CHAPTER 5
BACKCALCULATION OF LAYER MODULI

1.0 GENERAL

During the Phase I and Phase II studies, nondestructive deflection tests (NDT) were conducted on several rubblized pavement projects. The objectives of the tests include:

- Analyze the variations in the pavement deflections along and across the pavements.
- Backcalculate the moduli of the rubblized pavement layers.
- Assess the linearity of the pavement layers relative to load.

At each rubblized pavement project included in the NDT, a test section was selected and the section was divided into one or two 100-ft long test sites separated by 100-ft of pavement. At each test site, about forty FWD test locations were marked on the pavement surface as shown in figure 5. 1. The circles and the letter "X" in the figure indicate core and FWD test locations, respectively. The deflection data are discussed in later sections.

All NDT were conducted using the MDOT KUAB Falling Weight Deflectometer (FWD). The configuration and spacing of the 9 FWD deflection sensors are shown in figure 5. 2. All deflection data were recorded by an on-board computer to within 0.01 mils (0.00001 in.). Also at each FWD test location, the pavement and air temperatures were measured and the data were recorded. After the FWD tests were completed, between 5 and 12 pavement cores were extracted and the thickness of each core was measured. The thickness data were used as input to the backcalculation program. The deflections from sensors D1 through D7 (see figure 5. 2) were used to backcalculate the layer moduli using the MICHBACK computer software.

All FWD tests consisted of 4 drops, the deflection data from the first drop was not recorded while the data from the other three drops were recorded. Further, most tests were conducted using targeted 9000-lb load. On some projects, few FWD tests were conducted at different load levels in order to assess the linearity of the pavement response to load. Also on some projects, about ten FWD tests were conducted at the same test location in order to analyze the repeatability of the measured deflection data. Both linearity and repeatability are discusses in the next section.

2.0 REPEATABILITY AND LINEARITY OF THE DEFLECTION DATA

On seven pavement projects, several FWD tests were conducted at the same location for each of the following loads: 5,500, 9,000, 16,000 and 21,000 lb. The purposes of the test are to examine the repeatability and linearity of the deflection data at all seven sensor locations. Table 5.1 depicts the projects along which the repeatability and linearity tests were conducted along with the number of FWD tests (number of drops) for each load level. Typical results of the repeatability tests for I-69 EB, test section 1, site 1 are listed in table 5.2. The table provides a list of the average measured deflection at each sensor locations, the standard

Table 5.1 Pavement projects where repeatability and linearity tests were conducted

Test sites*	Load (lb)	Number of drops	Load (lb)	Number of drops	Load (lb)	Number of drops	Load (lb)	Number of drops
20273-21			9000	20	16000	10	21000	10
10692-12	5500	10	9000	20	16000	10	21000	10
30373-52	5500	10	9000	20	16000	10	21000	10
20102-11	5500	10	9000	20	16000	10	21000	10

* refer to the test sites reported in the investigations of rubblized pavements (Chapter 3)

Table 5.2 Averages and standard deviations of deflections D1 through D7 at different load levels, I-69 EB section 1 test site 1

Load (pound)	Number of drops	Statistics	Deflection (mils)						
			D1	D2	D3	D4	D5	D6	D7
5500	10	Average	4.93	3.40	2.85	2.42	2.09	1.56	0.84
		STDEV (mils)	0.07	0.04	0.04	0.04	0.03	0.03	0.04
		CV (%)	1.4	1.1	1.3	1.5	1.5	1.9	4.4
9000	20	Average	8.00	5.63	4.87	4.17	3.58	2.62	1.37
		STDEV (mils)	0.06	0.05	0.04	0.04	0.03	0.02	0.02
		CV (%)	0.8	0.9	0.9	0.9	0.8	0.9	1.6
16000	10	Average	14.35	10.24	8.93	7.59	6.58	4.77	2.55
		STDEV (mils)	0.04	0.04	0.10	0.04	0.03	0.03	0.03
		CV (%)	0.3	0.4	1.2	0.5	0.4	0.7	1.3
21000	10	Average	18.60	13.37	11.58	9.83	8.55	6.22	3.36
		STDEV (mils)	0.05	0.04	0.10	0.03	0.02	0.02	0.03
		CV (%)	0.3	0.3	0.9	0.3	0.3	0.3	0.8

STDEV = Standard deviation

CV = Coefficient of variation = standard deviation as a percent of the average

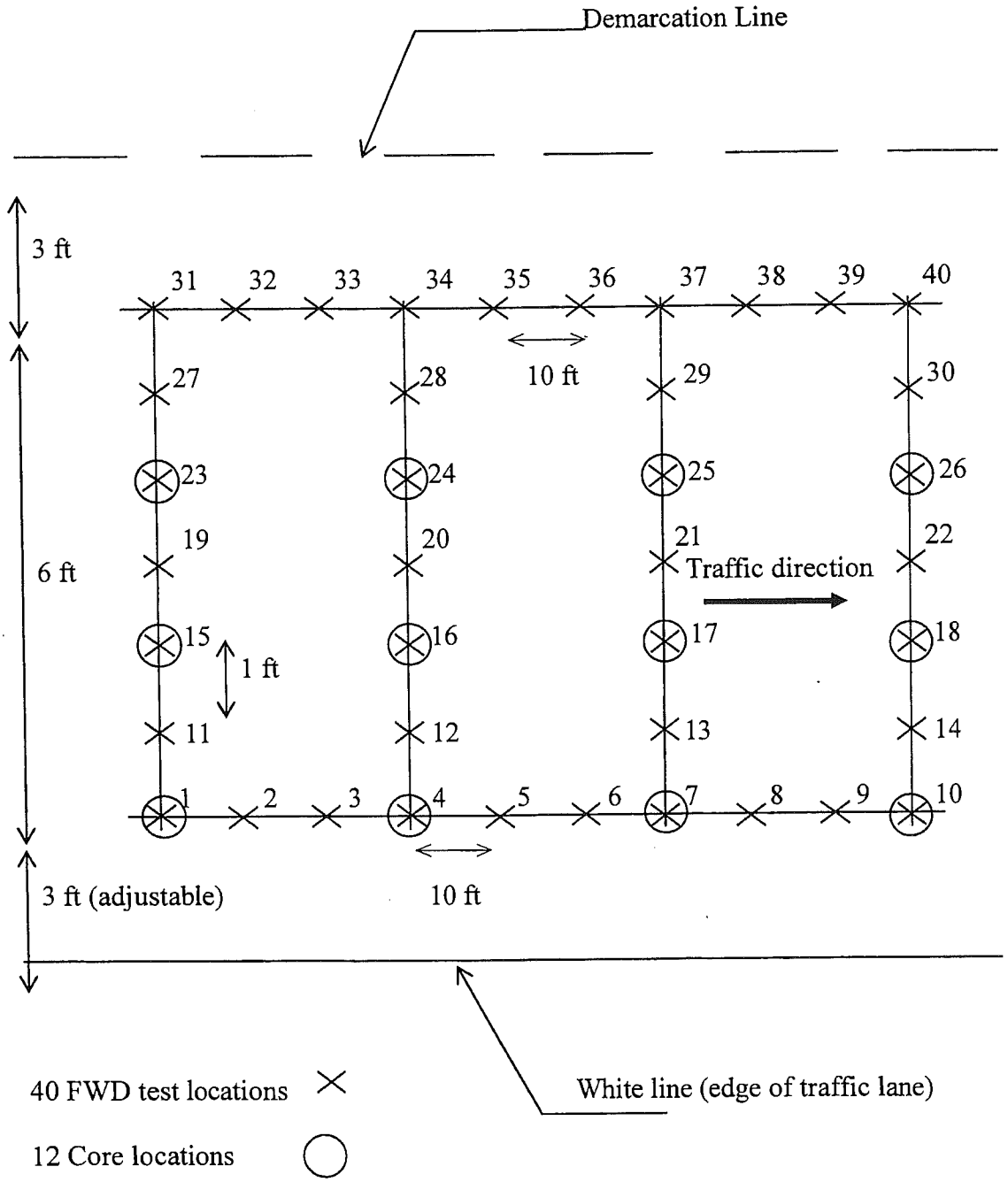

Figure 5.1 Typical FWD tests and cores layout

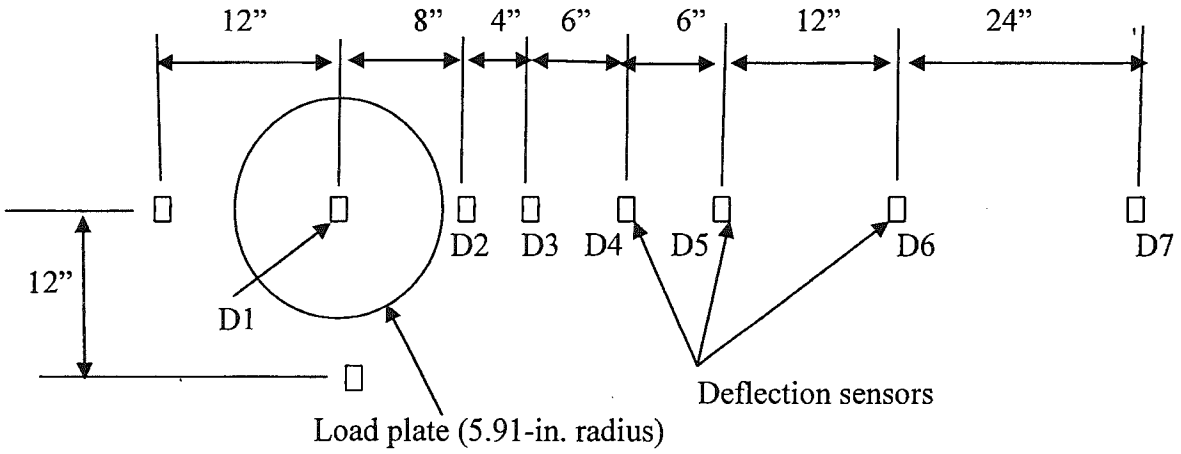

Figure 5.2 Schematic of FWD load plate and the deflection sensors

deviation and the coefficient of variation (standard deviation as percent of the average) of the deflection data at each load level. As can be seen, except for deflection sensor 3 (D3), the maximum standard deviation is 0.07 mils, which is well below the performance specifications for the FWD (1). Deflection sensor D3 shows good repeatability for the 5500- and 9000-lb load levels (standard deviation of less than 0.05 mils) and slightly higher standard deviation (0.1 mils) for the 16,000- and 21,000-lb loads, which is equal to the specified performance of FWD. Note that the impact of the repeatability (accuracy) of the measured deflection on the backcalculated layer moduli should not be measured in terms of absolute mils. It should be measured in terms of percent of the measured deflection. To illustrate, the impact of 0.07 mils error on 1.5 mils measured deflection is much higher than its impact on 9 mils measured deflection. Therefore, the coefficient of variation of each deflection sensor was calculated and is included in the table.

As stated above, linearity tests were also conducted together with the repeatability tests on seven pavement sections. As stated earlier, the purpose of the linearity tests is to assess whether or not the pavement response to load is linear. At each of the four load levels stated above, ten or twenty FWD tests were conducted. The average of the measured deflection data for each load level was calculated and then normalized relative to the average deflection at a 9,000-lb load. Typical results from I-69 EB, section 1, site 1 are provided in table 5.3. Figure 5.3 depicts the average measured deflections versus the applied load. The data in the table 5.3 and figure 5.3 indicate that, for all practical purposes, the pavement response to load is linear. Based on the linearity of the pavement response to load, the deflection data were used in the backcalculation of layer moduli using a linear elastic layered system.

3.0 DEFLECTION DATA

Pavement deflection represents its direct response to the applied load. Deflection can be thought of as an index expressing the structural capacity of the pavement. Hence, variations in the measured deflection reflect parallel variations in the structural capacity of the pavement. Tables 5.4 and 5.5 list the measured pavement deflections along and across the pavement of I-75 SB, section 1, test sites 1 and 2, respectively. Table 5.6 provides similar information for the flexible pavement along US 27 SB section 1test site 1.

The average and the coefficient of variation for D1 through D7 deflections are also listed in the three tables. Figures 5.4 and 5.5 depict plots of D1 through D7 deflections at the various test locations on test sites 1 and 2, respectively. The data in tables 5.4 and 5.5 and in figures 5.4 and 5.5 indicate that:

1. The variations in the deflections of the rubblized concrete pavement on I-75 SB, section 1, test sites 1 and 2 are much higher than the variation on flexible pavement (see table 5.6).

2. As it was expected, for both test sites, the peak pavement deflection (D1) shows the highest variation. The reason is that, the D1 deflection is a measure of the cumulative deflections of all pavement layers and of the roadbed soil. Hence, variations in these

Table 5.3 Average deflections D1 through D7 1 at different load levels normalized to the average deflection at 9,000 pound load, I-69 EB section 1 test site 2

Load (pound)	Deflection (mils)						
	D1	D2	D3	D4	D5	D6	D7
5500	4.93	3.40	2.85	2.42	2.09	1.56	0.84
9000	8.00	5.63	4.87	4.17	3.58	2.62	1.37
16000	14.35	10.24	8.93	7.59	6.58	4.77	2.55
21000	18.60	13.37	11.58	9.83	8.55	6.22	3.36
Normalized load	Normalized deflection						
	D1	D2	D3	D4	D5	D6	D7
0.6	0.62	0.60	0.59	0.58	0.58	0.60	0.61
1.0	1.00	1.00	1.00	1.00	1.00	1.00	1.00
1.8	1.79	1.82	1.84	1.82	1.84	1.82	1.87
2.3	2.33	2.37	2.38	2.36	2.39	2.38	2.46

Table 5.4 Deflections D1 through D7, I-75 SB section 1 test site 1

FWD Station	Deflection (mils)						
	D1	D2	D3	D4	D5	D6	D7
1	9.46	8.29	7.45	6.22	5.30	3.67	2.03
2	10.02	8.59	7.69	6.47	5.48	3.82	2.12
3	9.62	8.48	7.78	6.47	5.17	3.64	2.03
4	9.52	8.17	7.22	5.93	4.96	3.51	1.92
5	9.73	8.44	7.53	6.25	5.22	3.59	1.85
6	9.56	8.07	7.13	5.92	4.98	3.50	1.90
7	9.88	8.25	7.35	6.14	5.17	3.67	1.97
8	9.32	8.18	7.36	6.18	5.31	3.82	2.02
9	9.01	7.81	7.09	6.03	5.11	3.70	2.02
10	9.07	7.78	6.94	5.86	4.78	3.31	1.79
11	9.67	8.39	7.50	6.24	5.20	3.50	1.92
12	9.24	7.73	6.89	5.80	4.93	3.58	1.92
13	9.00	7.76	6.95	5.82	4.89	3.17	1.72
14	10.30	8.47	7.26	5.96	5.02	3.52	1.90
15	10.06	8.69	7.41	5.79	4.91	3.61	2.04
16	8.12	7.22	6.44	5.42	4.58	3.27	1.85
17	8.22	6.97	6.27	5.34	4.60	3.38	1.87
18	8.90	7.78	6.98	5.84	4.90	3.15	1.73
19	7.77	6.70	6.04	5.16	4.50	3.40	1.81
20	7.68	6.63	6.03	5.16	4.44	3.34	1.95
21	7.22	6.21	5.60	4.87	4.26	3.29	1.87
22	7.76	6.30	5.68	4.88	4.27	3.28	1.89
23	8.57	7.55	6.81	5.67	4.74	3.21	1.73
24	7.43	6.47	5.89	5.12	4.48	3.46	1.84
25	7.49	6.53	5.90	5.11	4.45	3.39	1.99
26	6.87	5.93	5.40	4.78	4.21	3.32	1.91
27	8.50	7.46	6.69	5.57	4.62	3.20	1.74
28	6.92	6.10	5.64	4.98	4.45	3.51	1.89
29	6.65	5.96	5.53	4.91	4.33	3.35	2.01
30	6.49	5.69	5.25	4.72	4.19	3.33	1.94
31	8.30	7.30	6.58	5.52	4.62	3.26	1.75
32	7.07	6.20	5.65	4.92	4.34	3.40	1.94
33	6.05	5.48	5.14	4.68	4.22	3.50	2.12
34	9.70	8.16	7.24	6.18	5.26	3.87	1.99
35	7.26	6.29	5.66	4.89	4.25	3.31	1.98
36	7.89	7.09	6.42	5.70	4.53	3.27	1.90
37	8.29	6.89	6.21	5.24	4.45	3.26	1.82
38	7.06	6.11	5.57	4.90	4.28	3.30	1.94
39	6.36	5.66	5.28	4.80	4.32	3.44	1.99
40	6.76	5.96	5.55	5.02	4.49	3.62	2.12
41	8.47	7.33	6.55	5.54	4.67	3.27	1.77
42	8.76	7.85	6.77	5.62	4.73	3.34	1.86
Average	8.33	7.21	6.48	5.51	4.70	3.44	1.91
CV (%)	14	13	12	10	8	5	6

CV = Coefficient of variation = standard deviation as a percent of the average

Table 5.5 Deflections D1 through D7, I-75 SB section 1 test site 2

FWD Station	Deflection (mils)						
	D1	D2	D3	D4	D5	D6	D7
1	10.45	8.53	7.37	5.95	4.87	3.45	1.89
2	9.30	7.84	6.92	5.74	4.80	3.46	1.83
3	9.98	8.42	7.38	6.08	5.07	3.51	1.78
4	8.38	7.15	6.41	5.45	4.68	3.34	1.66
5	10.55	8.38	7.07	5.61	4.60	3.26	1.68
6	9.12	7.68	6.74	5.53	4.56	3.14	1.60
7	8.98	7.39	6.44	5.24	4.31	2.90	1.46
8	10.01	8.00	6.85	5.43	4.33	2.85	1.32
9	10.83	8.70	7.35	5.82	4.61	2.93	1.25
10	9.33	7.49	6.49	4.89	4.07	2.81	1.41
11	7.85	6.66	5.85	4.82	3.95	2.72	1.42
12	10.30	8.34	7.11	5.58	4.45	2.82	1.29
13	9.31	7.62	6.68	5.51	4.63	3.40	1.83
14	8.37	7.50	6.54	5.39	4.57	3.23	1.70
15	9.40	7.23	6.22	4.91	4.03	2.74	1.36
16	6.86	6.05	5.37	4.50	3.80	2.70	1.45
17	8.09	6.57	5.81	4.97	4.25	3.22	1.84
18	8.17	7.05	6.29	5.34	4.55	3.24	1.72
19	9.03	6.76	5.78	4.66	3.88	2.68	1.35
20	6.16	5.40	4.90	4.24	3.64	2.69	1.42
21	7.68	5.99	5.27	4.52	3.93	3.09	1.81
22	8.03	6.93	6.29	5.50	4.85	3.26	1.76
23	8.63	6.41	5.51	4.48	3.72	2.60	1.36
24	6.79	5.80	5.12	4.37	3.77	2.80	1.50
25	6.79	5.96	5.25	4.32	3.63	2.62	1.41
26	7.22	5.82	5.19	4.50	3.95	3.14	1.87
27	7.89	6.82	6.23	5.51	4.89	3.35	1.79
28	7.52	6.08	5.20	4.26	3.59	2.58	1.40
29	7.16	6.22	5.48	4.49	3.74	2.18	1.34
30	6.47	5.72	5.18	4.58	4.08	3.24	1.92
31	8.08	7.05	6.37	5.60	4.96	3.37	1.80
32	7.53	6.22	5.32	4.41	3.76	2.79	1.54
33	7.52	6.46	5.70	4.67	3.88	2.68	1.37
34	6.57	5.69	5.14	4.47	3.91	3.13	1.89
35	6.53	5.77	5.34	4.72	4.11	3.18	1.82
36	7.26	6.38	5.78	4.94	4.24	3.20	1.80
37	8.73	7.58	6.82	5.88	5.11	3.42	1.74
38	5.93	5.27	4.84	4.28	3.77	2.97	1.67
39	6.65	5.84	5.28	4.53	3.92	2.97	1.65
40	7.65	6.31	5.51	4.58	3.90	2.89	1.57
41	7.20	6.21	5.63	4.89	4.30	3.17	1.69
42	10.54	7.66	6.54	5.28	4.47	3.26	1.80
43	8.40	6.82	5.99	4.92	4.05	2.81	1.42
Average	8.21	6.83	6.01	5.01	4.24	3.02	1.61
CV (%)	16	14	12	11	10	10	13

CV = Coefficient of variation = standard deviation as a percent of the average

Table 5.6 Deflections D1 through D7 on an asphalt pavement, US 27 SB section 1test site 1

FWD Station	Deflection (mils)						
	D1	D2	D3	D4	D5	D6	D7
1	7.50	6.48	5.81	4.91	4.18	2.93	1.43
2	7.39	6.36	5.68	4.79	4.07	2.86	1.44
3	7.33	6.34	5.69	4.80	4.07	2.85	1.37
4	7.58	6.48	5.80	4.85	4.11	2.86	1.36
5	7.32	6.27	5.64	4.75	4.03	2.84	1.40
6	7.52	6.40	5.74	4.85	4.12	2.91	1.40
7	7.68	6.60	5.90	4.97	4.24	2.99	1.47
8	7.51	6.45	5.78	4.91	4.15	2.95	1.44
9	7.58	6.41	5.80	4.93	4.18	2.94	1.46
10	7.43	6.34	5.71	4.84	4.12	2.90	1.46
11	7.44	6.36	5.75	4.89	4.14	2.90	1.43
12	7.44	6.34	5.66	4.75	3.99	2.80	1.36
13	7.49	6.37	5.73	4.87	4.15	2.90	1.44
14	7.24	6.22	5.59	4.75	4.03	2.87	1.44
15	7.23	6.23	5.60	4.71	4.03	2.82	1.43
16	7.32	6.20	5.55	4.64	3.93	2.75	1.35
17	7.28	6.30	5.65	4.79	4.10	2.91	1.42
18	7.12	6.12	5.51	4.69	3.98	2.78	1.44
19	7.05	6.14	5.53	4.68	3.97	2.85	1.41
20	7.16	6.13	5.48	4.60	3.93	2.74	1.34
21	7.09	6.11	5.50	4.71	3.98	2.86	1.45
22	7.13	6.09	5.50	4.66	3.97	2.81	1.44
23	7.03	6.08	5.46	4.64	3.96	2.86	1.45
24	7.17	6.12	5.47	4.62	3.93	2.79	1.39
25	7.06	6.07	5.48	4.67	4.01	2.86	1.46
26	7.22	6.20	5.60	4.72	4.04	2.86	1.48
27	7.14	6.20	5.57	4.69	4.01	2.80	1.38
28	7.15	6.19	5.58	4.75	4.05	2.93	1.45
29	7.27	6.25	5.65	4.80	4.07	2.94	1.49
30	7.17	6.22	5.60	4.75	4.06	2.89	1.45
31	7.32	6.31	5.71	4.80	4.08	2.88	1.45
32	7.43	6.41	5.80	4.93	4.15	2.93	1.45
33	7.23	6.26	5.66	4.81	4.10	2.88	1.43
34	7.06	6.10	5.47	4.67	3.97	2.79	1.39
35	7.10	6.13	5.53	4.73	4.04	2.88	1.42
36	7.31	6.29	5.69	4.83	4.13	2.91	1.44
37	7.22	6.21	5.58	4.72	4.02	2.85	1.45
38	7.15	6.18	5.56	4.75	4.02	2.88	1.49
39	7.51	6.43	5.76	4.89	4.15	2.92	1.45
40	7.27	6.19	5.55	4.62	3.92	2.74	1.39
Average	7.29	6.26	5.63	4.77	4.05	2.87	1.43
CV (%)	2	2	2	2	2	2	3

CV = Coefficient of variation = standard deviation as a percent of the average

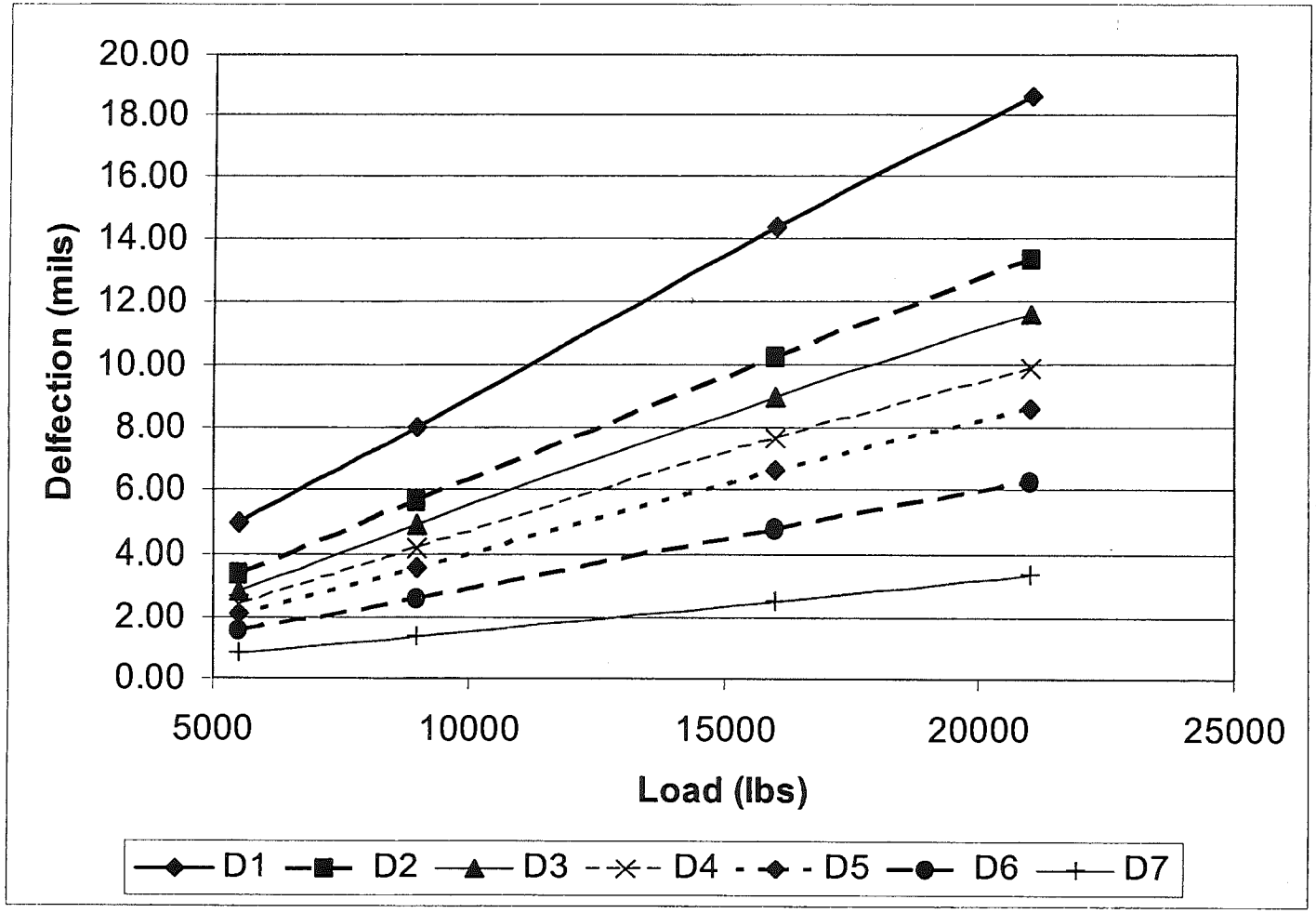

Figure 5.3 Average deflections D1 through D7 on I-69 section 1 site 1 at different load levels

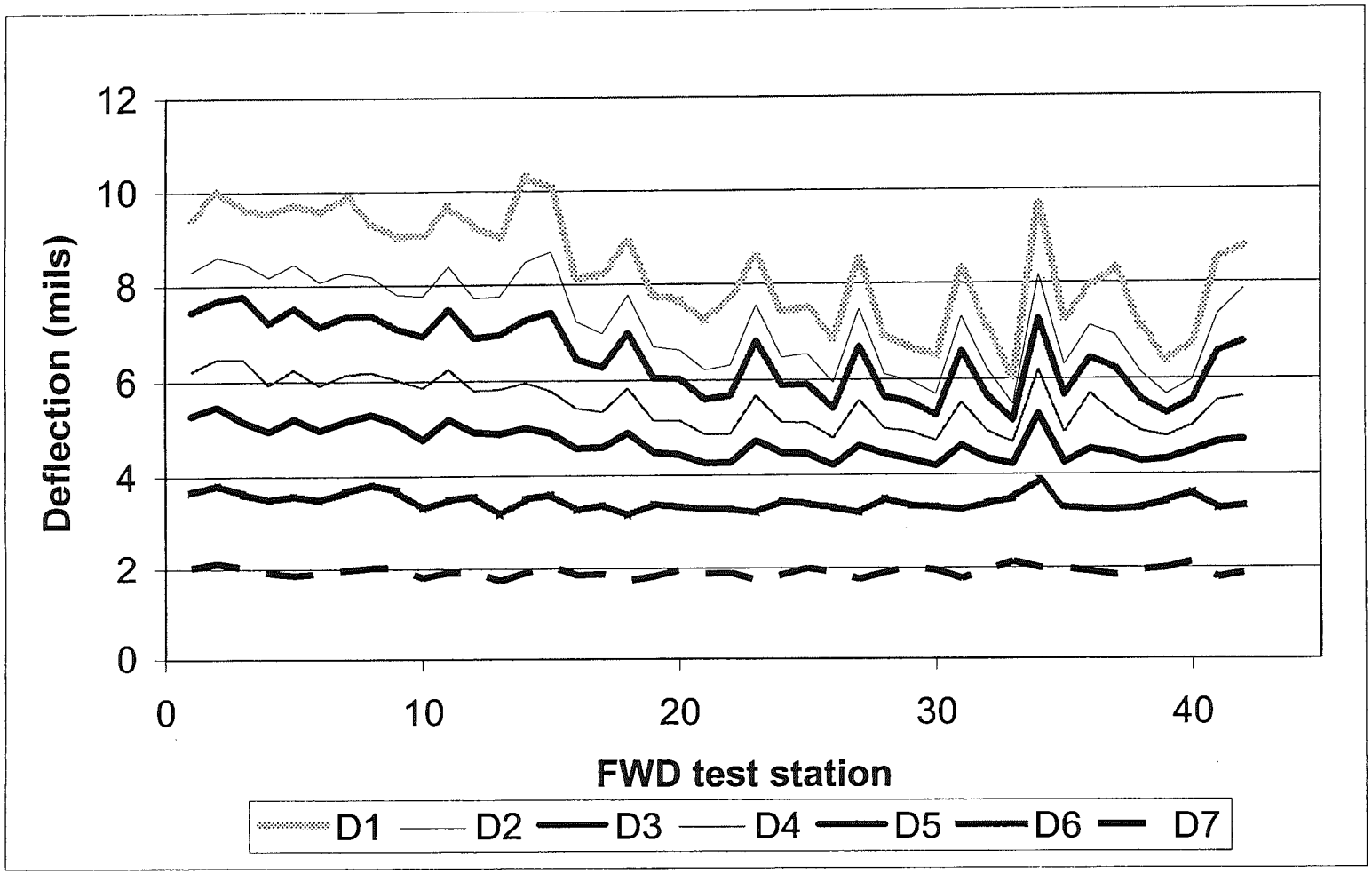

Figure 5.4 Variations of D1 through D7 deflections, I-75 SB, test section 1, site 1

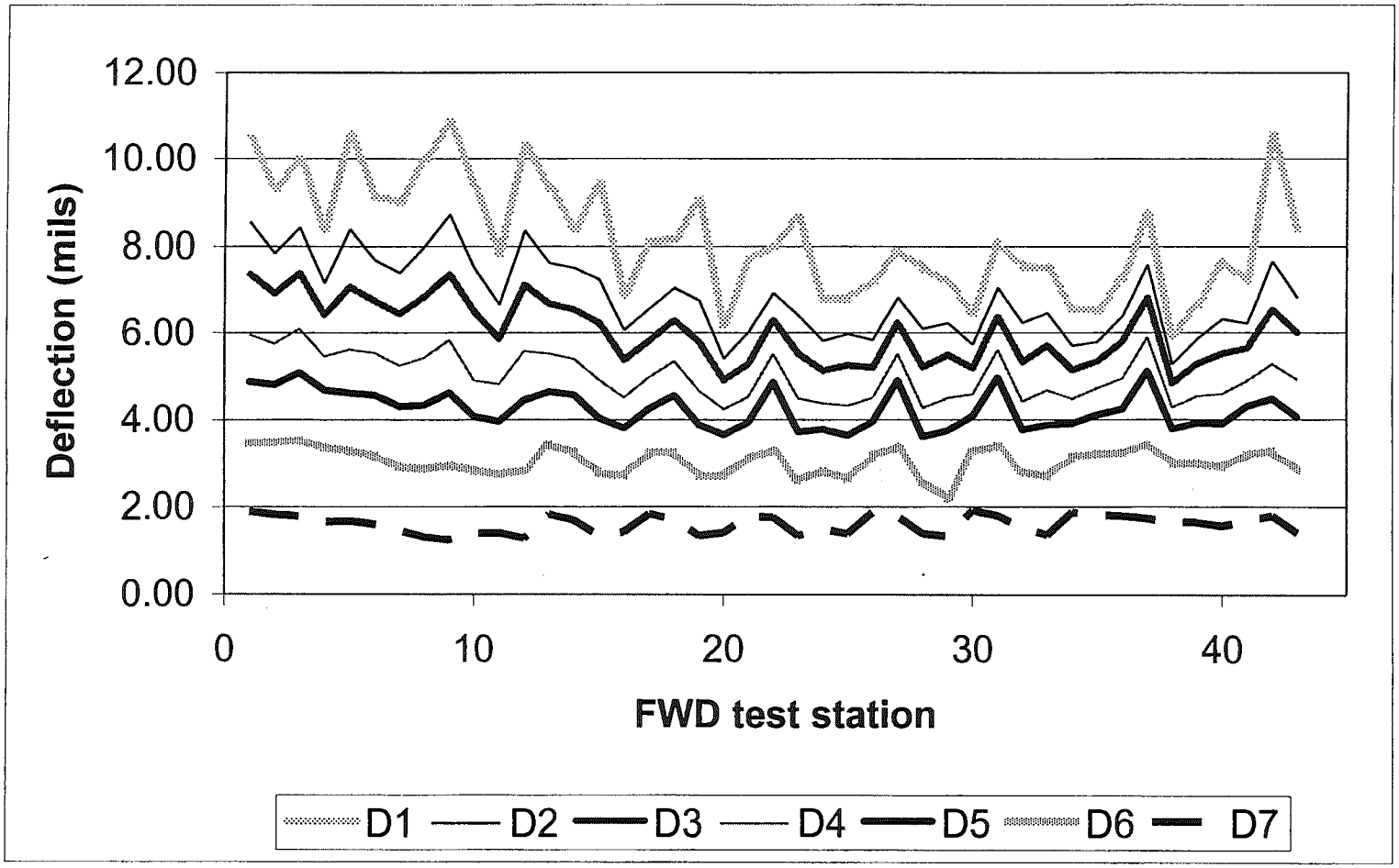

Figure 5.5 Variations of D1 through D7 deflections, I-75 SB, test section 1, site 2

layers and in the roadbed soil are reflected in the measured deflection. Further, the peak pavement deflection (D1) varies from about 6 to more than 10 mils.

3. The variations of D1 through D7 deflections for test site 1 are lower than those for test site 2.

4. The variation in the measured D7 deflection along test site 1 is much lower than that at test site 2.

The above observations are illustrated in figure 5.6. The figure shows the normalized D1 and D7 deflections for test sites 1 and 2. Examination of the figures indicates that relative to the normalized deflection value of 1:

1. The peak D1 deflections at test sites 1 and 2 vary by about $\pm$ 27 and $\pm$ 30 percent, respectively.

2. The D7 deflections at test sites 1 vary from about +10.3 to about – 8 percent whereas the variation at test site 2 is from about 10.3 to about – 27 percent.

For comparison purposes, the coefficients of variation of the measured D1 through D7 deflections for 18 test sites are listed in table 5.7. As can be seen, the coefficients of variation for I-75 SB section 1 test site 2 are relatively high compared to the other test sites.

Relative to table 5.7, it should be noted that the measured D1 through D7 deflections along all rubblized pavements included in this study show higher variation than the variation in the deflections of conventional flexible pavement. Given that the main difference between conventional flexible and rubblized pavement sections is the rubblized concrete slab, one can conclude that the high variations in deflections could be directly related to variations and/or non-uniformity of the rubblized concrete slab. Such non-uniformity was investigated while the pavement was being rubblized. Trenches were excavated in the rubblized concrete slab and the uniformity and thickness of the rubblized material were examined. It was observed that:

1. The rubblized concrete slab could be divided into two sublayers as follows:

   a) An upper rubblized material layer where the concrete has been broken to aggregate size material ranging in size from dust to more than 6-in.
   b) A lower fractured concrete layer where the rubblized concrete is semi-solid containing a network of micro cracks having random spacing.

2. The thickness of the rubblized material and the fractured concrete layers vary from zero to nine in. (the thickness of the concrete slab). Such variation yields geometry of the fractured concrete layer that consists of sharp peaks and valleys as shown in figure 5.7.

3. The temperature steel was occasionally debonded.

Table 5.7 Coefficients of variation in the measured D1 through D7 deflections for 18 test sites on rubblized pavements

Test site	Coefficient of variation of the measured D1 through D7 deflections (%)						
	D1	D2	D3	D4	D5	D6	D7
10692-11	9	10	11	10	10	10	15
10692-12	9	10	11	10	10	10	15
10753-11	14	13	12	10	8	5	6
10753-12	16	14	12	11	10	10	13
11941-21	8	7	7	7	7	7	4
11941-22	11	8	7	7	6	6	5
20102-11	7	7	7	7	7	7	6
20102-12	8	8	8	8	7	6	3
20233-11	12	12	11	10	8	7	15
20233-12	8	9	9	9	9	10	10
20273-21	15	13	11	8	6	4	4
20273-31	6	6	5	5	5	5	6
20273-41	8	12	11	9	7	6	4
20311-11	10	10	9	7	7	8	10
30373-21	19	14	10	17	14	12	10
30373-51	7	8	7	6	6	5	5
30373-52	15	16	15	14	14	13	11
30373-61	10	9	9	8	6	6	8

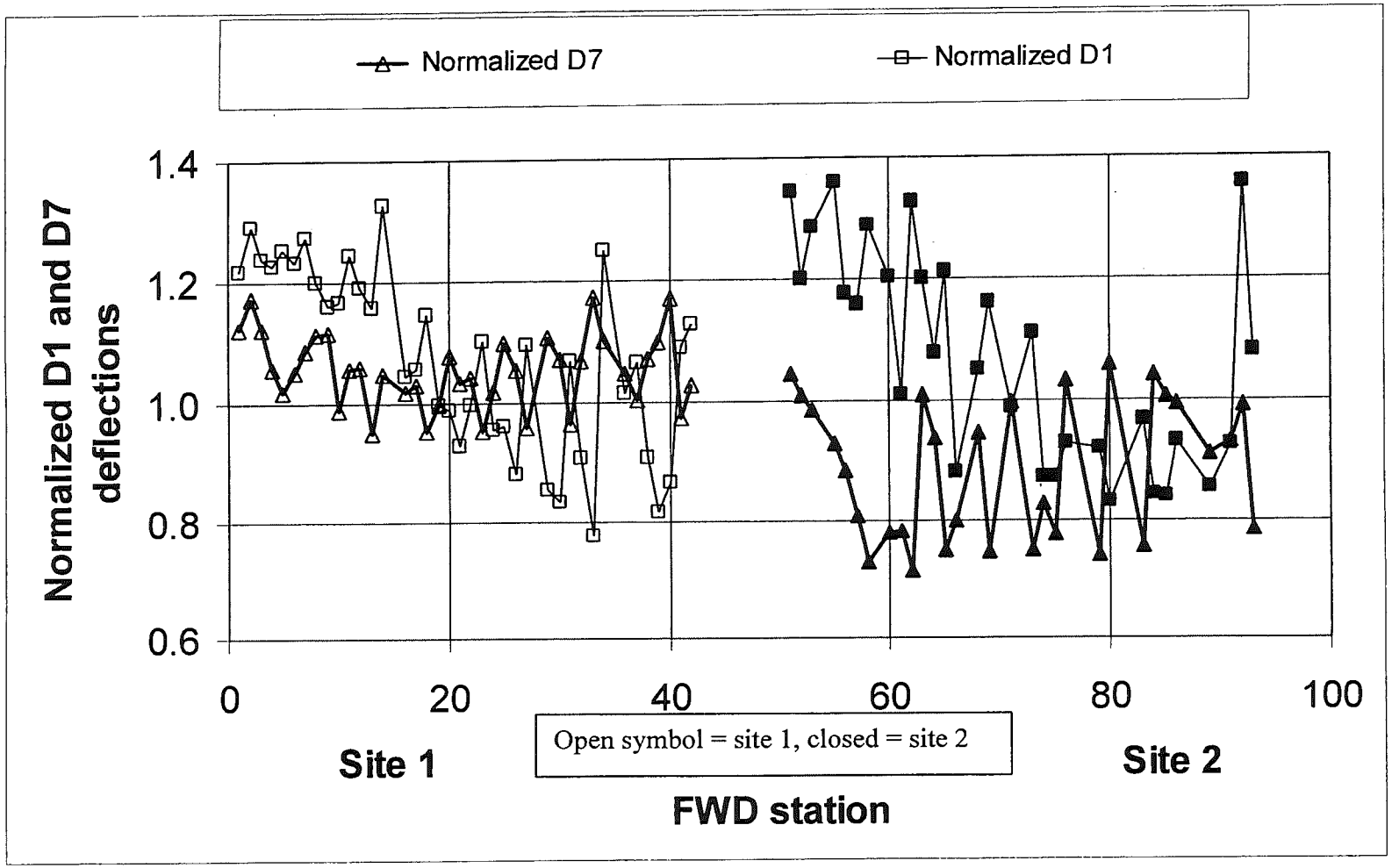

Figure 5.6 Normalized D1 and D7 deflection for I-75 SB, section 1, test sites 1 and 2

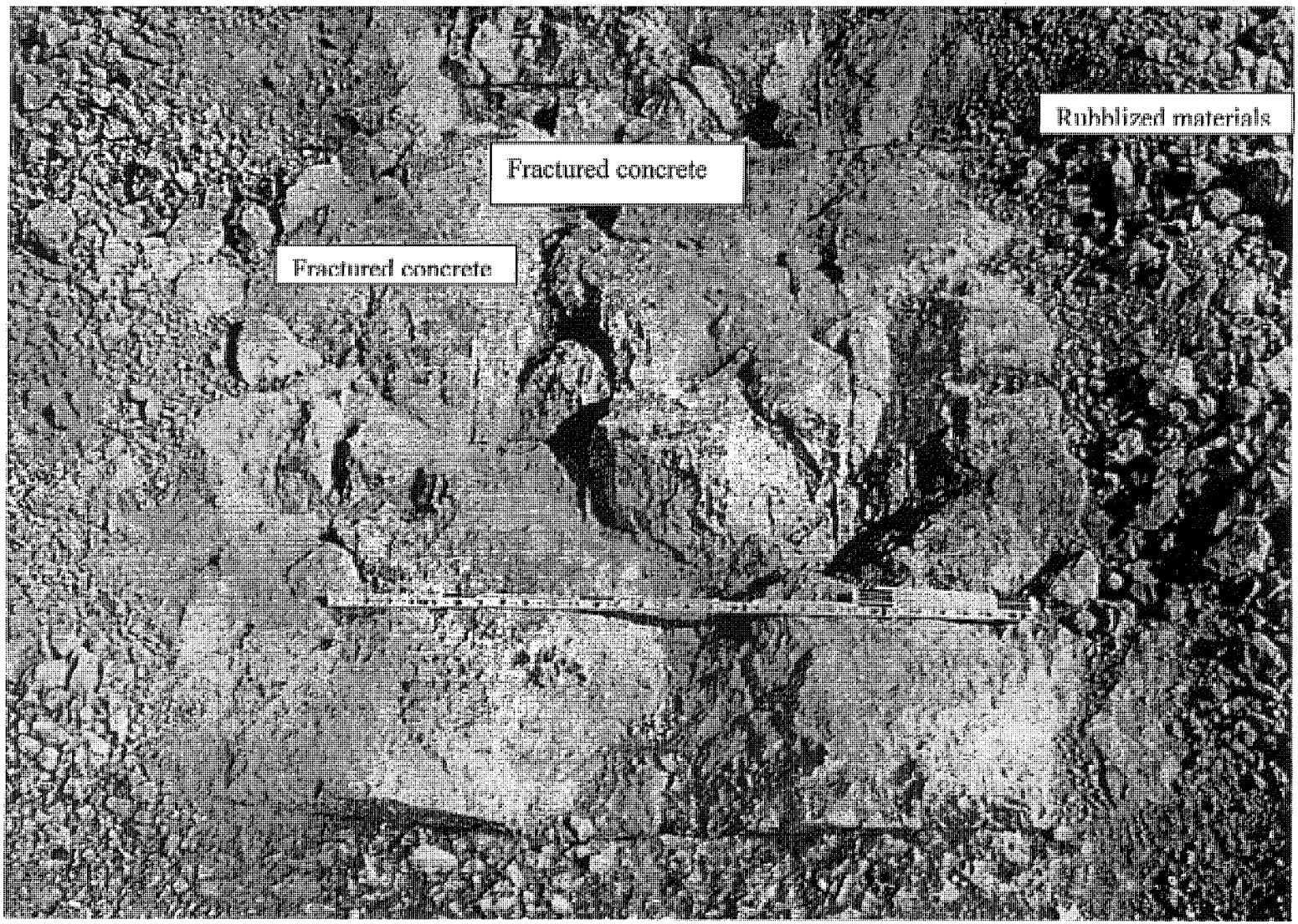

Figure 5.7 A typical trench in rubblized concrete pavement along US-10

Since variations in the thickness of the rubblized and fractured materials reflect the quality of the rubblization process and since said variations directly impact the variation in the measured deflection, the variation in the measured deflection could be used to express the quality of the rubblization process.

Finally variation in the outer deflection (sensor D7) is mainly related to the roadbed response to load. Said variation can be related to:

1. Variation in the roadbed soil in terms of moisture content, density, and material type.

2. Variations in the way the pavement layers distribute the load to the roadbed soil. For example, higher layer thickness causes decreases in the stress delivered to the roadbed soil due to the applied load and hence lower D7 deflection. Further, increases in the layer stiffness cause the applied load to be distributed to a wider area, which may cause higher D7 deflection. The reason is that the D7 deflection (located at 60-in. from the center of the load) may include some deflection from the subbase material.

The above scenario implies that, for some pavements or for some test locations, the D7 deflection may not correlate on one to one basis to the backcalculated roadbed soil modulus.

4.0 BACKCALCULATION PROCEDURE

Various computer software are available for the backcalculation of layer moduli. The differences between them are the forward software used to calculate pavement deflection and the convergence routine. The MICHBACK software uses the chevron-5 elastic layer system and a modified Newtonian algorithm (2 and 3) as a convergence routine to increment the modulus values of the various pavement layers. Hence, the use of MICHBACK is limited to 5-layer system including the stiff layer. In this study, pavements consisting of more than 5-layers were handled by combining two or more layers into one. Such combination was based on the proximity of the layer moduli of the combined layers and engineering judgment.

The accuracy of the backcalculation moduli is typically tested by conducting forward analyses of assumed pavement sections using a multilayer elastic computer program, backcalculating the layer moduli using the generated deflection basins and comparing the backcalculated moduli with the actual moduli used in the forward analysis. In general, the accuracy of the backcalculated moduli depends on several variables including:

1. The input seed modulus values
2. The accuracy of the measured deflection data
3. The number of deflection sensors
4. The accuracy and variability of the layer thicknesses
5. The number of pavement layers
6. The estimated depth to stiff layer

Unlike other backcalculation software, the results obtained from the MICHBACK computer software are independent of the assumed values of the seed modulus. For example, if the assumed seed modulus values are changed by ten folds, the backcalculated modulus values will change by less than 1 percent. The second item listed above (the accuracy of the measured deflection data) poses no problem as it was stated in the previous section regarding the repeatability of the MDOT FWD measured deflection data. Finally, the MDOT FWD is equipped with 9 deflection sensors spaced at 7 radial distances from the center of the loaded area. Hence, the deflection readings from three deflection sensors are similar and the deflection readings from only seven sensors can be used in the backcalculation of layer moduli. This limited number of deflection sensors causes no problem since, as stated earlier; the maximum number of pavement layers that can be handled by the Chevron-5 software (the forward engine in MICHBACK) is five. Indeed, the excess in the number of deflection sensors relative to the number of layers was advantageous in that it minimized the errors between the measured and the calculated deflection basins.

To minimize the errors due to the last three variables listed above; a backcalculation procedure was established and tested using forward and backward analyses. The procedure was used to backcalculate the layer moduli of all rubblized pavement sections included in this study after every step of it was verified. The procedure is detailed below relative to each of the three variables.

4.1 The Accuracy and Variability of the Layer Thicknesses

A typical rubblized pavement section consists of 4 or 5-layers situated on top of the roadbed soil as shown in figure 5.8. Relative to the two sections, the thickness of the pavement layers vary from one project to another. For example, the thickness of the:

- AC layer varies from about 4 to about 7 in. depending on the pavement section.
- Rubblized and fractured concrete layers is about 9 in. (the original thickness of the concrete pavement).
- Aggregate base varies from about zero (no aggregate base) to about 9 in.
- Sand subbase varies from about 9 to about 18 in.

Two unique features of the two typical sections shown in figure 5.8 are:

- For the same pavement section, the thickness of each of the rubblized and fractured concrete layers vary significantly from one point to another. For example, the thickness of the fractured concrete may vary along and across the pavement from zero to 9-in. Since the rubblized and fractured concrete layers are close to the pavement surface, such variation in their thicknesses significantly affects the accuracy of the backcalculated modulus values.
- The uneven surface between the rubblized material and the fractured concrete layer.

Further, note that for a given rubblized pavement section, the thicknesses of the AC, rubblized material, fractured concrete, aggregate base and sand subbase layers vary along and across the pavement. For example, a typical variation in the AC thickness along

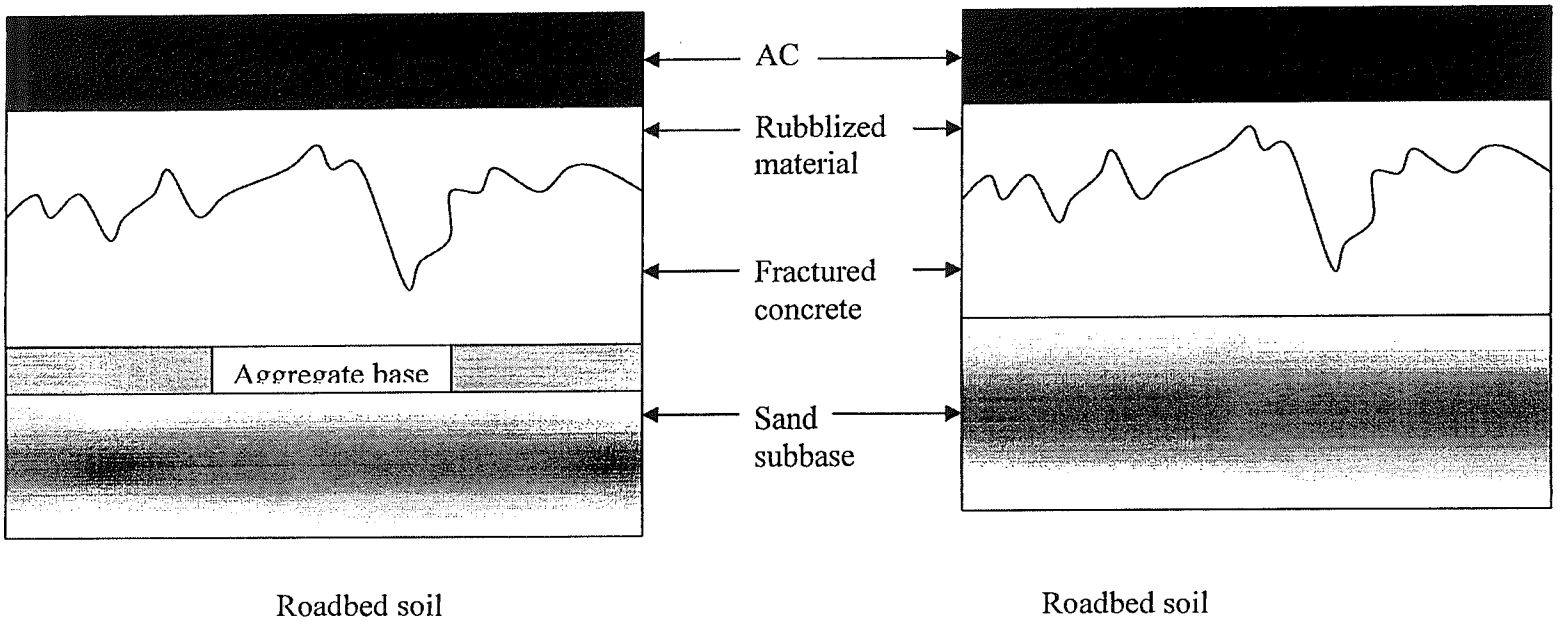

Figure 5.8 Typical rubblized pavement cross-sections

and across the pavement is about ± 1-in. Although variations in the thicknesses of the aggregate base and sand subbase have little impact on the backcalculated layer moduli, variation in the AC thickness has a substantial impact. Further, variation in the thickness of the rubblized material and fractured concrete impact their respective backcalculated moduli. To decrease the error in the backcalculated layer moduli due to variations in the AC thickness and the thicknesses of the rubblized and fractured concrete layers, the following procedure was adopted and used throughout the study.

4.1.1 The AC Thickness

At each test site, about 10 to 15 AC cores were extracted from the pavement and, for each core; four measurements of the AC thickness were made at the end of two orthogonal diameters. Hence, for each test site, a total of 40 to 60 AC thickness measurements were made. The average of all measurements was then calculated and used as input to the backcalculation routine. Examples of the variation in the AC thickness within 100 ft of pavement along I-75 SB, section 1, test sites 1 and 2 are shown in tables 5.8 and 5.9. As can be seen the AC thickness along test site 1 varies from 4.1 to 4.8 in. with an average of 4.5 in. and from 3.5 to 4.6 in. with an average of 4.1 in. for test site 2. Note that the MDOT inventory data for I-75 SB section 1 indicates that the AC thickness is 4.5 in. If this data is used in the backcalculation, one should expect larger errors in the backcalculated layer moduli for test site 2 than those for test site 1. Hence, efforts should be made to obtain the actual AC thickness from pavement coring. Nevertheless, the effect of using the average AC thickness on the backcalculated layer moduli was analyzed using forward and backward analysis. The forward analysis was based on an AC thickness of 4.5 in. The calculated pavement response (deflection) was then used to backcalculate the layer moduli. Ten trials were conducted where, in the backcalculation, the AC thickness was varied from 3.5 to 5.5 in. The results showed that, for a given error in the AC thickness, the backcalculated AC modulus varies relative to the true value. However, the average value of the ten backcalculated AC moduli has an insignificant error relative to the true modulus value.

To analyze the effect of using the average AC thickness on the backcalculated layer moduli, two backcalculation schemes were conducted as follows:

1. For each test site and at each core location, the measured deflection data and the measured core thickness were used to backcalculate the layer moduli at that location.

2. The layer moduli were backcalculated using the average measured AC thickness and the entire deflection data for the test site in question.

Table 5.8 Thickness, diameters and conditions of cores obtained from I-75 SB - section 1 test site 1

Core Designation	Total core thickness (in.)					Courses thickness (in.)			Core diameter (in.)	Crack/ defect
	1	2	3	4	Average	Surface	Leveling	Base		
10753-1101	4.2	4.4	4.5	4.2	4.3	1.5	1.1	1.7	5.7	None
10753-1104	4.1	4.1	4.3	4.1	4.2	1.5	1.0	1.7	5.7	None
10753-1107	4.8	4.5	4.4	4.8	4.6	1.6	1.0	2.0	5.7	None
10753-1110	4.0	4.1	4.1	4.0	4.1	1.4	1.0	1.7	5.7	None
10753-1115	4.6	4.6	4.8	4.6	4.7	1.8	1.4	1.5	5.7	Crack
10753-1116	4.8	4.6	4.6	4.7	4.7	1.6	1.1	2.0	5.7	None
10753-1117	4.8	4.7	4.8	4.8	4.7	1.8	1.1	1.8	5.7	None
10753-1118	4.3	4.4	4.5	4.3	4.3	1.6	1.0	1.7	5.7	None
10753-1123	4.8	4.8	4.8	5.0	4.8	1.8	1.0	2.0	5.6	None
10753-1124	4.5	4.5	4.6	4.5	4.5	1.7	1.0	1.8	5.7	None
10753-1125	4.8	4.5	4.8	4.6	4.7	1.8	1.0	1.9	5.7	None
10753-1126	4.5	4.5	4.5	4.5	4.5	1.7	0.9	1.9	5.6	None
10753-1150	4.8	4.8	4.5	4.6	4.7	1.8	1.0	1.9	N.A.	Broken
10753-1151	4.6	4.5	4.4	4.5	4.5	1.8	1.0	1.8	5.7	Crack
Average					4.5	1.7	1.0	1.8	5.7	
CV (%)					5	8	11	8	0	

Table 5.9 Thickness, diameters and conditions of cores obtained from I-75 SB - section 1 test site 2

Core Designation	Total core thickness (in.)					Courses thickness (in.)			Core diameter (in.)	Crack/ defect
	1	2	3	4	Average	Surface	Leveling	Base		
10753-1201	3.8	3.8	3.8	3.9	3.8	1.4	1.0	1.4	5.7	None
10753-1204	4.0	4.0	4.1	4.3	4.1	1.6	1.0	1.5	5.7	None
10753-1207	3.5	3.6	3.5	3.5	3.5	1.0	1.5	1.0	5.7	Crack
10753-1210	3.6	3.8	3.8	4.0	3.8	1.6	1.1	1.1	5.7	None
10753-1215	4.3	4.3	4.4	4.3	4.3	1.6	1.1	1.6	5.7	None
10753-1216	4.5	4.3	4.4	4.5	4.4	1.0	1.7	1.7	5.7	None
10753-1217	4.0	3.8	3.9	4.0	3.9	1.5	1.0	1.4	N.A.	Broken
10753-1218	4.2	4.2	4.2	4.2	4.2	1.6	1.0	1.6	5.7	None
10753-1223	4.4	4.4	4.4	4.5	4.4	1.7	1.1	1.6	5.6	None
10753-1224	4.5	4.8	4.6	4.5	4.6	1.9	1.0	1.7	5.7	None
10753-1225	4.3	4.3	4.4	4.3	4.3	1.7	1.0	1.6	5.7	None
10753-1226	4.3	3.9	3.9	4.0	4.0	1.6	1.1	1.3	5.7	None
10753-1250	3.6	3.5	3.5	3.5	3.5	1.5	0.9	1.1	5.7	None
10753-1251	4.4	4.3	4.3	4.4	4.3	1.7	1.0	1.6	5.7	None
10753-1252	3.5	3.5	3.5	3.5	3.5	1.0	1.4	1.1	N.A.	Broken
Average					4.1	1.6	1.1	1.4	5.7	
CV (%)					8	13	13	16	0	

Table 5.10 provides a list of the backcalculated moduli of the 2 schemes stated above. Examination of the results indicates that:

1. The backcalculated roadbed modulus based on the average AC thickness is almost the same as that based on the measured AC thickness (zero percent difference). This implies that errors in the AC thickness have no impact on the backcalculated layer moduli.

2. When the measured core thickness is lower than the average thickness of 4.5 in., the backcalculated AC and rubblized moduli based on the average thickness is lower than that based on the measured thickness (negative percent difference).

3. When the measured core thickness is equal to the average thickness of 4.5 in., the backcalculated AC and rubblized moduli based on the average thickness is almost the same as that based on the measured thickness (zero percent difference).

4. When the measured core thickness is higher than the average thickness of 4.5 in., the backcalculated AC and rubblized moduli based on the average thickness is higher than that based on the measured thickness (positive percent difference).

5. The average values of the moduli of the AC, rubblized and roadbed soil (that were backcalculated based on the average AC thickness of 4.5 in.) have insignificant differences (less than 3 percent) relative to those based on the measured core thickness.

6. The coefficients of variations of all the backcalculated moduli using the average AC thickness of 4.5 in. are similar to those backcalculated using the AC thickness at each core location.

The significance of the above observations is that, for each 100-ft long test site, when the thicknesses of the extracted cores are representative of the distribution of the thickness of the asphalt layer, the average core thickness could be used to backcalculate the layer moduli. In this study, the number of extracted cores within each 100-ft long test site is equal to or grater than 25 percent of the number of the FWD test locations. That is the ratio of the number of the FWD test locations to the number of extracted core is equal to or greater than 0.25. Further, for most test sites, the average core thickness is almost equal to the AC thickness found in the MDOT inventory file. The preliminary conclusion based on 18 test sites is that, when resources are not available, there is no absolute need (although it is highly recommended) to core the pavement section. The only requirement is to distribute about 40 FWD test locations along and across the asphalt mat within a short test site (e.g., 100-ft). In this regard, the FWD test layout shown in figure 5.1 is highly recommended.

Table 5.10 Backcalculated moduli at 14 core locations on I-75 SB section 1 test site 1 using the average AC thickness of 4.5-in. and the measured core thicknesses

Core no.	Measured AC thickness (in.)	Backcalculated modulus (psi)								
		Using the average AC thickness of 4.5-in.			Using the measured AC thickness at the core location			Error (%)		
		AC	Rubblized	Roadbed	AC	Rubblized	Roadbed	AC	Rubblized	Roadbed
10	4.1	1,917,561	102,669	17,752	2,371,494	110,442	17,752	-19	-7	0
4	4.2	1,317,448	125,546	16,779	1,526,898	131,539	16,784	-14	-5	0
1	4.3	2,041,531	106,098	15,865	2,262,151	110,175	15,866	-10	-4	0
18	4.3	2,728,687	68,577	18,406	3,060,106	71,237	18,402	-11	-4	0
26	4.5	2,346,427	101,879	18,372	2,352,325	101,679	18,373	0	0	0
51	4.5	536,489	452,420	18,055	536,530	452,393	18,055	0	0	0
24	4.5	1,365,183	302,454	16,820	1,364,897	302,484	16,820	0	0	0
7	4.6	1,115,255	133,978	16,190	1,077,134	131,401	16,188	4	2	0
25	4.7	960,796	467,837	17,498	954,398	442,757	17,458	1	6	0
15	4.7	677,201	142,011	16,919	649,673	136,186	16,907	4	4	0
16	4.7	2,144,219	147,111	17,682	1,958,521	141,734	17,679	9	4	0
17	4.7	1,196,843	215,286	17,415	1,140,703	206,343	17,403	5	4	0
23	4.8	2,454,067	211,126	17,330	2,235,075	196,141	17,326	10	8	0
Average	4.5	1,600,131	198,230	17,314	1,653,070	194,962	17,309	-3	2	0
CV (%)	5	44	66	4	47	65	4			

CV (%) = Coefficient of variation = standard deviation divided by average

Note that similar observations were also made on other test sites. Based on the above observations, the backcalculation of layer moduli was accomplished by using the average core thickness. The results are listed in Appendix B along with the average values and the coefficient of variation.

4.1.2 The Rubblized Material and the Fractured Concrete Thicknesses

Since the thicknesses of the rubblized and fractured concrete layers vary literally from one point to another, in the backcalculation, the two layers were treated as one combined layer. The thickness of the combined layer was assumed to be the same as the thickness of the original concrete slab. The impact of such an assumption on the backcalculated modulus values of the AC, base and subbase layers and on the roadbed soil was analyzed using forward and backward analyses of 111 pavement sections having the various layer thicknesses and modulus values that are listed below. Note that the variations in the layer properties were designed to simulate the spectrum of actual rubblized pavement sections in Michigan.

Layer	Modulus (ksi)	Thickness (in)	Poisson ratio
AC	500, 1000 and 2,000	6.0	0.3
Rubblized material	30, 100, 200, 300 and 400	3.0, 4.5, 5.0 and 7.0	0.4
Fractured concrete	300, 500, 1000 and 2,000	6.0, 4.5, 4.0 and 2.0	0.2
Base	20, 30, 40 and 60	4.0, 12.0, 15.0 and 18.0	0.4
Roadbed soil	10, 15, 20 and 40	infinite	0.45

As stated above, the forward analyses resulted in 111 deflection basins, which were used to backcalculate the layer moduli. In all backcalculation, the rubblized material and the fractured concrete layers were combined as one 9-in. thick layer. Figures 5.9 through 5.11 depict the backcalculated and the actual modulus values of the AC layer, roadbed soil and base layer, respectively. The straight line in the figures is the line of equality between the backcalculated and the actual layer moduli. Examination of the three figures indicates that combining the rubblized material and the fractured concrete layers into one layer produces:

1. Insignificant errors in the backcalculated moduli of the AC layer (figure 5.9) and roadbed soil (figure 5.10) relative to the actual modulus values.

2. Significant error in the backcalculated base modulus when the base thickness is 4 in. and insignificant error when the base thickness is between 12 and 18 in. as shown in figure 5.11.

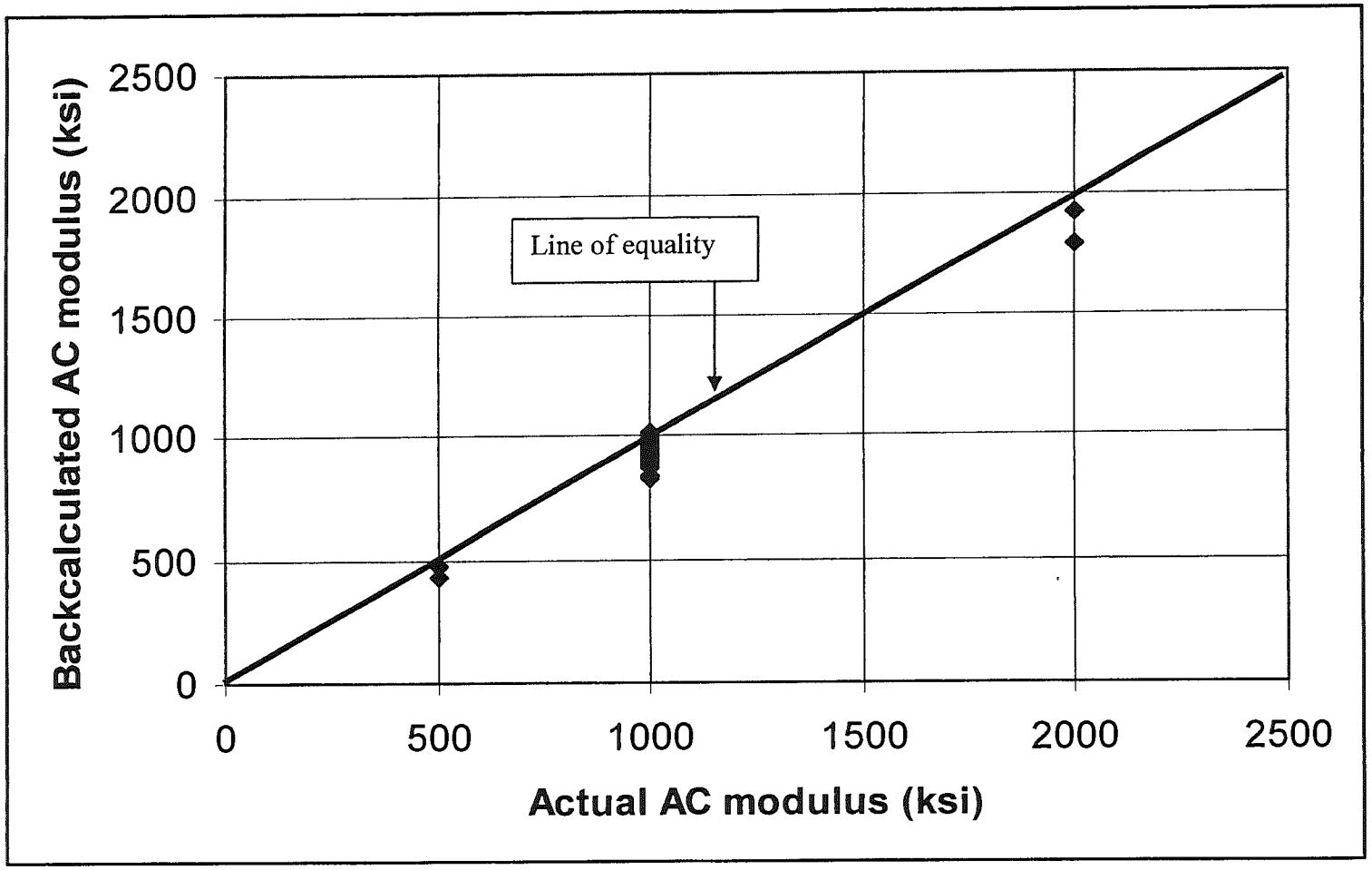

Figure 5.9 Backcalculated AC moduli when the rubblized and fractured concrete layers are combined as one layer

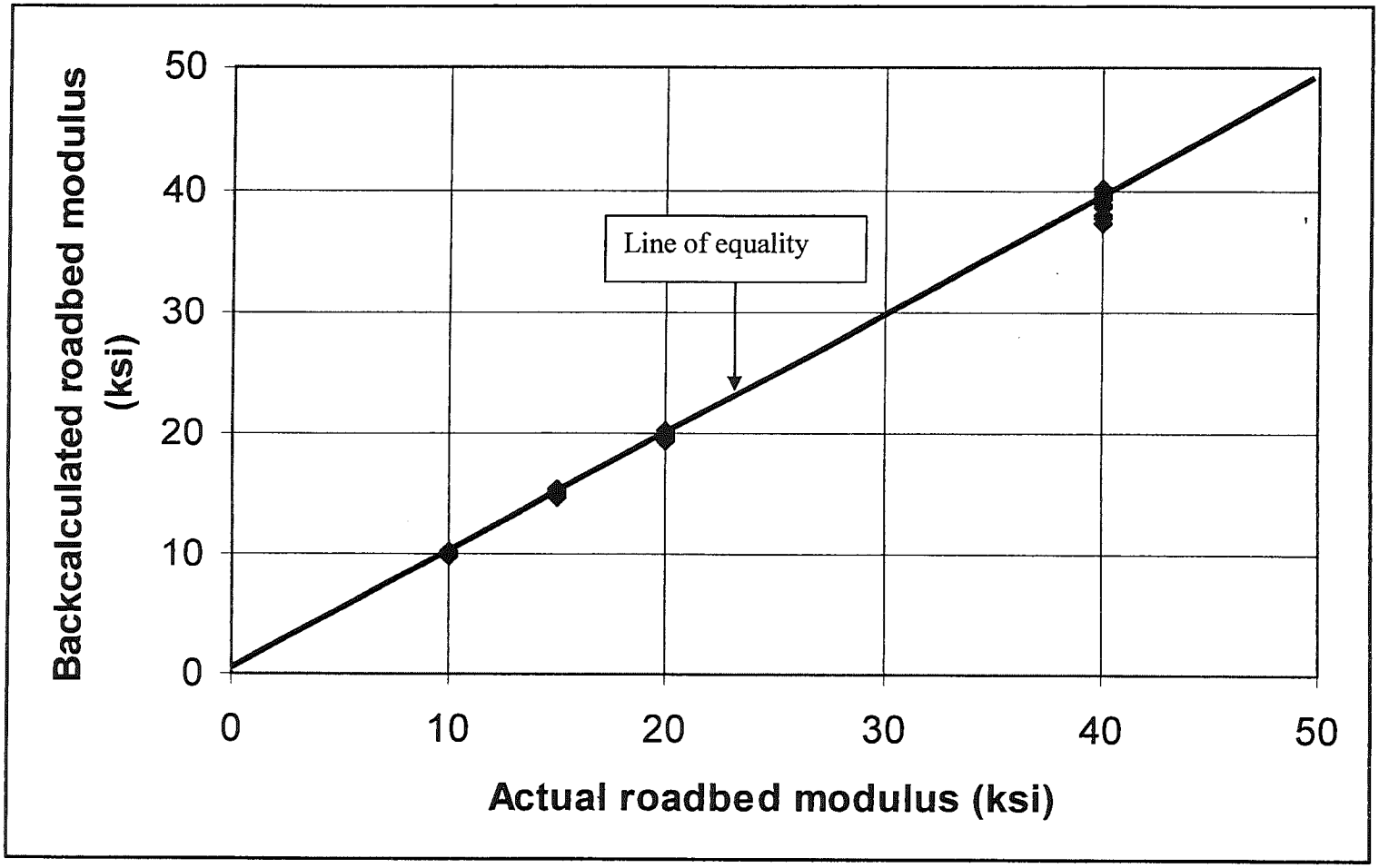

Figure 5.10 Backcalculated roadbed soil moduli when the rubblized and fractured concrete layers are combined as one layer

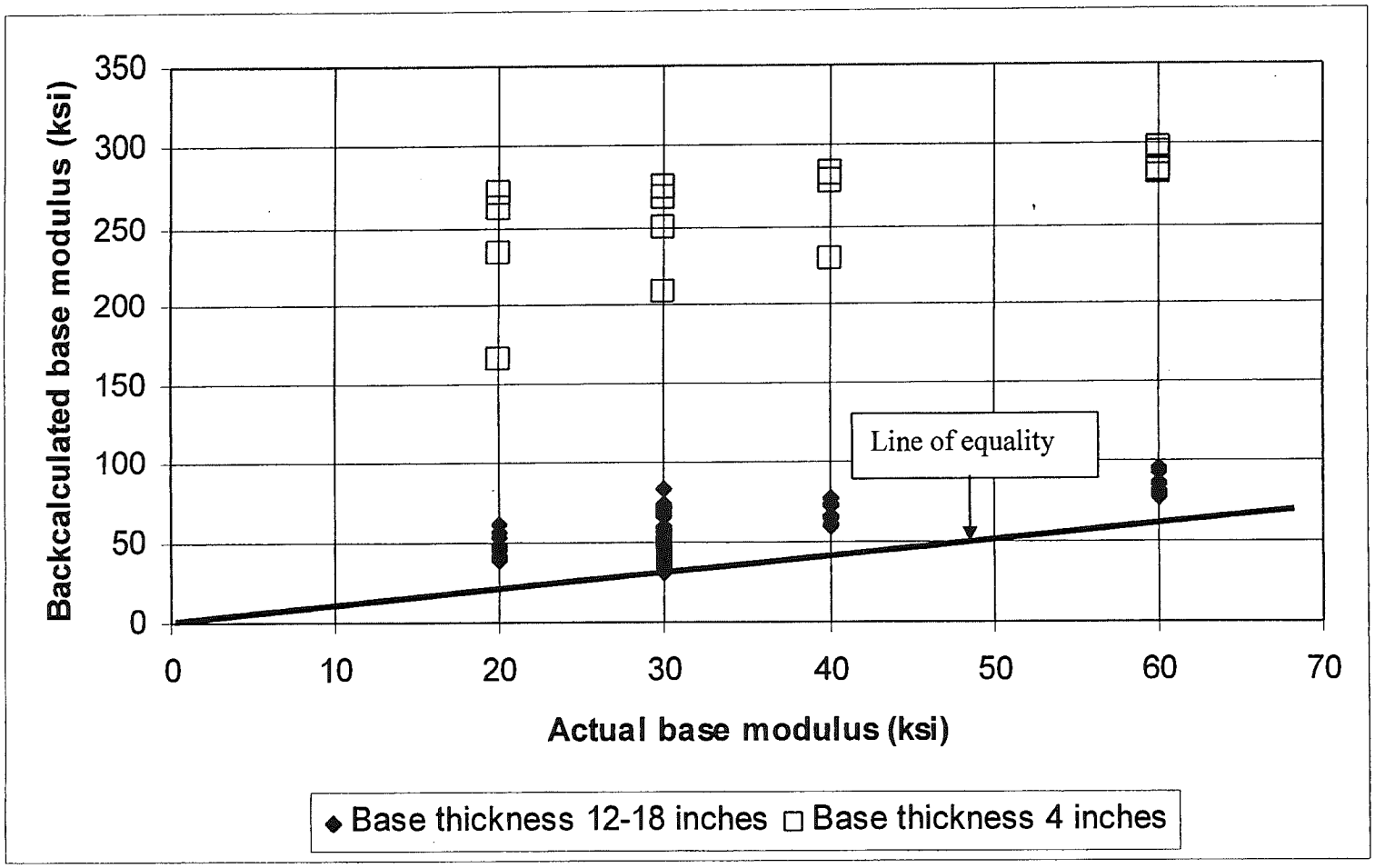

Figure 5.11 Backcalculated base moduli when the rubblized and fractured concrete layers are combined as one layer

A second backcalculation was also conducted using the 111 deflection basins where the rubblized material and the fractured concrete layers were handled separately and the thickness of each was assigned value of 4.5 in. The results of this backcalculation showed similar trends to those shown in figures 5.9 through 5.11. However, backcalculation of layer moduli based on the separation of the rubblized material and the fractured concrete layers cannot be extended to the measured deflection data for two reasons:

1. The high variability in the thickness of both layers.

2. For some pavement sections, the separation of the two layers makes the total number of layers more than five (AC, rubblized, fractured, base, roadbed and stiff layer). The reason is that the Chevronx computer program (which is the forward engine in MICHBACK) is limited to 5-layer systems.

For these two reasons, and for consistency, the backcalculation of layer moduli of all rubblized pavements were accomplished by combining the rubblized material and the fractured concrete layers into one layer.

Finally, the impact of variation in the thicknesses of the AC, rubblized material and fractured concrete layers on the backcalculated moduli of the AC and base layers and on the roadbed soil were also examined using forward and backward analyses. A total of twenty pavement sections having the material properties listed below were analyzed and the resulting deflection basins due to a 9000 lb load were calculated.

Properties	AC	Rubblized material	Fractured concrete	Base layer	Roadbed soil
Thickness (in.)	5.0	2.0	7.0	15.0	Infinite
	5.5	4.0	5.0		
	6.0	6.0	3.0		
	6.5	8.0	1.0		
	7.0				
Modulus (psi)	1,000,000	100,000	1,000,000	15,000	15,000
Poisson's ratio	0.3	0.4	0.2	0.45	0.45

The calculated deflection basins of the twenty pavement sections were then used to backcalculate the known layer moduli. In the backcalculation, the rubblized material and the fractured concrete layers were combined into one 9-in. thick layer. Further, an average AC thickness of 6 in., a base thickness of 15 in. and an infinite depth of the roadbed soil were used in the backcalculation. These and other layer properties (Poisson's ratio) and the average backcalculated layer moduli of the twenty pavement sections are listed below. For each layer used in the backcalculation, the percent error of each backcalculated layer modulus relative to the true modulus is also listed below.

Layer properties for backcalculation				
Properties	AC	Rubblized concrete slab	Granular base layer	Roadbed soil
Thickness (in.)	6.0	9.0	15.0	-
Poisson' ratio	0.3	0.3	0.4	0.45
Backcalculated layer moduli (psi)				
Average backcalculated moduli (psi)	902,265	203,470	16,180	14,697
Error (%)	9.77		7.86	2.02

Examination of the layer moduli used in the forward analyses, the average backcalculated layer moduli, and the percent errors listed above indicates that:

- The backcalculated moduli of the AC and base layers and the roadbed soil are not significantly affected by combining the rubblized material and the fractured concrete layers into one rubblized concrete slab layer. The percent error for the AC and base layers are less than 10 percent and for the roadbed soil is less than 2.5 percent.

- The average backcalculated AC modulus is not significantly affected by the variation in the AC thickness used in the forward analyses. Note that, for those locations where the true AC thickness was $\pm$ 1 in. from that used in the backcalculation, the backcalculated AC modulus values were significantly different than the actual values. However, the average backcalculated AC modulus value (the average of the twenty tests) was not significantly affected. The implication of this is that, in the field, the impact of variation in the AC thickness on the backcalculated results could be significantly decreased by increasing the number of FWD tests along a project and by using the average AC core thickness in the backcalculation.

- The backcalculated modulus of the rubblized concrete slab does not resemble the moduli of the rubblized material nor the fractured concrete layers. It represents the weighted average modulus of the two layers based on their space location and thickness.

The above observations are more or less similar to those reported earlier using the 111 forward analyses. Based on the analyses of the 131 pavement sections (111 + 20) presented above and the MDOT pavement design and construction practice (the thickness of the combined base and subbase layers for rigid pavement is 12 in. or more), the procedure of combining the rubblized material and the fractured concrete layers into one layer was adopted and used throughout the study. The results (the

backcalculated moduli of the AC and base layers and of the roadbed soil) were found, for most cases, to be acceptable. On the other hand, given the high variations in the thicknesses of the rubblized material and fractured concrete layers; the moduli of these two layers cannot be accurately backcalculated. Consequently, statistical procedures were developed in this study to estimate these moduli. The procedures are presented in section 5 of this chapter.

In the remaining parts of this report the combination of the rubblized material and the fractured concrete layers is termed "the rubblized concrete slab". The applicability of combining the rubblized material and the fractured concrete layers into one layer procedure to real deflection data is illustrated in section 6.0 of this chapter using the measured deflection data on I-75 SB, section 1, test sites 1 and 2.

4.1.3 The Granular Base Thickness

The impact of errors in the thickness of the aggregate base and sand subbase on the backcalculated layer moduli was also analyzed using forward and backward analyses. Since, for rubblized pavements the influence of the surface load on the base and subbase layers is small (they are separated from the load by the AC and the rubblized concrete slab), the impact of errors in their thicknesses was found to be insignificant. For example, variations in the aggregate base and sand subbase thicknesses of $\pm$ 2 in. yield less than ten percent error in the backcalculated layer moduli. Based on the results of the analyses, it was concluded that the thickness of the sand subbase and the aggregate base can be obtained from available cross-section records (pavement coring is not required). Note that the above scenario is not valid for conventional asphalt pavements because only the AC layer separates the aggregate base from the surface load.

4.1.4 The Roadbed Soil

In some locations in the State of Michigan, the roadbed soil consists of a thick sand deposit. At these locations, the original concrete slab was constructed either on top of the roadbed soils or on top of an aggregate base (minimum thickness of 4 in.) that was placed on top of the roadbed soil. Therefore, the pavement section was treated either as a 3-layer (AC and rubblized concrete slab layers situated on a roadbed soil) or as a 4-layer (AC, rubblized concrete slab, and base layers situated on a roadbed soil) system.

4.2 Backcalculation Parameters

In this section, the parameters used in the backcalculation of the layer moduli for the 18 rubblized projects are summarized.

Table 5.11 Typical pavement layer properties used in the backcalculation

Layers	Thickness/ (Source of data)	Poison's ratio	Seed moduli (ksi)	
			minimum	maximum
AC	Coring (inventory data)	0.3	30	4,000
Rubblized	4.5-in.	0.4	30	4000
Fractured	4.5-in.	0.2	30	10,000
Combination of rubblized and fractured	9.0-in.	0.3	30	4000
Conventional aggregate base	Drilling (inventory data)	0.4	10	200
Roadbed	Infinite or finite depth	0.40 (sand) 0.45 (clay)	1	100
Stiff layer depth	Infinite or finite depth	0.2	2,000	2,000

Table 5.12 Lab test moduli of various types of sand and clay (4)

Soil types	Modulus of elasticity (psi) min.-max.
Loose sand	1,500-3,500
Medium dense sand	2,500-4,000
Dense sand	5,000-8,000
Silty sand	1,500-2,500
Sand and gravel	10,000-25,000
Soft clay	600-3000
Medium clay	3,000-6,000
Stiff clay	6,000-14,000

4.2.1. Seed Moduli and Poisson's Ratio

Table 5.11 provides a list of Poisson's ratios and seed moduli used in the backcalculation of the layer moduli of all rubblized pavements. The table also provides some information regarding the layer thicknesses and the source from which the data can be obtained. It is strongly recommended that the AC thickness be verified through coring and the other layer thicknesses be obtained from the inventory data or from drilling. Finally table 5.12 provides a list of typical lab modulus values of various roadbed soils. The data in the table can be used as guidelines keeping in mind that the backcalculated modulus values are about three times higher than those reported in the table.

4.2.2. Convergence Control

The MICHBACK program allows the users to specify the parameters of the convergence control criteria. The values of the parameters used in this study for the backcalculation of layer moduli using 3- and 4-layer systems are listed below.

1. Calculate the gradient matrix after each two iterations
2. Maximum number of iterations is sixty
3. Modulus tolerance was set at 0.1 percent
4. The desired RMS tolerance was set at 0.1%
5. Precision of deflection entries 3 decimal places

Note that lower percent modulus an RMS tolerances yields more accurate solution but requires more iterations. Detailed information regarding the effect of each parameter on the results of the backcalculation can be found in MICHBACK user's manual (7).

4.3 The Number of Pavement Layers

The two typical rubblized pavement sections shown in figure 5.8 indicate that a rubblized pavement consists of either 4- or 5-layers situated on a roadbed soil. In addition, the density and modulus of the roadbed soil typically change with depth. In a multilayer elastic system, an infinite depth is assigned to the last layer (the roadbed soil). Hence, the modulus of the roadbed soil is explicitly assumed as constant throughout its depth. This creates errors in the backcalculated layer moduli. To overcome the problem, a stiff layer is typically placed at certain depth below the pavement surface and the layer moduli are backcalculated (for more detail see the next section). Such placement is problematic in that the depth to stiff layer and its properties (modulus and Poisson's ratio) are not known. In addition, for MICHBACK, the inclusion of stiff layer increases the total number of layers beyond the capability of the chevron-5 program. Consequently, some layers must be combined to reduce the total number of layers to 5 or less.

The first layer combination (addressed in section 4.1.2) is that of the rubblized material and the fractured concrete layers. The two layers cannot be separated mainly because the

thickness of each layer is unknown and may vary from zero to 9 in. within the deflection basin. Typically the original base (if it exists) and subbase of the old concrete pavement are also combined as one layer in the backcalculation to reduce the number of the pavement layers. The combination of the base and subbase into one layer, on one hand, and that of the rubblized material and fracture concrete layers, on the other hand, reduce the total number of layers including the roadbed soil to 4 or 5 as follows:

1. AC layer
2. Rubblized concrete slab (a combined layer of the rubblized material and fractured concrete layers)
3. Base (a combined layer of base and subbase layers)
4. Roadbed soil
5. A stiff layer (optional)

The backcalculation was then performed using 4-layer system (AC, rubblized concrete slab, and combined base and subbase layers, and roadbed soil) with an option to incorporate a stiff layer at certain depth. Further, as stated in the previous section, in certain scenarios, based on available information in the inventory data, the base and subbase layers and the roadbed soil were combined into one layer. Hence, for such scenario, a 3-layer system was used with the option of incorporating a stiff layer at certain depth.

Note that in the MICHBACK computer program, the stiff layer is not counted as a layer while it is counted in the chevron-5 program. For example, if a 4-layer system is specified in MICHBACK and if a stiff layer is incorporated, the total number of layers to be analyzed by the chevron-5 program is 5.

From this point forward, the number of layers used in the backcalculation will be counted in accordance with the MICHBACK computer program.

To summarize, the backcalculation of layer moduli must be based on the measured deflection data and on accurate information regarding the pavement cross-section specifically the top pavement layers. Given the lack of such information relative to the rubblized material and fractured concrete layers, the two layers must be combined to backcalculate the moduli of the roadbed soil and the AC layer. When accurate information are available regarding the base, subbase and the roadbed soil, two or more of these materials could be combined into one layer and the backcalculation could be accomplished based on 3 or 4-layer systems. The exact number of layers to be used in the backcalculation depends not only on accurate information but also on the possible incorporation of a stiff layer. These and other issues are addressed in detail in the next section along with some examples.

4.4 Depth to Stiff Layer

As stated earlier, most backcalculation software typically use mechanistic-based layer analysis routines to calculate stresses, strains and deflections induced in a given pavement section with known properties due to an applied load. For example, the MICHBACK software uses the Chevronx computer program (5-layer linear elastic program) as the forward

engine to calculate pavement deflections. Like other two dimensional mechanistic programs, the chevronx algorithm is based on the assumption that the last layer (the roadbed soil) is semi-infinite. Therefore the calculated strain in that layer is integrated over an infinite depth while in reality, the load induced-stresses and strains in most pavement sections dissipate to insignificant values within few feet from the pavement surface. For this reason, most backcalculation software including the MICHBACK were designed to allow the users to place a stiff layer at a certain depth below the pavement surface. Such placement is problematic in that, if the estimated depth to stiff layer is incorrect, it produces errors in the backcalculated layer moduli. For example, for a 4-layer system, if the depth to stiff layer is erroneously estimated at 400 in. rather than the true 200 in. then the backcalculated roadbed and base moduli could be as high as70 percent and the error in the AC modulus could be of the order of 10 percent. The error in the backcalculated AC modulus could be more significant for a 3-layer system.

In most cases, the actual depth to stiff layer (the depth at which the load-induced stresses and strains are zero) is not known. Therefore, a depth to stiff layer is typically assumed. The problem with such an assumption is that there is a wide range of depths to stiff layer that existing backcalculation software including the MICHBACK could successfully produce layer moduli to closely match the measured deflection basin. The question becomes which set of modulus values are correct. For certain pavement sections where concrete culvert and/or cross-drains can be found, the depth to stiff layer must be specified to match the vertical distance between the pavement surface and the top of the culvert. In some others, where deep deposit of soft layer is encountered, no stiff layer needs to be included. The important point is that relatively accurate information regarding the original soil strata and the under pavement structures would assist a great deal in estimating the depth to stiff layer. Such information could be obtained from soil maps published by the Soil Conservation Service of the U.S. Department of Agriculture. When such information is lacking, a trial and error method must be used where the layer moduli are backcalculated using various depths to stiff layer and the resulting modulus values are selected based on engineering criteria and judgment.

So the first step needs to be taken is to answer the question "is there a need to incorporate a stiff layer?" The answer to this question can be easily obtained with the help of Boussinesq equivalent modulus procedure (8). In this procedure, the pavement is treated as a one layer system and the modulus of that layer is calculated using equation 5.1:

$$E = \frac{P\left(1-\upsilon^2\right)}{\pi(r)\left(d_r\right)} \qquad (5.1)$$

Where
E = modulus
P = applied load = 9000 lb for the normalized deflection file
υ = Poisson's ratio (assume 0.4)
R = radial distance from the center of the load (in.)
d_r = deflection at distance r from the center of the load (in.)

To determine whether or not a stiff layer should be incorporated, do the following steps"

1. Calculate E for each deflection sensor location excluding the center sensor.

2. Plot the calculated E versus the distance from the loaded area (the distance between the center of the load plate and the deflection sensor in question).

3. The E versus distance curves will have three possible shapes as follows:

   a) If the modulus "E" decreases with distance and then it increases (see figure 5.12), a stiff layer should be incorporated. Higher rates of increasing modulus imply shallower depths to stiff layer.
   b) If the modulus decreases with distance until it reaches almost a constant value, the stiff layer is about 400 in. deep.
   c) If the modulus continuously decreases with distance; the stiff layer is more than 500-in. deep or there may not be any stiff layer.

The above three scenarios are illustrated in figure 5.12. It can be seen that the shape of the curve changes with depth to stiff layer.

Next, one needs to determine the depth to stiff layer using a trial and error procedure. To illustrate such a procedure, three pavement sections were established. Each section consists of a 3-layer system; AC, rubblized and base, supported on roadbed soil and a stiff layer located 300 in. below the pavement surface. In each section, the base and roadbed soil were assigned equal modulus values of 30,000, 20,000 and 10,000 psi. The three sections were analyzed and the pavement deflections due to a 9,000-lb load were calculated. The calculated deflection and the pavement layer thicknesses were then used to backcalculate the layer moduli using variable depths to stiff layer and 3- and 4-layer systems. The 3-layer system consisted of AC and rubblized concrete slab layers situated on roadbed soil while the 4-layer system consisted of AC, rubblized slab and base layers situated on roadbed soil. A stiff layer was incorporated in both systems. The results of the backcalculation for the 20,000 psi base and roadbed modulus are shown in figures 5.13a, 5.13b and 5.13c. The figures depict each backcalculated modulus obtained by using 3 (closed symbols) and 4 (open symbols) layer systems and for different depths to stiff layer. Examination of the figures indicates that:

1. The backcalculated layer moduli vary significantly with the assumed depth to stiff layer except the modulus of the AC, which is the least sensitive to the depth to stiff layer.

2. Backcalculation of layer moduli using 3 and 4 layer systems produce different results for all depths to stiff layer except for the true depth of 300 in.

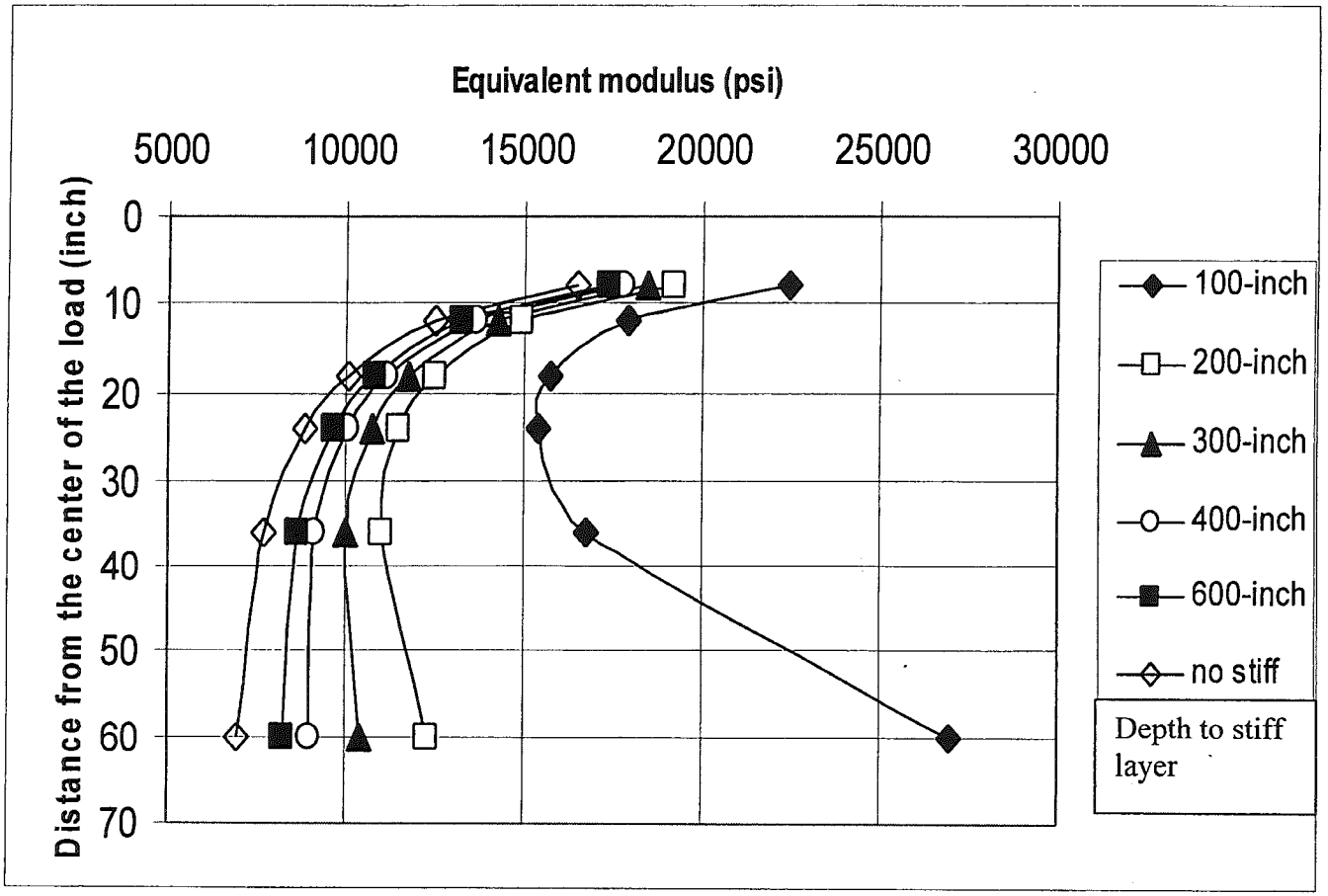

Figure 5.12 Equivalent moduli as function to the deflection sensor locations (Boussinesq procedure) for various depths to stiff layer

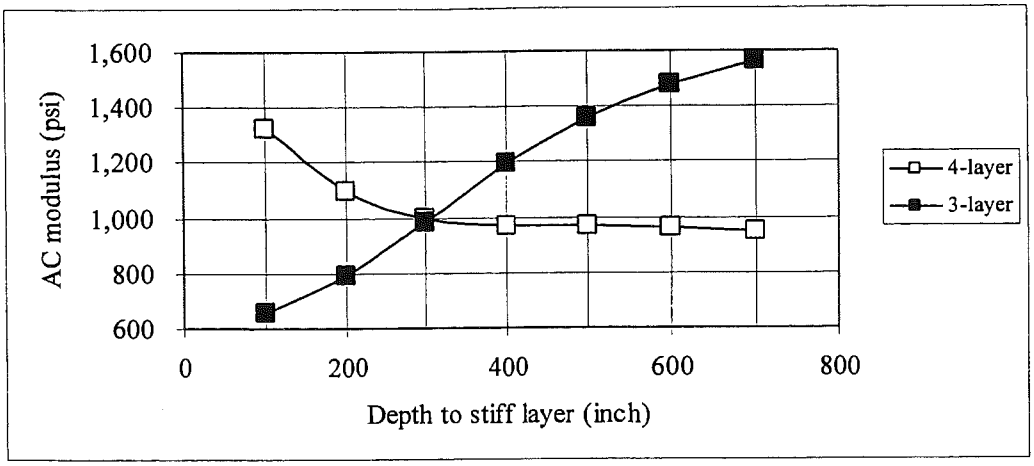

a) AC modulus (psi)

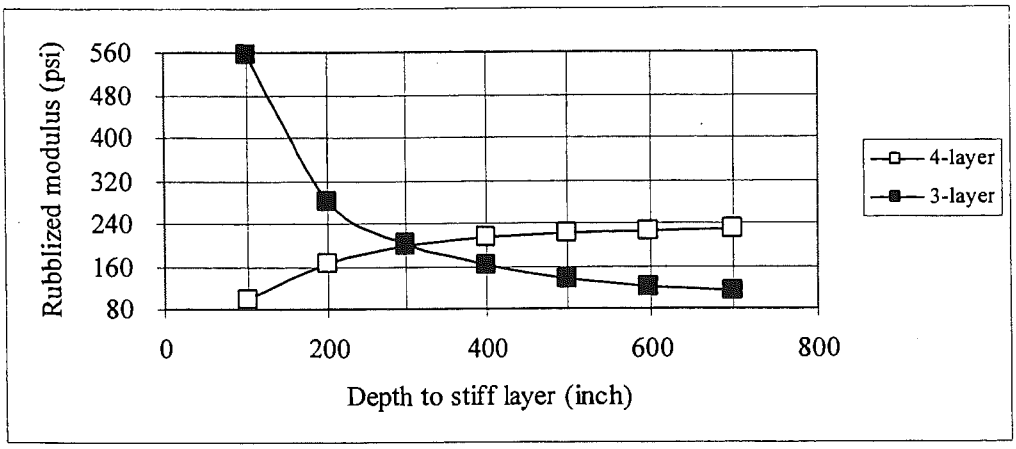

b) Rubblized modulus

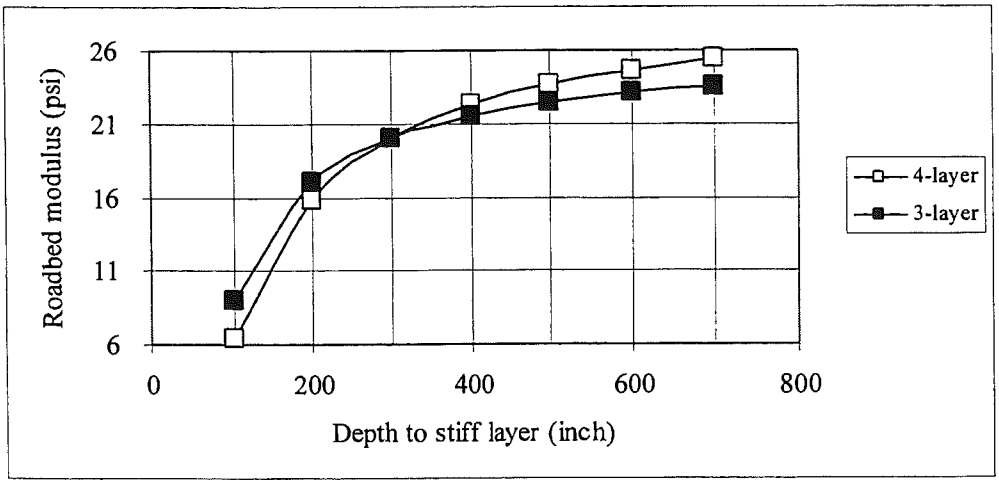

c) Roadbed modulus

Figure 5.13 Backcalculated layer moduli using 4 and 3 layer systems versus depth to stiff layer

3. At the true depth to stiff layer of 300 in., the backcalculated layer moduli (AC, rubblized concrete slab and roadbed) obtained from 3- and 4-layer systems are equal (the two curves intersect).

4. At a stiff layer depth of 300 in., all the backcalculated modulus values are within a fraction of one percent of their true values.

Recall that the forward analyses were conducted using equal modulus for the base and roadbed soil. For this case, the above findings can also be made by examination of figure 5.13. The figure shows the backcalculated base and roadbed modulus using a 4-layer system as a function of the depth to stiff layer. It can be seen that the two moduli are equal only at the true depth to stiff layer of 300 in.

The significance of figure 5.14 is that the figure can also be used to estimate the depth to stiff layer when the modulus of the roadbed soil is not equal to the modulus of the base layer. For such pavement layers, the curves representing the moduli of the base and roadbed soil as functions of the stiff layer depth will also intersect. On one side of the intersection, the base modulus will be lower than that for the roadbed soil. Since for most pavements the opposite is true (the base modulus is higher than that of the roadbed soil), then the true depth to stiff layer is within the region defined by the two curves where the modulus of the base is higher than that of the roadbed soil.

The above example illustrates that although the backcalculated modulus values were obtained based on trial and error (different depths to stiff layer), the true values can be obtained by a careful examination of the results. The application of the above and other procedures (the effects of the accuracy of layer thicknesses and the number of pavement layers) to measured pavement deflections are presented in the next section.

Figure 5.15 shows the results of the 30,000 and 10,000 psi base and roadbed moduli. It can be seen that the figure shows similar trends to those shown in figure 5.13. Finally, regardless of the procedure used to estimate the depth to stiff layer, the values of the backcalculated moduli must be scrutinized using engineering judgment. In this endeavor, three steps can be used as follows:

1. The variation in the backcalculated moduli should be the mirror image of the variation in the measured deflection. Such variations reflect the variability of the structural capacity of the pavement. For some pavement sections, the backcalculated layer moduli could vary as much as 100 percent along and across the pavement. For some others, this variation could be as low as 10 percent. In general, variations in the measured pavement deflections could be the direct results of:

   a) Variations in the layer thicknesses especially the AC, the rubblized material and the fractured concrete layers.
   b) Variations in the density/air voids of the compacted asphalt mat that may be caused by temperature and/or particle segregation.

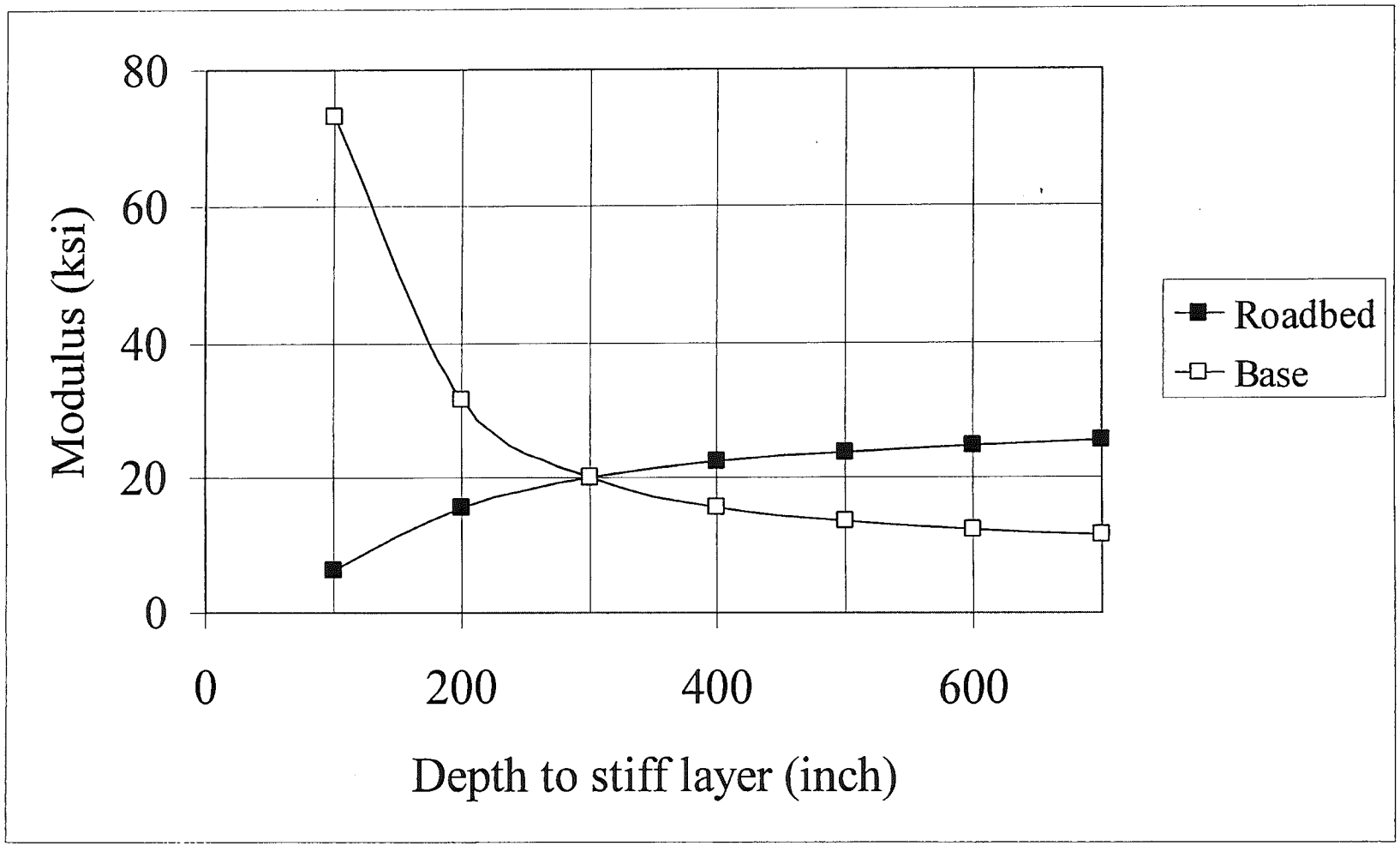

Figure 5.14 Backcalculated roadbed and base modulus using 4-layer system

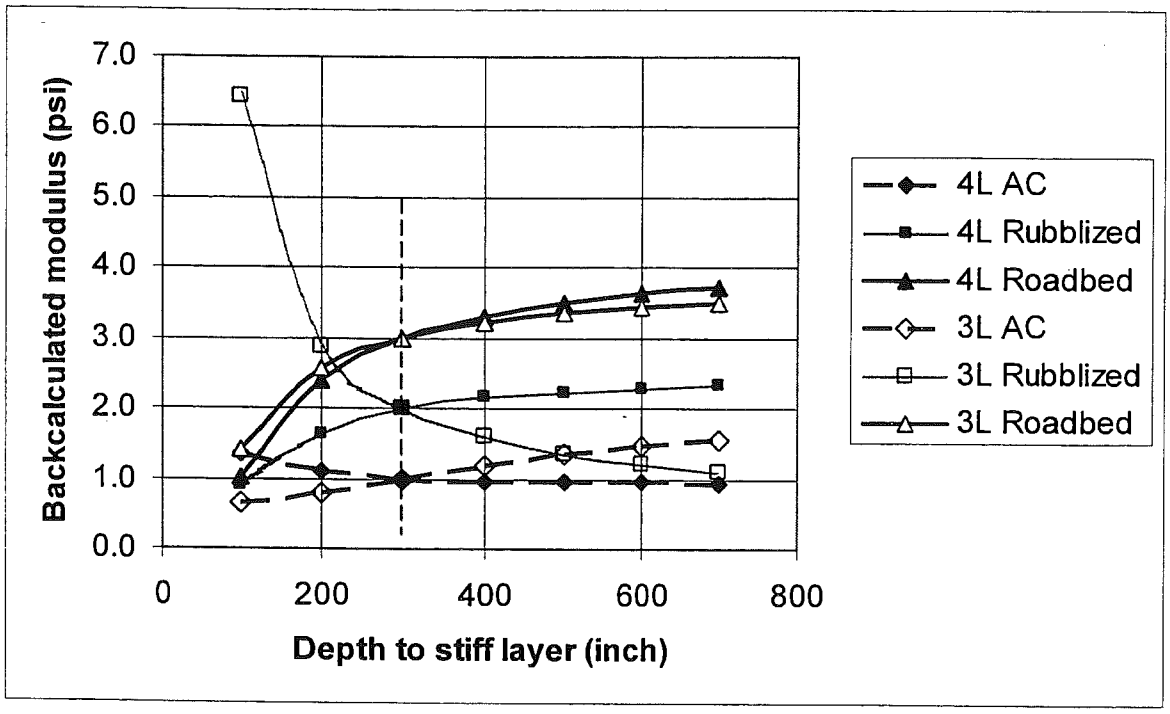

a) Base and roadbed moduli of 30,000 psi

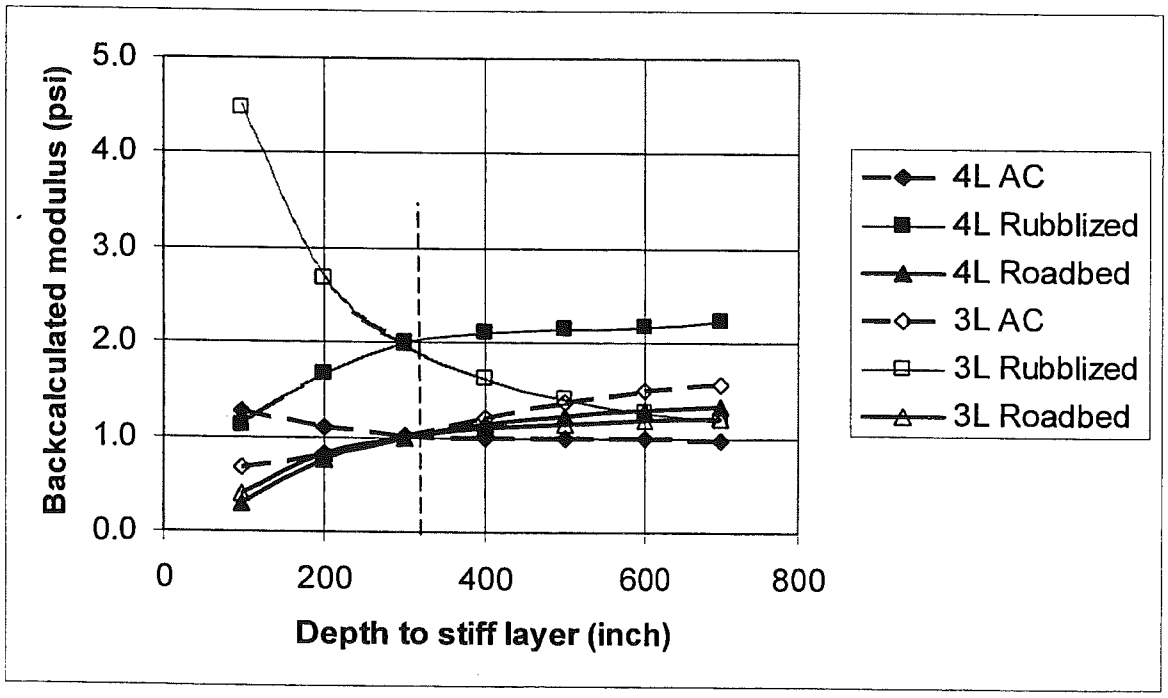

b) Base and roadbed moduli of 10,000 psi

Figure 5.15 Backcalculated modulus (AC $*10^6$, rubblized concrete slab$*10^5$, and roadbed $*10^4$) of 3 pavement sections with actual depth to stiff layer of 300 in.

2. The values of the backcalculated roadbed soil moduli should be reasonable. The data listed below could be used as guidelines for acceptance. Note that these values are based on laboratory tests, backcalculated moduli are typically much higher than those listed below.

Material	Modulus (psi)	
	Low	High
Clay	1,800	42,000
Sand	4,500	24,000

Further, the AASHTO Design Guide provides the following equation, which was derived from the Boussinesq equation by assuming a value of Poisson's ratio of 0.5, for estimating the modulus of the roadbed soil.

$$MR = \frac{0.24 * P}{D_r * r} \qquad (5.2)$$

Where

MR = estimated roadbed soil modulus (psi)
P = applied load (lb)
r = radial distance from center of load (in)
D_r = deflection at the radial distance "r" (in)

It is highly recommended that measured deflection at distances of 50 in. or more from the center of the FWD load plate be used in the above equation. Further, the ASHTO Design Guide recommends that the roadbed modulus to be used in design be one third the backcalculate value.

3. Plots of the backcalculated roadbed modulus and the inverse of the measured outer sensor deflection along a project (see figure 5.16) should overlap.

5.0 THE MODULI OF THE RUBBLIZED MATERIAL AND FRACTURED CONCRETE LAYERS

As previously noted, a rubblized concrete slab can be divided into two distinctive layers; rubblized and fractured concrete layers. The insitu modulus of the rubblized and fractured concrete layers are very difficult or almost impossible to backcalculate from the measured deflection data. The reasons include:

1. The extreme variations in the thicknesses of the rubblized material and the fractured concrete layers.

2. The uneven interface between the rubblized material and the fractured concrete layers.

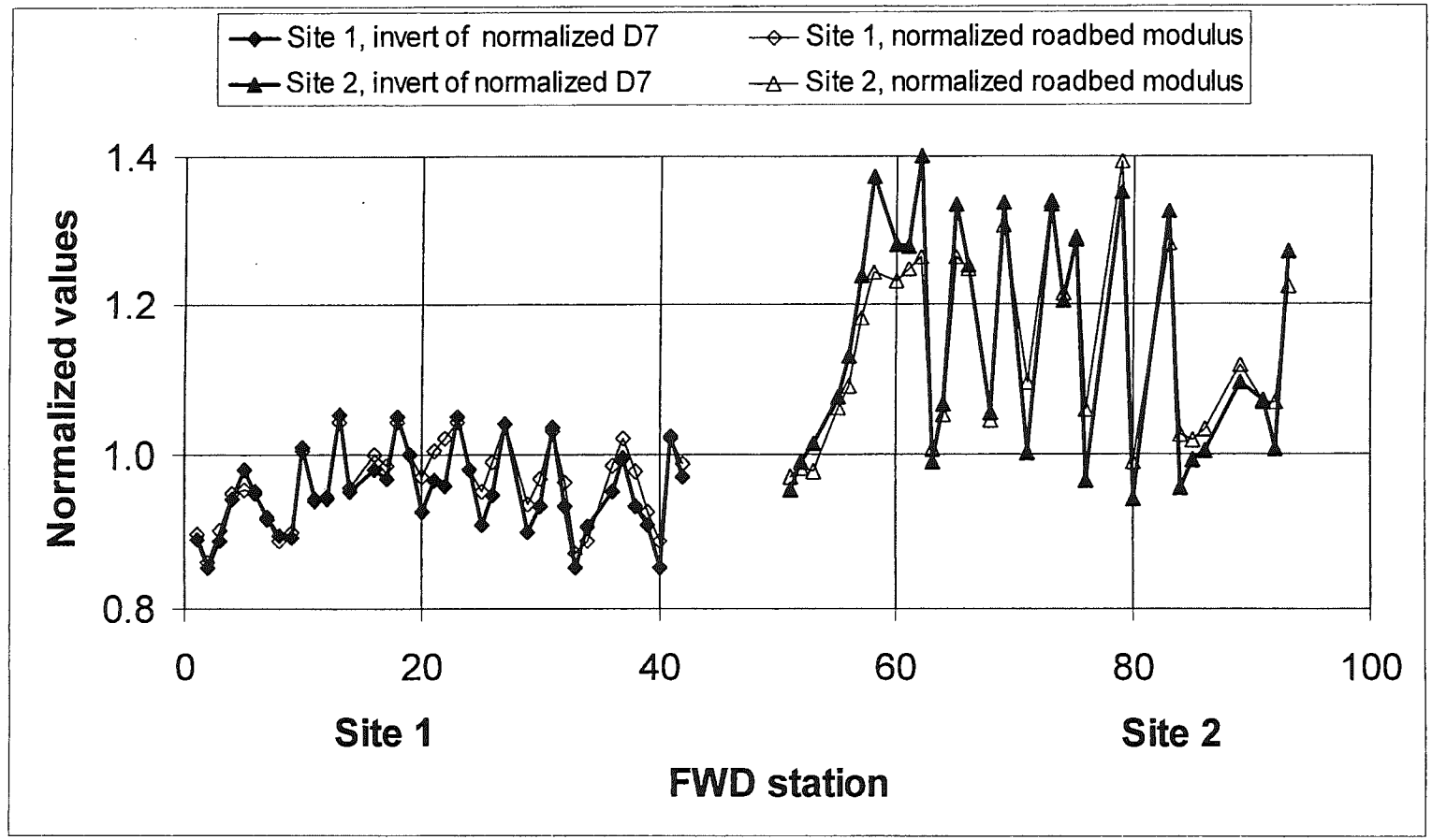

Figure 5.16 Normalized roadbed moduli and the invert of normalized D7 deflection at various test stations along I-75 SB, section 1, test sites 1 and 2

3. The random distribution of the crack network in the fractured concrete layer.

4. The number of rubblized material pieces larger than 6 in.

Because of these, the rubblized material and the fractured concrete layers were combined into one 9-in. thick layer (the rubblized concrete slab) and its modulus was backcalculated using the measured deflection data. It was shown in subsection 4.1.2 of this chapter that the combination of the rubblized material and the fractured concrete layers had no impact on the accuracy of the AC, base and roadbed soil moduli when the base is thicker than 12-in. Unfortunately, no procedure was found to verify the accuracy of the backcalculated modulus of the rubblized concrete slab.

Also as stated in section 4.1.2, a statistical equation (equation 5.3) was developed to estimate the modulus of the rubblized material layer. The equation is based on the backcalculated AC and roadbed soil moduli and on the measured deflection data. After estimating the modulus of the rubblized material, the modulus of the fractured concrete layer was estimated using equation 5.4. The latter equation is based on the mechanics of stress dissipation through the pavement structure and the relative geometry of the rubblized material and the fractured concrete layers.

$$E_{rubb} = (0.001*F_1/F_2) / (F_4* (1.055*F_3^{-1.5262}) * F_2^{2.22}/F_3^{0.15}) \quad (5.3)$$

$$E_{fract} = (E_{RCS}*9-4.5* E_{rubb}) / (4.5*((T_1+0.25*9)/(T_1+0.75*9))) \quad (5.4)$$

where

E_{rubb} = Estimated rubblized material modulus (ksi)
E_{fract} = Estimated fractured concrete modulus (ksi)
E_{RCS} = Backcalculated modulus of the rubblized concrete slab (ksi)
F_1 = Stress in rubblized concrete slab (psi)
$= 82*((5.91/(5.91+0.95*T_1))^2)*2.4*F_3^{0.1}$
F_2 = Compression in rubblized concrete slab (in.)
$= (0.8*\delta_1-(T_1*0.082*(5.9/(5.9+1.7*T_1/2))^2)/E_{AC})/(-0.002289*T_2+0.823492+\delta_2/10)$
F_3 = Compression in AC (in.)
$= T_1* (5.91/(5.91+T_1*0.7))^2*82/(E_{AC}*1000)$
F_4 = $(0.0632*T_1+0.7628)*(0.0128*T_2+0.7505)$
T_1 = AC thickness (in.)
T_2 = Base thickness (in.)
δ_1 = D1-D2 (in.)
δ_2 = D6-D7 (in.)
E_{AC} = Backcalculated AC modulus (ksi)

Note that both equations 3 and 4 were developed based on the assumption that the thickness of the rubblized material and the fracture concrete layers are 4.5 in. When the actual thickness of the rubblized material is more than 4.5 in., equation 3 will yield lower estimates of the modulus relative to the actual modulus. The inverse is also true, that is, when the actual thickness of the rubblized material is less than 4.5 in., equation 3 will yield higher

estimates. Since the actual thicknesses of the rubblized material and the fractured concrete layers vary along and across the pavement from 0 to 9 in., their estimated moduli using equations 3 and 4 will also vary substantially from one point to another. To overcome this problem, the thicknesses of the two layers were measured in more than thirty trenches that were excavated during the rubblization operation. It was found that the average thickness of each layer is about 4.5 in. and that the average thickness varies only slightly from one project to another. Consequently, the modulus of the rubblized material and the fractured concrete layers were estimated using two averaging methods as follows:

Individual-Average – In the first step of this method, the moduli of the rubblized material and the fractured concrete layers were estimated for each accepted individual FWD test location using equations 3 and 4. In the second step, the average of the estimated moduli and their coefficients of variation were calculated.

Average-Average - In the first step of this method, for each test site, the average deflection and the average backcalculated AC and roadbed soil moduli for all accepted FWD test locations were calculated. In the second step, the average moduli of the rubblized material and the fractured concrete layers were estimated using equations 3 and 4 and the above averages.

Examination of the estimated moduli of the rubblized material and the fractured concrete layers using the two methods indicate that:

1. The individual-average method yielded unreasonable estimated modulus values of the fractured concrete layer at few FWD test locations, which substantially affected the estimated average modulus. Further, the estimated moduli of the rubblized materials and the fractured concrete layers were highly variable. For example, some individual modulus values of the fractured concrete layer at few test sites were higher than the modulus of concrete of 4,000,000 psi and the coefficient of variation was very high. The main reason for this is the high variability in the thicknesses of the two layers. The thickness of each layer may vary from 0 to 9 in. along and across the pavement.

2. The average-average method produced reasonable modulus values of the fractured concrete such that the forwarded calculated deflection basins using these and the average backcalculated layer moduli closely simulate the measured deflection basins. Further, the advantage of this method is that the impact of the variability of the thicknesses of the rubblized material and the fractured concrete layers is minimized. The reason is that, on average, the thickness of each layer is about 4.5 in.

Based on these observations, it was decided to adopt the average-average method. Table 5.13 provides a list of:

1. The test site designation number (a total of 18 FWD test sites were included in this study).

2. The number of FWD tests that were conducted at each test site.

Table 5.13 Backcalculated and estimated pavement layer moduli of 18 rubblized pavement test sites

Test site	No of FWD stations			Backcalculated moduli (ksi)					Estimated moduli (ksi)	
	Total	Converged	Accepted	AC	TCAC	RCS	Base	Roadbed soil	Rubblized material	Fractured concrete
10692-11	40	40	39	317	534	122	25	14	65	256
10692-12	40	40	40	295	573	159	29	17	73	352
10753-11	42	39	34	1,732	1,297	225	[illegible]	17	27	704
10753-12	43	31	20	2,104	1,701	182	[illegible]	19	14	600
11941-21	36	36	27	1,567	1,468	225	44	23	201	360
11941-22	43	42	20	1,247	1,500	182	37	21	144	322
20102-11	40	40	39	710	1,640	61	27	16	44	119
20102-12	40	40	35	517	1,657	46	23	16	31	92
20233-11	52	51	51	433	1,484	50	34	10	15	135
20233-12	26	26	25	150	743	114	29	9	46	287
20273-21	45	41	35	1,891	2,285	117	36	21	24	350
20273-31	40	40	29	470	936	55	17	13	36	109
20273-41	40	39	31	237	608	1,064	50	22	297	2,774
20311-11	40	40	35	637	1,620	414	40	22	191	949
30153-11	43	42	31	2,364	2,165	71	37	20	28	183
30373-51	40	40	35	411	1,192	275	31	16	179	561
30373-52	40	39	38	392	1,407	134	25	15	67	307
30373-61	33	26	17	2,126	2,337	234	38	16	90	592
Minimum				150	534	46	17	9	14	92
Maximum				2,364	2,337	1,064	50	23	297	2,774

TCAC = Temperature corrected asphalt concrete, RCS = Rubblized concrete slab

3. The number of FWD test locations for which the backcalculation of layer moduli routine successfully converged.

4. The backcalculated layer moduli of the AC, rubblized concrete slab and base layers and the roadbed soil.

5. The temperature corrected AC modulus and the design AC modulus (temperature corrected minus two standard deviations).

6. The estimated moduli of the rubblized material and the fractured concrete layers using equations 3 and 4.

The modulus values listed in table 5.13 were used to arrive at the recommended design values. This and other design issues such as the AASHTO layer coefficients are presented in Chapter 6. The applicability of equations 3 and 4 to measured deflection data and discussion of the results are presented in the next section.

6.0 DETAILED EXAMPLE OF BACKCALCULATION OF I-75 SB SECTION 1, TEST SITES 1 AND 2

One of the rubblized pavement projects is located in a rolling terrain in the northern part of the lower peninsula of Michigan along SB I-75 just north of the I-75 and US 31interchange. The original soil consists of Roscommon muck and a deep deposit of poorly drained highly permeable Battlefield sand with gravel. Prior to construction of the original rigid pavement, the muck was excavated and replaced with Battlefield sand, which was compacted to specifications. On site, a seasonal (autumn to spring) high water table exists at a depth of about 0.5 to 1.5 feet from the original ground level. The cross-section of the original concrete pavement consisted of the following layers:

- Nine-in. rubblized JRCP
- Four-in. 22A base
- Four-in. 23A subbase
- Ten-in. class II aggregate subbase

The concrete pavement was rubblized in 1988, and it was capped by an asphalt layer whose thickness varies from 3.5 to 4.8 in.

A test section was selected on the south bound of I-75 about 0.5 miles north of the I-75 and US 31 interchange. Two 100-ft long test sites were marked along the test section such that the two sites were separated by 100-ft. At each test site, FWD tests were conducted and pavement cores were extracted in 2001. The average core thickness for test site 1 was 4.5 in. and for test site 2 was 4.1 in. The measured deflection data were then used to backcalculate the layer moduli using the procedure outlined above. Details of the backcalculation are presented in the next subsections.

6.1 Stiff Layer - Boussinesq Equation

In order to determine whether or not a stiff layer should be incorporated in the backcalculation, the Boussinesq equation (repeated here for convenience) was used to calculate an equivalent modulus.

$$E = \frac{P\left(1-\upsilon^2\right)}{\pi(r)\left(d_r\right)} \qquad (5.1)$$

Where E = equivalent modulus
P = applied load = 9000 lbs for the normalized deflection file
υ = Poisson's ratio (assume 0.4)
R = radial distance from the center of the load (in.)
d_r = deflection at distance r from the center of the load (in.)

For each test site, three sets of measured deflection data were selected and for each set, the measured data at each deflection sensor and the Boussinesq equation were used to calculate the equivalent moduli. The results are plotted in figure 5.17. Examination of the figure and comparing it to figure 5.12 indicate that; for test site 1, the calculated equivalent modulus decreases to almost an asymptotic value with increasing distance from the center of the load whereas it decreases and then increases for test site 2.

The two observations imply that a stiff layer should be incorporated in the backcalculation of layer moduli and that the stiff layer for test site 1 is deeper than that for test site 2. The latter finding was confirmed through field investigation. Because of the hilly terrain, test site 1 is located entirely in a 4- to 5-ft deep fill area (after about 4 to 5 ft of muck was removed) while the fill at test site 2 is about 1 ft. That is the original battlefield sand at test site 1 is about 7 ft below the existing pavement surface and at about 3 ft at test site 2. Having determined that a stiff layer should be incorporated into the backcalculation of layer moduli, the next step is to determine the actual depth to stiff layer for both test sites. This was accomplished by comparing the results of the backcalculation obtained by using 3- and 4-layer systems as presented below.

6.2 Depth to Stiff Layer

After scrutinizing the cross-section information of the rubblized pavement on SB I-75, it was assumed that the base and the two subbase layers have similar modulus and therefore they could be combined into one 18-in. thick layer. Hence the backcalculation could be conducted using 4-layer system (AC, rubblized concrete slab, subbase, and roadbed soil) and a stiff layer. Alternatively, the deep gravelly battlefield sand subgrade could also be combined with the base and subbase material and the backcalculation could be conducted using 3-layer system (AC and rubblized concrete slab layers situated directly on roadbed soil) and a stiff layer. The average backcalculated layer moduli of the 4- and 3-layer systems

Table 5.14 Backcalculated layer moduli using 4-layer system with different depths to stiff layer, I-75 SB section 1 test site 1

Depth to stiff layer (in.)	Number of stations converged	Average moduli (psi) and coefficients of variation								Average RMS (%)
		AC	CV (%)	Rubblized	CV (%)	Base	CV (%)	Roadbed	CV (%)	
150	35	1,983,950	46	204,385	103	40,924	70	10,612	8	0.49
200	37	1,948,166	48	223,162	98	30,183	72	13,601	9	0.49
250	37	1,852,974	49	239,186	94	23,018	51	15,702	11	0.49
300	**37**	**1,792,123**	**49**	**249,483**	**91**	**19,699**	**44**	**17,210**	**12**	**0.49**
350	37	1,758,721	49	255,885	90	17,872	42	18,334	13	0.50
400	37	1,744,236	49	259,716	88	16,722	42	19,203	14	0.50
500	38	1,787,859	50	257,718	89	19,590	138	20,359	15	0.52

Table 5.15 Backcalculated layer moduli using 3-layer system with different depths to stiff layer, I-75 SB section 1 test site 1

Depth to stiff layer (in.)	Number of stations converged	Average moduli (psi) and coefficients of variation								Average RMS (%)
		AC	CV (%)	Rubblized	CV (%)	Base	CV (%)	Roadbed	CV (%)	
150	14	1,216,576	24	435,999	46			12,240	6	2.26
200	32	1,407,587	36	298,240	76			14,754	6	1.71
250	38	1,606,831	43	248,394	73			16,143	5	1.28
300	**39**	**1,778,413**	**40**	**218,816**	**72**			**17,042**	**5**	**1.05**
350	37	1,986,909	39	176,534	67			17,750	5	0.96
400	39	2,147,277	40	162,832	67			18,227	5	1.01
500	36	2,295,899	37	136,458	73			18,983	5	1.01

CV (%) = Coefficient of variation = standard deviation divided by average

Table 5.16 Backcalculated layer moduli using 4-layer system with different depths to stiff layer, I-75 SB section 1 test site 2

Depth to stiff layer (in.)	Number of stations converged	Average moduli (psi) and coefficients of variation								Average RMS (%)
		AC	CV (%)	Rubblized	CV (%)	Base	CV (%)	Roadbed	CV (%)	
150	39	1,873,089	55	163,702	58	34,576	35	13,024	14	0.53
200	41	1,799,901	57	186,045	54	26,623	40	16,343	13	0.60
250	**41**	**1,685,368**	**58**	**201,607**	**52**	**22,858**	**43**	**18,630**	**13**	**0.61**
300	42	1,674,405	59	209,546	51	20,776	43	20,290	12	0.63
350	42	1,638,025	60	215,912	50	19,378	44	21,494	12	0.65
400	42	1,620,314	60	220,111	50	18,412	44	22,417	13	0.67
500	42	1,609,033	61	225,294	49	17,173	44	23,733	13	0.70

Table 5.17 Backcalculated layer moduli using 3-layer system with different depths to stiff layer, I-75 SB section 1 test site 2

Depth to stiff layer (in.)	Number of stations converged	Average moduli (psi) and coefficients of variation								Average RMS (%)
		AC	CV (%)	Rubblized	CV (%)	Base	CV (%)	Roadbed	CV (%)	
150	20	912,221	98	722,106	88			15,193	12	3.56
200	29	1,481,824	68	381,263	113			17,529	10	1.93
250	**31**	**1,693,455**	**58**	**274,789**	**116**			**19,357**	**10**	**1.53**
300	31	1,806,179	61	256,115	113			20,160	11	1.36
350	30	1,816,340	63	226,722	118			21,226	11	1.36
400	30	1,806,183	67	223,407	111			21,630	11	1.42
500	27	1,814,783	69	209,135	113			22,418	11	1.59

CV (%) = Coefficient of variation = standard deviation divided by average

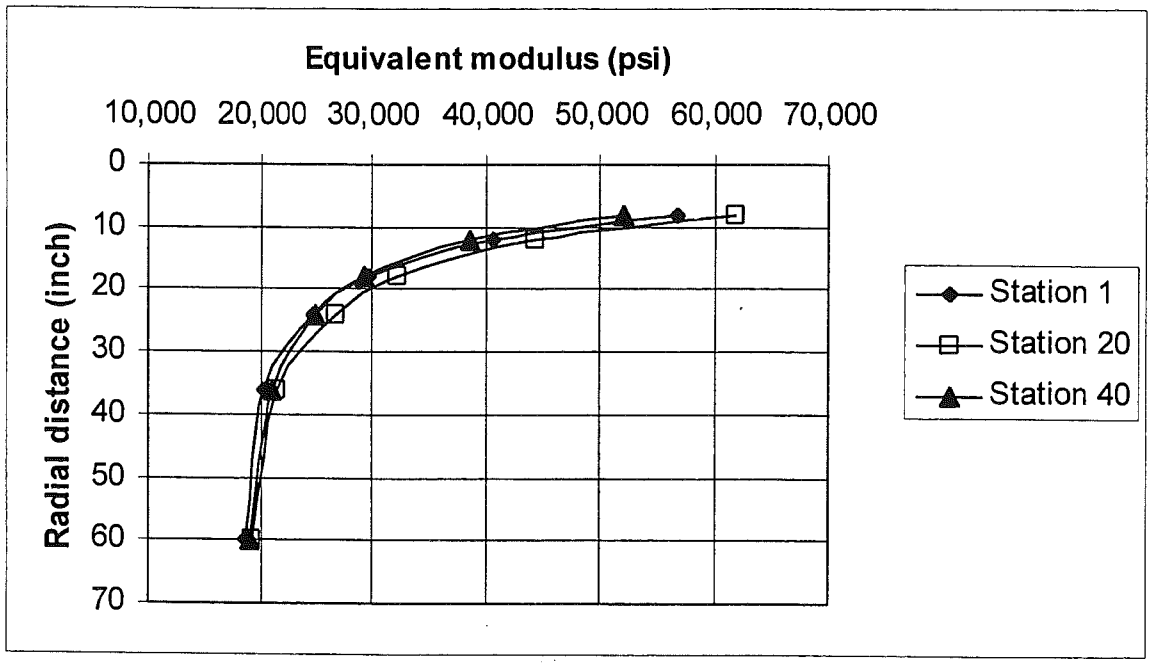

a) Test site 1

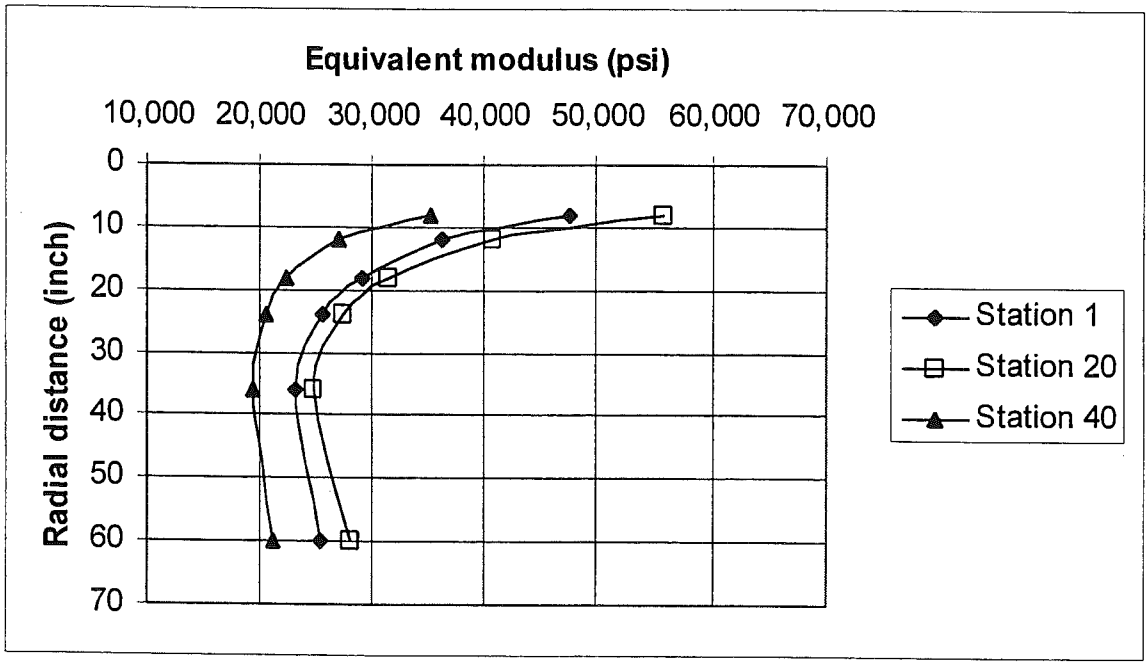

b) Test site 2

Figure 5.17 Plots of Boussinesq equivalent modulus of three set of FWD deflections from each test site on I-75 SB section 1

stated above for various depths to stiff layer are listed in tables 5.14 through 5.17. For test site 1, table 5.14 (4-layer system) and table 5.15 (3-layer system) provide lists of:

1. The depths to stiff layer used in the backcalculation.

2. The number of test locations for which the backcalculation was successful (convergence between the measured and calculated deflection basins was achieved).

3. The average backcalculated modulus and the coefficients of variation of:

   - The AC
   - The rubblized concrete slab
   - The base layer (in table 5.14, the base layer is the combination of the one base and two subbase layers stated above).
   - The roadbed soil (in table 5.15, the roadbed soil represents all the material below the rubblized concrete slab).

4. The average root mean square of the errors between the measured and calculated deflection basins.

Tables 5.16 and 5.17 provide similar results for test site 2.

Relative to test site 1 (tables 5.14 and 5.15), the data indicate that the moduli of the various pavement layers and the roadbed soil vary from one FWD test location to another. This is because of the variability in the measured deflection data (see tables 5.4 and 5.5 and figures 5.4 and 5.5), which is caused by variable thicknesses of the AC, rubblized material and fractured concrete layers. Note that among the 18 rubblized projects that were FWD tested in 2001, the measured deflection data along SB I-75 show the highest variation (see table 5.7) and consequently the highest variation in the backcalculated layer moduli (see table 5.18). Finally, the data for site 2 (tables 5.16 and 5.17) show similar results.

Now, let us use the measured deflection data along SB I-75, section 1, test sites 1 and 2 to illustrate the applicability of the procedure, which was presented in the previous subsection, for determining the stiff layer depth. Recall that the backcalculation was accomplished using 3- and 4-layer systems and variable depth to stiff layer. The backcalculated moduli of the AC and roadbed soil for the two test sites are plotted in figure 5.18 (Note that in order to plot the moduli of the two materials on the same graph, the AC modulus was divided by 1,000,000 and the roadbed soil by 10,000 psi). Figure 5.18a shows that the curves representing the backcalculated AC modulus using three and four layer systems intersect around a stiff layer depth of 300 in. Similarly, the curves for the roadbed soil modulus intersect at around 300-in. For test site 2 (figure 5.18b), these intersections are between 240 in. for the AC and 280 in. for the roadbed soil. Although these last two intersections should theoretically be at the same stiff layer depth, the high variation in the measured deflection data makes this not possible. The data, however, suggest that the stiff layer for test site 2 is shallower than 280 in., which is shallower than that for test site 1. This finding is

Table 5.18 Backcalculated moduli and their coefficients of variation of 18 rubblized pavement test sites

Test site	Depth to stiff layer (in.)	Number of stations converged	Modulus (psi)								Average RMS (%)
			AC	CV (%)	Rubblized	CV (%)	Base	CV (%)	Subgrade	CV (%)	
10692-11	150	40	317,448	14	120,329	48	24,826	25	13,785	12	0.54
10692-12	150	40	294,737	20	158,793	32	28,730	21	16,513	15	0.55
10753-11	300	39	1,778,413	40	218,816	72			17,042	5	1.05
10753-12	250	31	1,693,455	58	274,789	116			19,357	10	1.53
11941-21	No stiff layer	36	1,494,031	30	244,821	36	39,767	36	23,438	5	0.43
11941-22	No stiff layer	42	1,457,345	33	205,137	45	39,340	50	17,582	5	0.30
20102-11	500	40	712,346	17	61,512	37	26,261	26	16,248	6	0.45
20102-12	500	40	516,364	14	48,853	35	21,316	33	15,766	3	0.53
20233-11	200	51	437,318	22	50,064	38	34,381	24	10,303	5	0.84
20233-12	200	26	154,165	34	112,020	59	29,107	17	9,198	9	0.81
20273-21	300	41	1,776,844	28	108,717	48	36,515	21	20,765	3	0.68
20273-31	225	41	460,330	18	58,254	34	15,778	24	13,561	5	0.49
20273-41	300	39	230,377	19	1,401,144	76	42,099	52	23,744	35	0.53
20311-11	500	40	619,688	23	671,698	114	35,306	49	22,460	14	0.61
30153-11	500	42	2,182,399	23	90,987	83	31,453	47	20,387	9	0.26
30373-51	400	40	421,812	12	284,801	33	28,806	34	15,878	8	0.63
30373-52	400	39	393,301	25	132,980	46	24,516	33	14,750	10	0.52
30373-61	200	27	2,083,677	27	311,434	52	28,356	62	16,686	11	0.38

CV (%) = Coefficient of variation = standard deviation divided by average

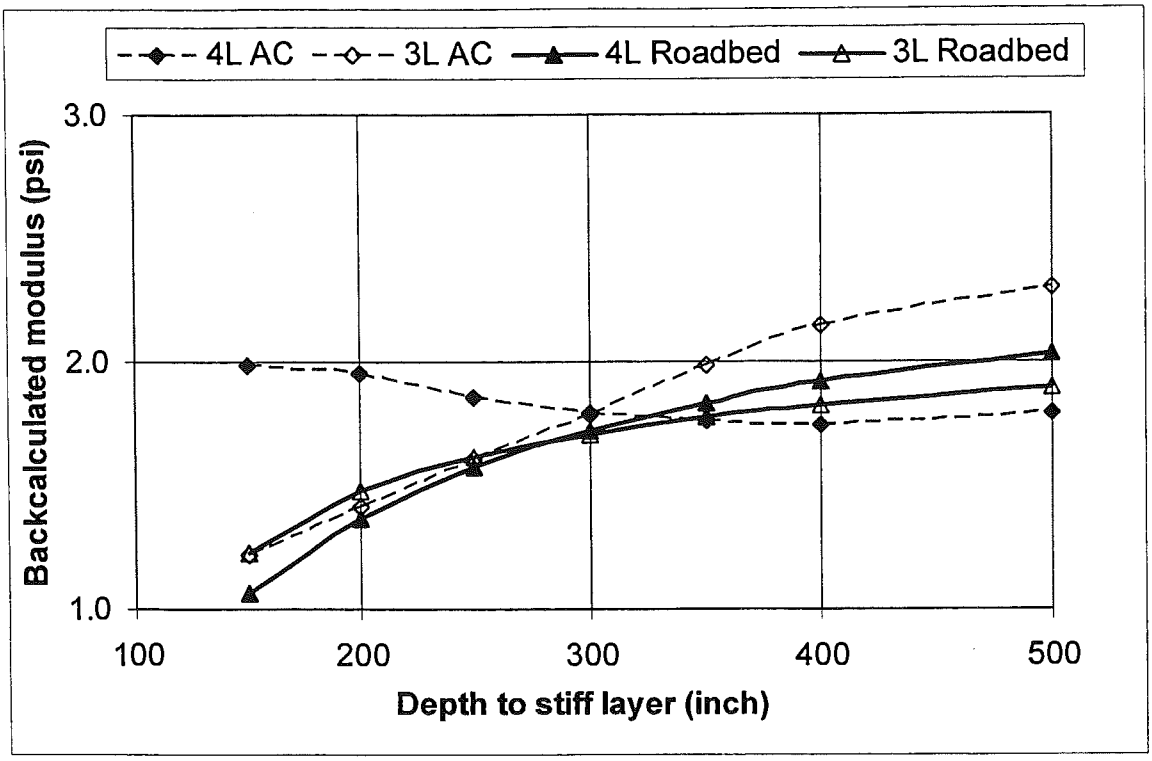

a) Test site 1

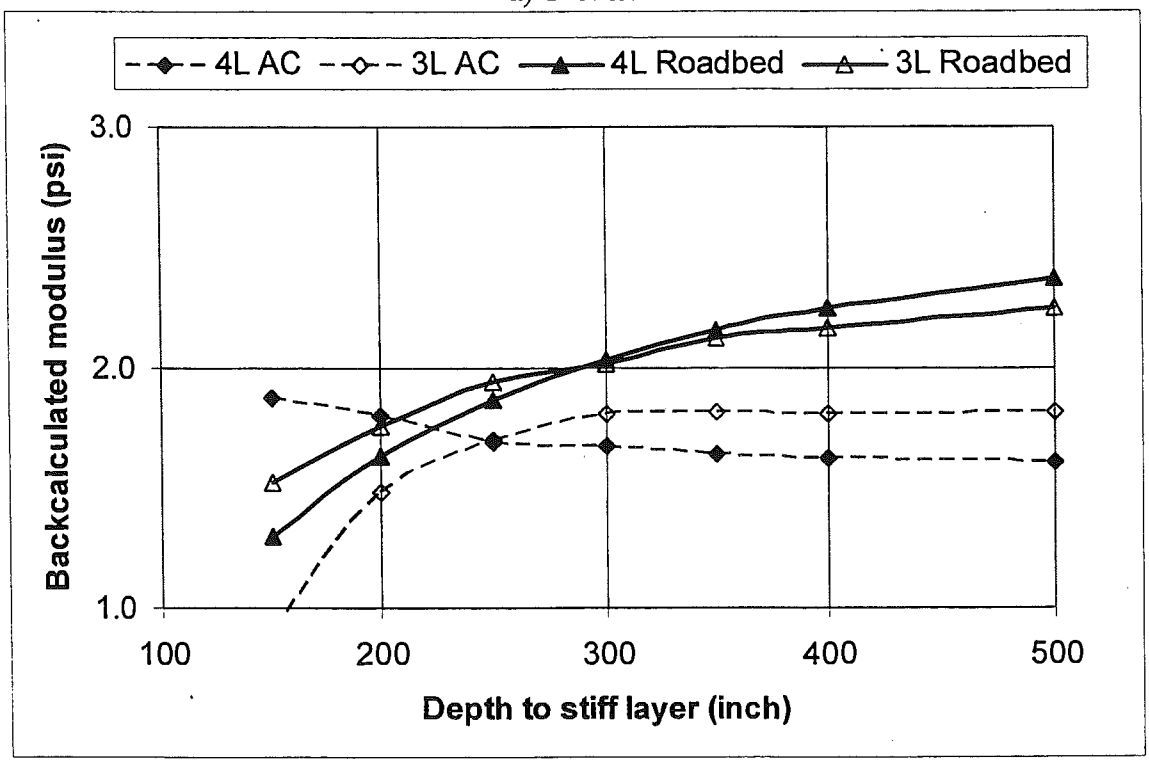

b) Test site 2

Figure 5.18 Intersections of backcalculated AC ($*10^5$) and roadbed soil ($*10^4$) moduli using 3 and 4-layer systems (3L and 4L)

also supported by that stated earlier based on Boussinesq equation. One other indicator of the relative depths to stiff layer was found by plotting the backcalculated base and roadbed soil moduli using the 4-layer system against the depth to stiff layer as shown in figure 5.19. The data in the figure indicate that:

- The base and roadbed moduli for test sites 1 and 2 intersect at stiff layer depths of 350 and 300 in., respectively.
- The base modulus is lower than the roadbed modulus at deeper stiff layer depths, which is not probable.
- The stiff layer at test site 2 is shallower than that at test site 1.

Based on the data in figures 5.17, 5.18 and 5.19 and on field observations (the fill thickness at test site 1 is higher than that at test site 2 by about 4 ft) it was decided to use 3-layer system and stiff layer depths of 300 and 250 in. for test sites 1 and 2, respectively for the backcalculation of layer moduli.

Finally, the backcalculated moduli of the rubblized concrete slab were not used in the determination of the stiff layer depths because of the high variability in the thicknesses of the rubblized material and fractured concrete. Such variability significantly affects the accuracy of the backcalculated moduli of the rubblized concrete slab.

6.3 Layer Moduli for SB I-75, Section 1, Test Sites 1 and 2

After the depths to stiff layer was estimated at 250 and 300 in. for test sites 2 and 1, respectively, the deflection data were used to backcalculate the layer moduli using a 3-layer system and the MICHBACK computer program. Results of the MICHBACK include the layer moduli, the root mean square (RMS) of the errors between the measured and calculated pavement deflections and whether or not they converged. After the backcalculation was accomplished, the resulting modulus values of converged FWD test stations were scrutinized. They were rejected when:

1. The RMS was larger than 2 percent.

2. The FWD test was conducted over cracked area.

3. The base modulus satisfies the following equation:

$$MR_{Base} < MR_{RB}/1.1$$

MR_{Base} = backcalculated base modulus; and
MR_{RB} = backcalculated roadbed modulus.

Based on the above criterion, some of the I-75 SB backcalculation results were rejected and the rest of them were accepted and used to calculate the average backcalculated moduli of test sites 1 and 2. Tables 5.19 and 5.20 provide the backcalculated layer moduli for test sites 1 and 2, respectively. The tables also provide the moduli of the rubblized material and the

Table 5.19 Results of the backcalculation and the estimated layer moduli for I-75 SB -section 1 test site 1

FWD station	MDT (^{0}C)	Backcalculated modulus (ksi)					Estimated moduli (ksi)		RMS (%)	Converged	Accepted
		AC	TCAC	RCS	Base	RB	Rubblized material	Fractured concrete			
1	13.1	2040	1472	106	-	16	18	538	1.13	Y	Y
2	13.2	1511	1097	118	-	15	17	611	1.01	Y	Y
4	13.3	1312	958	126	-	17	27	623	1.00	Y	Y
5	13.4	2358	1733	69	-	17	10	357	0.28	Y	Y
6	13.7	1192	889	133	-	17	23	672	0.67	Y	Y
7	13.7	1116	832	134	-	16	20	688	0.33	Y	Y
8	13.7	2411	1797	102	-	16	15	527	0.56	Y	Y
9	14.0	2072	1572	132	-	16	16	686	0.37	Y	Y
10	14.2	1916	1464	103	-	18	14	532	1.08	Y	Y
11	14.4	1986	1540	87	-	17	14	445	1.41	Y	Y
12	14.4	1032	800	168	-	17	31	848	0.24	Y	Y
13	14.6	2533	1985	73	-	18	9	381	1.93	Y	Y
14	14.8	678	537	142	-	17	38	683	1.02	Y	Y
16	15.2	1197	969	215	-	17	42	1080	0.16	Y	Y
18	15.2	1809	1464	204	-	18	31	1045	1.24	Y	Y
19	15.3	1378	1119	265	-	17	56	1317	1.07	Y	Y
20	15.4	1090	892	351	-	18	111	1643	0.55	Y	Y
21	15.4	2826	2313	80	-	18	15	405	1.15	Y	Y
22	15.8	2543	2126	207	-	17	23	1088	1.71	Y	Y
23	15.6	1347	1118	304	-	17	82	1463	0.80	Y	Y
24	15.6	962	799	467	-	17	198	2047	0.58	Y	Y
25	15.4	2352	1931	102	-	18	19	512	1.09	Y	Y
27	15.5	3147	2593	304	-	17	42	1569	0.29	Y	Y
28	15.1	1039	841	561	-	17	308	2259	0.76	Y	Y
29	15.0	2675	2150	104	-	18	17	533	0.50	Y	Y
30	14.8	1552	1239	334	-	17	89	1608	0.71	Y	Y
31	14.6	2966	2341	510	-	15	96	2570	1.19	Y	Y
32	14.6	1255	991	143	-	16	20	737	1.40	Y	Y
35	14.6	941	740	225	-	18	46	1125	0.79	Y	Y
36	14.8	1271	1011	370	-	17	96	1790	0.47	Y	Y
37	14.8	1632	1303	491	-	16	175	2240	1.78	Y	Y
38	14.9	844	677	664	-	16	586	2063	1.10	Y	Y
39	15.1	2235	1808	118	-	18	16	610	0.55	Y	Y
40	15.2	1663	1351	131	-	17	64	551	1.82	Y	Y
3	12.2	2114	1457	91	-	16	-	-	2.32	Y	N
15	16.0	2137	1800	147	-	18	-	-	1.28	Y	N
17	16.0	2719	2289	69	-	18	-	-	2.21	Y	N
34	14.8	2957	2351	132	-	17	-	-	2.65	Y	N
42	14.3	533	412	454	-	18	-	-	1.76	Y	N
26		-	-	-	-	-	-	-	2.32	N	N
33		-	-	-	-	-	-	-	1.74	N	N
41		-	-	-	-	-	-	-	3.85	N	N
Average	14.7	1732	1366	225	-	17	70	1054	0.90		
CV (%)	5	39	40	70	-	5	159	61	53		

MDT = Mid-depth temperature, TCAC = Temperature corrected asphalt concrete, RCS = Rubblized concrete slab, RB = Roadbed, RMS = Root mean square error

Table 5.20 Results of the backcalculation and the estimated layer moduli for I-75 SB -section 1 test site 2

FWD station	MDT (°C)	Backcalculated modulus (ksi)					Estimated moduli (ksi)		RMS (%)	Converged	Accepted
		AC	TCAC	RCS	Base	RB	Rubblized material	Fractured concrete			
2	15.0	1193	957	170	-	17	28	912	0.67	Y	Y
3	14.8	1596	1269	114	-	16	13	627	0.24	Y	Y
4	15.1	3241	2622	123	-	18	7	696	1.55	Y	Y
6	15.2	1743	1412	119	-	18	13	661	0.27	Y	Y
9	15.4	853	702	132	-	21	22	705	1.98	Y	Y
10	15.4	2060	1694	141	-	21	16	779	0.71	Y	Y
12	15.7	2463	2054	136	-	18	33	699	1.20	Y	Y
13	16.2	597	510	150	-	21	24	806	0.62	Y	Y
14	16.2	3050	2606	181	-	21	24	984	0.75	Y	Y
16	16.5	2328	2027	167	-	17	15	931	0.36	Y	Y
22	16.5	2275	1981	208	-	22	38	1102	1.30	Y	Y
30	16.6	2602	2277	133	-	21	13	738	0.31	Y	Y
32	16.5	3088	2688	341	-	17	28	1906	0.41	Y	Y
33	16.4	2134	1849	273	-	17	35	1489	0.84	Y	Y
35	16.3	3220	2777	395	-	18	40	2189	0.83	Y	Y
36	16.3	2325	2005	303	-	19	38	1658	0.50	Y	Y
38	16.1	2659	2271	238	-	18	15	1346	1.17	Y	Y
40	15.9	1210	1023	159	-	21	14	889	0.39	Y	Y
41	16.0	1527	1292	118	-	20	8	664	0.51	Y	Y
42	15.9	1921	1617	50	-	21	3	287	1.28	Y	Y
43	15.9	1419	1195	307	-	20	-	-	0.55	Y	N
7	14.8	1574	1252	71	-	21	-	-	1.41	Y	N
17	15.9	404	341	214	-	22	-	-	1.38	Y	N
5	15.4	563	460	148	-	18	-	-	2.11	Y	N
8	14.8	2333	1855	33	-	21	-	-	2.58	Y	N
19	14.2	168	130	1309	-	18	-	-	3.77	Y	N
21	16.4	431	374	240	-	23	-	-	2.32	Y	N
23	14.2	207	160	1465	-	18	-	-	3.36	Y	N
24	17.5	562	516	385	-	17	-	-	3.19	Y	N
26	18.6	2637	2563	127	-	23	-	-	6.06	Y	N
39	16.9	111	99	571	-	18	-	-	4.82	Y	N
1	-	-	-	-	-	-	-	-	2.98	N	N
11	-	-	-	-	-	-	-	-	2.05	N	N
15	-	-	-	-	-	-	-	-	2.64	N	N
18	-	-	-	-	-	-	-	-	0.80	N	N
20	-	-	-	-	-	-	-	-	2.27	N	N
25	-	-	-	-	-	-	-	-	2.48	N	N
27	-	-	-	-	-	-	-	-	1.23	N	N
28	-	-	-	-	-	-	-	-	2.23	N	N
29	-	-	-	-	-	-	-	-	2.84	N	N
31	-	-	-	-	-	-	-	-	2.48	N	N
34	-	-	-	-	-	-	-	-	1.91	N	N
37	-	-	-	-	-	-	-	-	1.99	N	N
Average	15.9	2104	1782	182	-	19	21	1003	0.79		
CV (%)	3	37	38	47	-	10	54	48	60		

MDT = Mid-depth temperature, TCAC = Temperature corrected asphalt concrete, RCS = Rubblized concrete slab, RB = Roadbed, RMS = Root mean square error

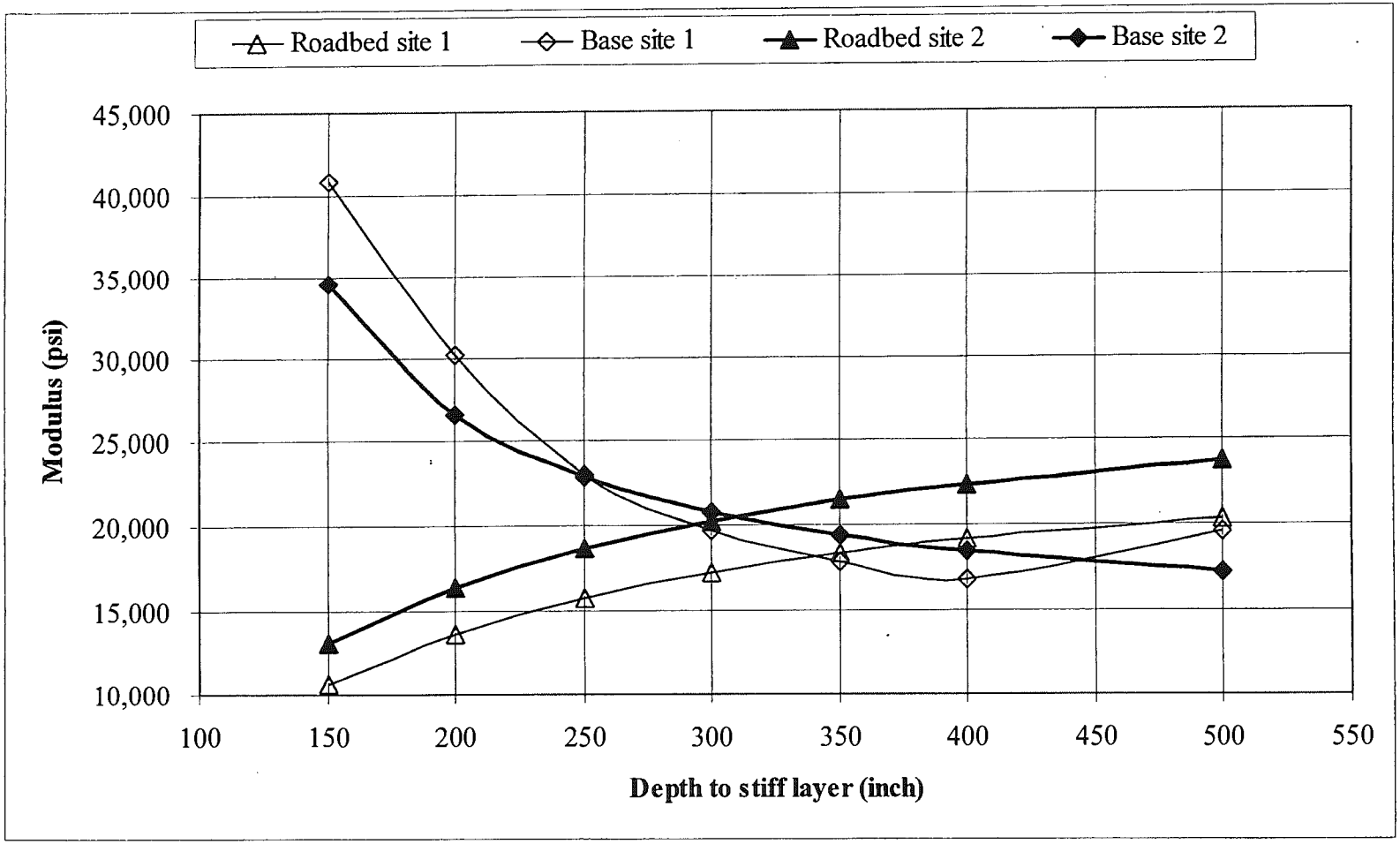

Figure 5.19 Base and roadbed moduli versus depth to stiff layer for I-75 SB, section 1, test sites 1 and 2

fractured concrete layers at each accepted stations that were estimated using equations 3 and 4. As can be seen from the tables, the moduli of the two layers are highly variable. The modulus of the rubblized material varies from 9 to 586 ksi for test site 1 and from 3 to 40 for test site 2. Likewise, the modulus of the fractured concrete layer varies from 357 to 2570 ksi for test site 1 and from 287 to 2189 for test site 2. Once again, the reason for such variation is that the thicknesses of the rubblized material and the fractured concrete layers are not known at any specific location. For this reason, the moduli of the two layers were estimated using equations 3 and 4 and the averages of the AC, roadbed moduli and the average of the measured deflections at the accepted FWD test locations for each test site. The results of the later estimates of the moduli of the two layers are listed in table 5.13 and discussed in section 5 of this chapter.

One last note, for I-75 SB, section 1, test sites 1 and 2, the estimated moduli of the rubblized material and the fractured concrete layers using the individual-average and the average-average methods are listed below. As can be seen, the average-average method yields lower modulus values and more reasonable than the individual-average method.

Test site	Method of calculation	Estimate4d modulus values (ksi)	
		Rubblized material layer	Fractured concrete layer
10753-11	Individual-average	70	1054
	Average-average	27	704
10753-12	Individual-average	21	1003
	Average-average	14	600

Results of the backcalculation of 18 rubblized pavements are summarized in Appendix J along with the deflection.

7.0 SUMMARY

Various nondestructive deflection test and backcalculation of layer moduli issues are discussed in this chapter. These include:

1. The repeatability of the measured deflection data; the MDOT FWD produces repeatable data.

2. The pavement response to load was tested using the FWD. For the pavement projects included in this study, the pavement response to load is more or less linear. Hence, a linear layered-elastic system can be used for the analysis of the pavement sections and for the backcalculation of layer moduli.

3. The measured deflection data along and across a pavement section (within 100-ft test site) are highly variable. Hence, one should expect high variability in the structural capacity of the pavement and in its performance. The variability in the deflection data of rubblized pavement structures is in order of magnitude higher than that for conventional flexible pavements.

4. The sensitivity of the backcalculated layer moduli to several pavement and site variables was discussed. These variables include the accuracy of the layer thicknesses and the depth to stiff layer.

5. A backcalculation procedure was developed during this study and discussed in this chapter. The procedure was successfully applied to real sets of measured deflection data. It is shown that the most difficult problem in the backcalculation of layer moduli is the uncertainty of the thicknesses of the rubblized material and the fractured concrete layers.

6. A statistical model was developed and presented in this chapter for the estimation of the modulus of the rubblized material. The model uses as input, the deflection data and the backcalculated moduli of the AC and roadbed soil.

7. The modulus of the fractured concrete layer can be estimated based on the principles of stress dissipation and on the geometry of the rubblized pavement.

REFERENCES

1. Irwin, L.H., W.S., Yang, and R.N. Stubstad, "Deflection Reading Accuracy and Layer Thickness Accuracy in Backcalculation of Pavement Layer Moduli." The American Society for Testing and Material, STP 1026 1989, Bush/Baladi, editors

2. Harichandran R.S., T. Mahmood and G.Y. Baladi, "Backcalculation of Pavement Layer Moduli, Thicknesses and Stiff Layer Depth Using a Modified Newton Method." The American Society for Testing and Materials, ASTM STP 1198, Philadelphia, PA 1994, Von Quintas, Bush and Baladi, editors

3. Harichandran, R.S., T. Mahmood, A. Raab and G.Y. Baladi "A Modified Newton Algorithm for Backcalculation of Pavement layer properties," Transportation Research Record, 1384, 15-22, 1993

4. Das, Braja M., Principles of Foundation Engineering, 4th edition, 1998

5. AASHTO Guide for Design of Pavement Structures, 1993

6. "Soil Survey of Cheboygan County, Michigan", United States Department of Agriculture, Soil Conservation Service; September 1991.

7. Harichandran, R. S., Ramon, C. M., and Baladi, G. Y., "MICHBACK user's manual.", Department of Civil and Environmental Engineering, Michigan State University, East Lansing, Michigan, 1994

8. Per Ullidtz "Pavement Analysis", Elsevier Science Publishing Company, New York, New York, 1987.

CHAPTER 6
RUBBLIZED PAVEMENT DESIGN PARAMETERS

1.0 PAVEMENT DESIGN PROCEDURES

The design of rubblized concrete pavements can be accomplished by using three different design methods, empirical, mechanistic-empirical or catalogue-based design. Each of the three methods has benefits and drawbacks. Currently, MDOT uses a modified version of the AASHTO 93 empirical design procedure. The inputs to the procedure include the modulus of the various pavement layers and the AASHTO layer coefficients. Hence, one of the objectives of this study is to determine the moduli and coefficients of the rubblized concrete slab.

As noted in chapter 5, the modulus values of the AC, rubblized concrete slab, and base layers and of the roadbed soil were obtained using the MICHBACK computer program and the measured deflection data. Based on the backcalculated modulus of the rubblized concrete slab, on the AC and roadbed modulus values and on the measured deflection data, the modulus values of the rubblized material and the fractured concrete layers were estimated. The estimated and the backcalculated modulus values were reported in table 6.13 (which is, for convenience, repeated herein as table 6.1) and discussed in chapter 5. This chapter addresses the modulus and the layer coefficient values of the rubblized concrete slab, the rubblized material and the fractured concrete layers to be used in mechanistic-based or the AASHTO pavement design procedures.

2.0 RUBBLIZED PAVEMENT DESIGN PARAMETERS

Table 6.1 provides a list of results of the backcalculated and estimated layer moduli of 18 test sites. The list includes:

1. The total number of FWD tests that were conducted at each test site.

2. The number of FWD test locations at which the backcalculation routine achieved convergence between the measured and the calculated deflection data.

3. The number of FWD test stations that were accepted based on the acceptance criteria discussed in chapter 5.

4. For each test site, the average backcalculated modulus values of the AC, rubblized concrete slab, base layers and the roadbed soil. Note that the AC modulus values have been corrected to the standard temperature of 68°F and listed under the title TCAC.

5. The average estimated modulus values of the rubblized material and the fractured concrete.

Table 6.1 Backcalculated and estimated pavement layer moduli of 18 rubblized pavement test sites

Test site	No of FWD stations			Backcalculated moduli (ksi)					Estimated moduli (ksi)	
	Total	Converged	Accepted	AC	TCAC	RCS	Base	Roadbed soil	Rubblized material	Fractured concrete
10692-11	40	40	39	317	534	122	25	14	65	256
10692-12	40	40	40	295	573	159	29	17	73	352
10753-11	42	39	34	1,732	1,297	225		17	27	704
10753-12	43	31	20	2,104	1,701	182		19	14	600
11941-21	36	36	27	1,567	1,468	225	44	23	201	360
11941-22	43	42	20	1,247	1,500	182	37	21	144	322
20102-11	40	40	39	710	1,640	61	27	16	44	119
20102-12	40	40	35	517	1,657	46	23	16	31	92
20233-11	52	51	51	433	1,484	50	34	10	15	135
20233-12	26	26	25	150	743	114	29	9	46	287
20273-21	45	41	35	1,891	2,285	117	36	21	24	350
20273-31	40	40	29	470	936	55	17	13	36	109
20273-41	40	39	31	237	608	1,064	50	22	297	2,774
20311-11	40	40	35	637	1,620	414	40	22	191	949
30153-11	43	42	31	2,364	2,165	71	37	20	28	183
30373-51	40	40	35	411	1,192	275	31	16	179	561
30373-52	40	39	38	392	1,407	134	25	15	67	307
30373-61	33	26	17	2,126	2,337	234	38	16	90	592
Minimum				150	534	46	17	9	14	92
Maximum				2,364	2,337	1,064	50	23	297	2,774
Average						207			87	503

TCAC = Temperature corrected asphalt concrete, RCS = Rubblized concrete slab

6. The maximum and minimum values of the modulus of each material.

7. The overall average (the average of all test sites) modulus values of the rubblized concrete slab, the rubblized material and the fractured concrete. The overall average modulus values of the AC and base layers and of the roadbed soil are not included because various asphalt mixes, base material, and roadbed soil were found at the test sites

Examination of the modulus values of the rubblized concrete slab, and the rubblized material and the fractured concrete layers listed in table 6.1 indicates that the average modulus varies significantly from one test site to another. Indeed, it was shown that the modulus values within one test site also vary significantly. It was discussed in chapter 5 that the main reason of the variations in the modulus within a test site is the high variation in the thicknesses of the rubblized material and the fractured concrete layers. The variation between the test sites is related to the quality (strength) of the concrete before rubblization and to the rubblization process itself. Some projects were rubblized using the resonant frequency breaker whereas others using the multi-hammer breaker. Hence, the issue herein is what modulus value or values should be used in the rubblized pavement design process? These and other design issues are addressed in the next two subsections.

2.1 Design Modulus Values

To satisfactorily answer the question posted above, two step- analyses were undertaken as follows:

1. FWD deflection data obtained from various conventional flexible pavements were used to backcalculate the layer moduli of the pavements. Results of the analysis indicate that the backcalculated modulus values were about twice as high as those used in the pavement design process. Therefore, it was decided to divide the modulus of the rubblized material listed in table 6.1 by a factor of 2. The inherent assumption is that the rubblized material performs like a conventional aggregate base.

2. FWD deflection data obtained from various composite pavements were used to backcalculate the layer moduli of the pavements. Results of the analysis indicate that the backcalculated modulus value of the concrete slab varied from 2,500,000 to 4,500,000 psi. The implication of this is that the backcalculated values are representative of the modulus of the AC slab. Therefore, it was decided to use the backcalculated or estimated modulus values of the rubblized concrete slab and the fractured concrete layer as the design moduli.

Based on the results of the analyses from the two steps, the recommended design modulus values for the rubblized concrete slab, the rubblized material and the fractured concrete layers were calculated and are provided, for each test site, in table 6.2. The table also lists the minimum and maximum modulus values and the overall average moduli of the three materials.

Table 6.2 Recommended design moduli and layer coefficients

Test site	Modulus (ksi)			Layer coefficient					
				AASHTO-based			Mechanistic-based		
	RCS	Rubblized material	Fractured concrete	RCS	Rubblized material	Fractured concrete	RCS	Rubblized material	Fractured concrete
10692-11	122	32.7	256	0.18	0.15	0.23	0.20	0.16	0.25
10692-12	159	36.5	352	0.21	0.16	0.27	0.23	0.17	0.29
10753-11	225	13.7	704	0.26	0.05	0.34	0.26	0.08	0.36
10753-12	182	6.8	600	0.23	-0.02	0.33	0.24	0.02	0.34
11941-21	225	100.6	360	0.26	0.27	0.27	0.26	0.26	0.29
11941-22	182	72.1	322	0.23	0.23	0.26	0.24	0.23	0.28
20102-11	61	22.1	119	0.09	0.10	0.15	0.13	0.12	0.18
20102-12	46	15.6	92	0.06	0.07	0.12	0.10	0.09	0.15
20233-11	50	7.6	135	0.07	-0.01	0.17	0.11	0.03	0.19
20233-12	114	23.2	287	0.17	0.11	0.25	0.19	0.13	0.27
20273-21	117	11.9	350	0.18	0.04	0.27	0.20	0.07	0.29
20273-31	55	18.1	109	0.08	0.08	0.14	0.12	0.11	0.17
20273-41	1,064	148.5	2,774	0.45	0.31	0.49	0.42	0.30	0.49
20311-11	414	95.7	949	0.33	0.26	0.38	0.32	0.26	0.39
30153-11	71	13.8	183	0.11	0.05	0.20	0.15	0.08	0.22
30373-51	275	89.4	561	0.28	0.26	0.32	0.28	0.25	0.33
30373-52	134	33.3	307	0.19	0.15	0.25	0.21	0.16	0.27
30373-61	234	44.9	592	0.26	0.18	0.32	0.27	0.19	0.34
Minimum	46	6.8	92	0.06	-0.02	0.12	0.10	0.02	0.15
Maximum	1,064	148.5	2,774	0.45	0.31	0.49	0.42	0.30	0.49
Average	207	43.7	503	0.20	0.14	0.26	0.22	0.15	0.28

Based on the analyses and the overall average of the moduli of the three materials, it is strongly recommended that the following design modulus values be used in the design of rubblized pavement section:

Material	Design modulus (ksi)
Rubblized concrete slab	207
Rubblized material	43
Fractured concrete	503

2.2 AASHTO Layer Coefficients

Two methods were used to estimate the layer coefficients of the rubblized concrete slab, the rubblized material and the fractured concrete layers. The first method is based on the AASHTO design procedure and the second is based on mechanistic analysis. The two methods are presented and discussed in the next two subsections.

2.2.1 AASHTO-Based Layer Coefficients

In the AASHTO-based layer coefficient method, three procedures were used as follows:

1. The rubblized concrete slab
2. The fractured concrete layer
3. The rubblized material

The three procedures are presented below.

Procedure One - The Rubblized Concrete Slab – In this procedure, the following assumptions were made based on the state of distress of the original concrete pavement prior to rubblization:

1. Since the rubblized concrete slabs consist of two layers; a rubblized material layer and a fractured concrete layer, the rubblized concrete slabs can be treated as a deteriorated concrete slabs in need of AC overlay.

2. The relationship between the modulus of the rubblized concrete slabs and the layer coefficient is analogous to that between cement treated bases and the layer coefficient since both behave like a strong base layer under the AC surface. Hence, the AASHTO proposed relationship between the cement-treated bases and the layer coefficient was used as follows:

$$a_2 = 0.2187*\text{Ln}(E_{RCS}) - 2.7547 \qquad (6.1)$$

where: E_{RCS} = the modulus of the fractured concrete slab (ksi); and
Ln = natural logarithm

3. For each mile, the average number of deteriorated joints and transverse cracks in the concrete is 155. This makes the average distance between deteriorated joints and transverse cracks 35 ft. For such a state of distress, the AASHTO design procedure recommends reducing the a_2 value by a factor of 0.65.

4. On average, the concrete pavement has 75 working transverse cracks per mile. That is the average distance between working transverse cracks is about 70 ft. For this scenario, the AASHTO design procedure recommends reducing the a_2 value by a factor of 0.9.

Incorporating the two reduction factors of items 3 and 4 above into equation 6.1 yields the following equation, which relates the design modulus to the AASHTO layer coefficient.

$$a_2 = 0.65*0.9*(0.2187*Ln(E_{RCS})-2.7547) \qquad (6.2)$$

Based on equation 6.2, the layer coefficient of the rubblized concrete slab at each test site was calculated and the results are listed in table 6.2 along with the minimum, maximum and the overall average layer coefficient value.

Procedure Two – The Fractured Concrete Layer – For this material, the first two assumptions (assumptions 1 and 2) of the first procedure were upheld for the same argument. However, assumptions 3 and 4 are not valid for the fractured concrete layer. The layer includes deteriorated joints and transverse cracks as well as micro cracks created by the rubblization process throughout the layer. To account for the micro cracks, the product of the reduction factors (0.65 and 0.9) was further reduced by a factor of 0.85. That is, the reduction factor for the fractured concrete layer is the product of 0.65, 0.9 and 0.85 or 0.5. The final equation relating the modulus of the fractured concrete to its AASHTO layer coefficient is as follows:

$$a_2 = 0.5*(0.2155*Ln(E_{FCL})-0.7266) \qquad (6.2)$$

where: E_{FCL} = the modulus of the fractured concrete layer (ksi); and
Ln = natural logarithm.

The calculated values of the AASHTO layer coefficients of the fractured concrete layer are listed in table 6.2 along with the minimum, maximum and the overall average layer coefficient value.

Procedure Three – The Rubblized Material – The rubblized material layer was assumed to perform like a conventional aggregate base. Therefore the AASHTO recommended relationship between the modulus and the layer coefficient was used as follows:

$$a2 = 0.249*Log(E_{RML})-0.977 \qquad (6.3)$$

where: E_{RML} = the modulus of the rubblized material layer (psi); and
Log = base 10 logarithm.

The calculated values of the AASHTO layer coefficients of the fractured concrete layer are also listed in table 6.2 along with the minimum, maximum and the overall average layer coefficient value.

Based on the assumptions and on the analyses, it is strongly recommended that the following layer coefficients be used in the AASHTO design procedure.

Material	Design modulus (ksi)
Rubblized concrete slab	0.2
Rubblized material	0.14
Fractured concrete	0.26

2.2.2 Mechanistic-Based Layer Coefficients

The layer coefficients of the rubblized concrete slab, the rubblized material and the fractured concrete were also determined using mechanistic-based design (the MICHPAVE computer program was used) coupled with the AASHTO empirical pavement design procedure. Unlike the AASHTO-based layer coefficient, the determination of the mechanistic-based layer coefficients entailed a more in depth procedure as presented below.

1. For each test site, the backcalculated and estimated modulus values of the AC, rubblized slab, aggregate base and roadbed soil were used to determine the design modulus as follows:

    a) For the AC layer, 67 percent of the average backcalculated and temperature adjusted modulus.
    b) For the rubblized concrete slab, the rubblized material and the fractured concrete, the design modulus values listed in table 6.2 were used.
    c) For the aggregate base, 50 percent of the average backcalculated modulus values.
    d) For the roadbed soil, the average value of the backcalculated layer moduli was divided by three as per AASHTO recommendation.

2. The actual layer thicknesses were obtained by coring or from the MDOT project files and used in the analyses.

3. The MICHPAVE computer program was then used to analyze the pavement section and to estimate its fatigue life in terms of 18-kip ESAL.

4. The AASHTO flexible pavement design procedure was then used with the following inputs:

a) The fatigue life obtained from the MICHPAVE program in terms of 18-kip ESAL.
b) The design modulus values of all layers.
c) For all layers except the one whose layer coefficient is being determined, the layer coefficient which was obtained using the design modulus value and the proper AASHTO equation or chart. For the layer in question, a layer coefficient value of 0.25 was assumed.
d) All layer thicknesses except the one whose layer coefficient is being determined.

5. Based on the above input, the AASHTO procedure was used to determine the required thickness (d_{req}) of the layer whose coefficient is being determined.

6. The mechanistic-based layer coefficient was then calculated using the following equation.

$$a_{2Mechanistic} = .25 * \left(\frac{d_{REQ}}{Actual\ thickness} \right) \qquad (6.3)$$

The procedure was then repeated for each layer (the rubblized concrete slab, the rubblized material and the fractured concrete).

The mechanistic based layer coefficients of the three materials are also listed in table 6.2. Examination of the AASHTO-based and the mechanistic-based layer coefficients indicate that, on average, the two procedure produce compatible results.

Note that, in all analyses the thickness of each of the rubblized material and the fractured concrete layers was assumed as 4.5-inch (based on a total concrete thickness of 9 in.). The AASHTO-based and the mechanistic-based layer coefficients listed in table 6.2 indicate that the structural number (SN) of the rubblized concrete slab is almost the same as that of the rubblized material and the fractured concrete. That is the pavement designer has the option of using either a 9-inch rubblized concrete slab with a layer coefficient of 0.2 or 4.5 in. rubblized material with a layer coefficient of 0.14 and 4.5 in. of fractured concrete with a layer coefficient of 0.26. This is so because the two methods produce the same structural number as follows:

$$SN = 9*0.2 = 4.5*.14 + 4.5*.26$$

The above observation indicates that the layer coefficients are reasonable and balanced. One word of caution should be exercised however is that, in the above analysis, the AC thickness was fixed at the actual field value obtained by coring. In real life, the pavement design engineer may use the AASHTO design procedure to

determine the thickness of the AC. For that case, the required AC thickness will be different if the designer uses one rubblized slab layer than if he/she uses rubblized material and fractured concrete layer. The reason is that the design modulus of the rubblized slab is different than that of the rubblized material. Therefore, the rubblized slab layer will result in a thinner AC thickness.

3.0 SUMMARY

Based on the FWD deflection data and the actual layer thickness, the design modulus value for the rubblized concrete slab, the rubblized material and the fractured concrete were estimated. Two sets of layer coefficients were obtained; one is AASHTO-based and the other is based on mechanistic analysis and design of the pavement structure augmented by the AASHTO empirical pavement design procedure. It is shown that the two sets of layer coefficient values are compatible and almost the same.

CHAPTER 7
MECHANISTIC ANALYSIS OF RUBBLIZED PAVEMENTS

1.0 FIELD OBSERVATIONS

Based on field investigations and observations that were conducted during the rubblization operation and after the completion of construction, the causes of the underperformance of rubblized concrete pavement projects can be related to several attributes as follows:

1. The rubblization procedure
2. The construction of the asphalt mat
3. The asphalt mix

The effects of these attributes on the performance of rubblized concrete pavements are addressed in Chapter 4 and, for convenience, are summarized below. The three attributes may cause the following defects in the rubblized concrete pavements:

1. Joint reflective cracking if the integrity of the joints in the concrete pavement is not completely destroyed.

2. Reflective cracking if the integrity of the concrete in the vicinity of the crack is not destroyed and/or if the temperature steel is not completely debonded or if the rubblized material contains independent large concrete pieces (larger than 6 in.).

3. Localized shear failure if the rubblization procedure caused some large concrete pieces to break loose and rotate or penetrate into the subbase material. Fixing such shear failure requires removal of the AC, base and subbase layers and appropriate compaction of the roadbed soil before AC patches can be placed.

4. Raveling if the asphalt mix was segregated during transportation and/or lay-down operation or if the asphalt content is low (a dry mix). The extent and severity of raveling will depend on the extent and degree of segregation.

5. Top-down cracking due to segregation and/or differential stiffness between the pavement layers. This scenario would happen if the rubblization procedure produces rubblized and fractured concrete sublayers (a soft layer sandwiched between two harder layers), or when the construction procedure causes temperature and/or particle segregations in the AC.

6. Top-down cracking if the rubblization procedure produces uneven surface between the rubblized and fractured concrete sublayers as shown in figures 7.1 and 7.2.

The first two defects are well understood and repeatedly observed in composite pavements. The third one is analogous to bearing capacity failure of the base material. The fourth one (raveling) is observed on all types of AC surfaced pavements and was also studied by various

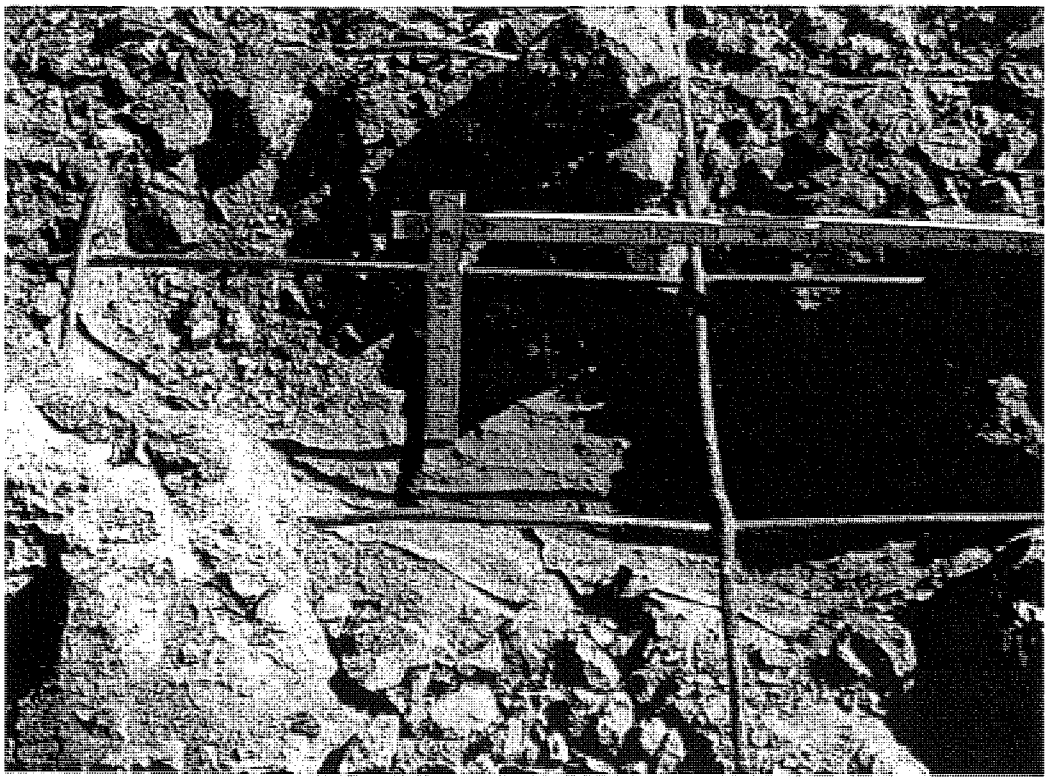

Figure 7.1 Excavated trench in a rubblized concrete slab showing the sand subbase and the fractured concrete

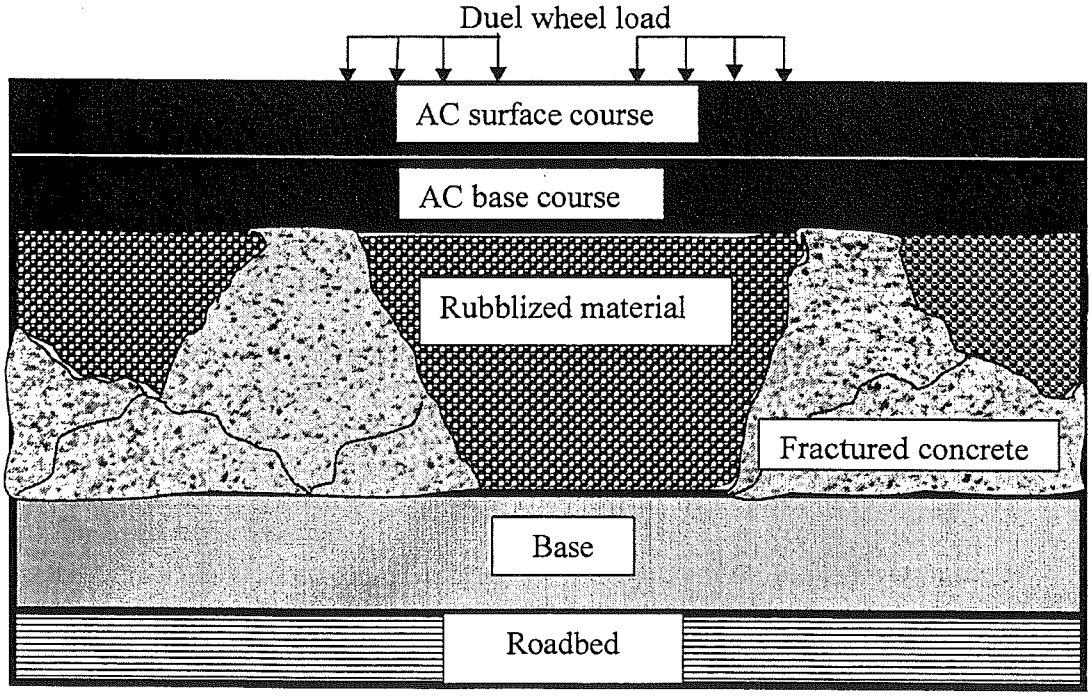

Figure 7.2 Schematic representation of the trench area of figure 7.1 after construction

researchers (see the segregation report submitted to MDOT by the PRCE). Finally, top-down cracking which has recently been reported as a dominant distress in flexible pavements and has been studied by few researchers (see Appendix K). Some stated that TDC are caused by aging of the AC mix, others by environmental conditions, and still others blamed the appearance of TDC on the increasing use of radial tires. Therefore, TDC deserve a special attention and detailed study. In this research study, mechanistic analyses of rubblized pavements were conducted to study the effects of various attributes on the TDC potential. The analyses were based on the following hypothesis:

The main cause of TDC is load-induced surface tensile stresses magnified by asphalt aging, differential stiffness between the pavement layers, segregation and environmental condition.

To verify the hypothesis and to analyze the factors affecting TDC potential, two and three dimensional mechanistic analyses were conducted and the results are presented and discussed in the next sections.

2.0 MECHANISTIC ANALYSIS

As stated above, two and three dimensional mechanistic analyses were conducted to calculate the maximum load-induced surface tensile stress. The analyses were conducted using the following computer programs:

1. CHEVRONX – The CHEVRONX program is a closed form solution of multilayer linear elastic systems. The program is capable of analyzing maximum of 5-layer systems and, for each layer; it requires the input of layer modulus, Poisson's ratio and thickness. In this analysis, the lower layer (the roadbed soil) is assumed to have an infinite extent

2. MICHPAVE – The MICHPAVE is a two-dimensional (2-D) finite element computer program capable of modeling the pavement structure as linear or nonlinear multilayer elastic systems. The linear model was used in this study.

3. ABAQUS – ABAQUS is a finite element computer program capable of modeling the pavement structure as linear or nonlinear multilayer elastic, viscoelastic or plastic systems in two and three dimensions (2-D and 3-D). The linear 3-D elastic system was used in this study.

The objectives of the mechanistic analyses include:

1. Calculate the magnitude and location of the maximum load-induced surface tensile stress and compare the results to field measurements.

2. Study the impact of variations in the thickness and moduli of the AC courses, rubblized materials and fractured concrete layers and variations in the moduli of base and roadbed soil on the maximum load-induced surface tensile stress.

3. Analyze the impact of the geometry of the interface between the rubblized materials and the fractured concrete layers on the load-induced surface tensile stress.

4. Assess the sensitivity of the maximum load-induced surface tensile stress to various rubblization and construction factors.

Based on the objectives and the capabilities of the three computer programs, two basic pavement models were used; they are presented in the next section.

3.0 PAVEMENT MODELS

Two basic pavement models were used in the mechanistic analysis of rubblized concrete pavements. The characteristics of the pavement (thicknesses and moduli) were varied to simulate various pavement cross-section and the effects of the environment and aging on the asphalt mix properties. The two models are detailed below.

1. Figure 7.3 shows two alternatives of the first rubblized pavement model. Both alternatives consist of five layer system as follows:

   Alternative one:

   - A 1.5-in. thick AC surface course.
   - A variable thickness AC base course
   - A 9-in. thick rubblized concrete slab.
   - A variable thickness aggregate base layer.
   - A roadbed soil.

   Alternative two:

   - A variable thickness AC layer.
   - A 4.5-in. thick rubblized material.
   - A 4.5-in. fractured concrete
   - A variable thickness aggregate base layer.
   - A roadbed soil.

   Since the 2-dimensional (2-D) CHEVRONX and MICHPAVE computer programs were used in the analysis of both models, the duel tire was simulated by a 9000-lb single wheel load. In addition, few cases were analyzed using the 2-D option of the ABAQUS computer program. This allowed comparison of the results of the three computer programs. The two alternatives of this pavement model are called the 2-D model.

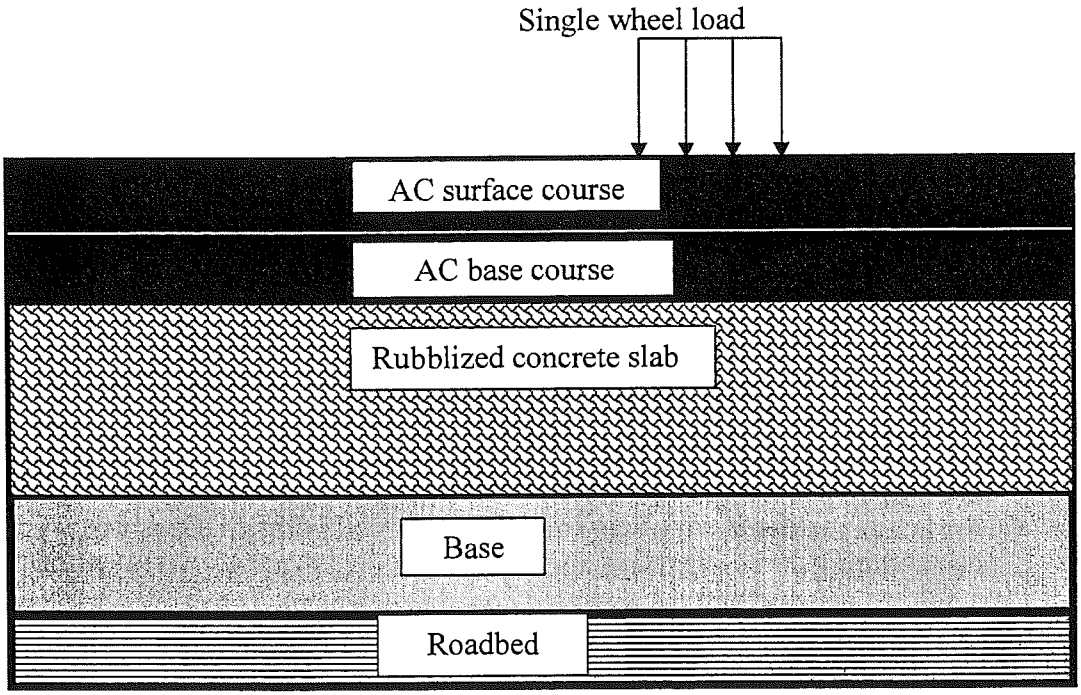

a) Rubblized pavement (2 AC courses and a rubblized concrete slab)

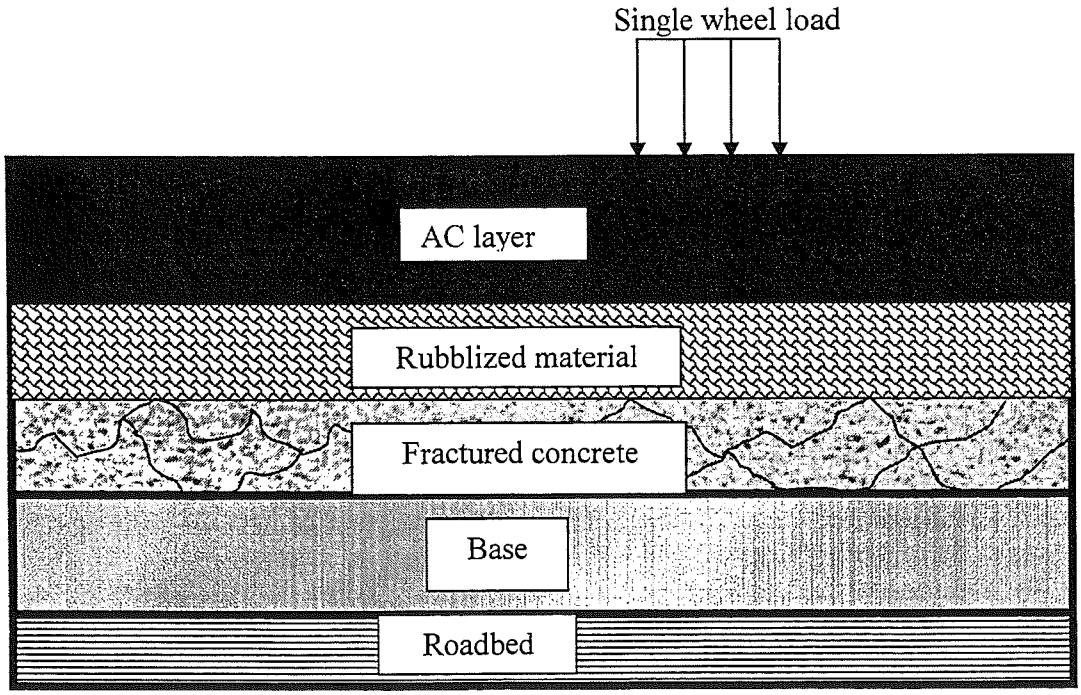

b) Rubblized pavement (an AC, rubblized material and fractured concrete layers)

Figure 7.3 Five layer rubblized pavement models

2. Also two alternatives were used in the second basic rubblized pavement model, uneven with variable geometry and even interface between the rubblized material and the fractured concrete layers as shown in figures 7.2 and 7.4. Both alternatives consist of 6-layer system as follows:

   - Variable AC surface course thickness.
   - Variable AC base course thickness
   - Variable rubblized material thickness.
   - Variable fractured concrete thickness
   - Variable aggregate base layer thickness.
   - A roadbed soil.

   The actual layer thicknesses used in each analysis were the same as the pavement section being analyzed. For example, in the analysis of the rubblized pavement sections along I-75, I-69 and M-37, the actual measured layer thicknesses were used in the analysis. Nevertheless, this 3-D model was used to simulate dual wheel load and the actual rubblized pavement condition observed in the trenches that were excavated during the rubblization operation. This includes the variable thicknesses of the rubblized material and the fractured concrete layers and the various geometry of their interface. The pavement was subjected to a 9000-lb dual wheel load and only the 3-D finite element program, ABAQUS, was used in this analysis. Hence, the model is called the 3-D model.

The main reason for conducting analyses of the two models is to compare the results (the load-induced stresses and strains) obtained from both models. If no significant differences are found, then one can use the first model, which is much simpler, easier to use and less time consuming than the analyses of the second model, which require 3-D type analyses.

Results of the analyses of the two rubblized pavement models and the steps that need to be taken to minimize the TDC potential are presented and discussed in the remaining sections of this chapter.

4.0 MECHANISTIC ANALYSIS USING THE 2-D MODEL

As noted above, due to limitation of the CHEVRONX program, each alternative of the 2-D model consists of 5 layer system as shown in figure 7.3. In the first alternative, the effects of differential stiffness between the AC courses due to aging and/or temperature on the maximum surface tensile stress were analyzed. In the second alternative, the effects of differential stiffness between the rubblized material and the fractured concrete layers on the maximum surface tensile stress were analyzed. In both alternatives, the standard 18-kip single axle load was simulated using a 9000-lb single wheel load having a tire pressure of 100 psi and uniform circular contact area with 5.781-in. radius. In the analysis, the pavement cross-section (layer thicknesses) and the layer properties (modulus) were varied to simulate the actual field condition and the results obtained from the backcalculation.

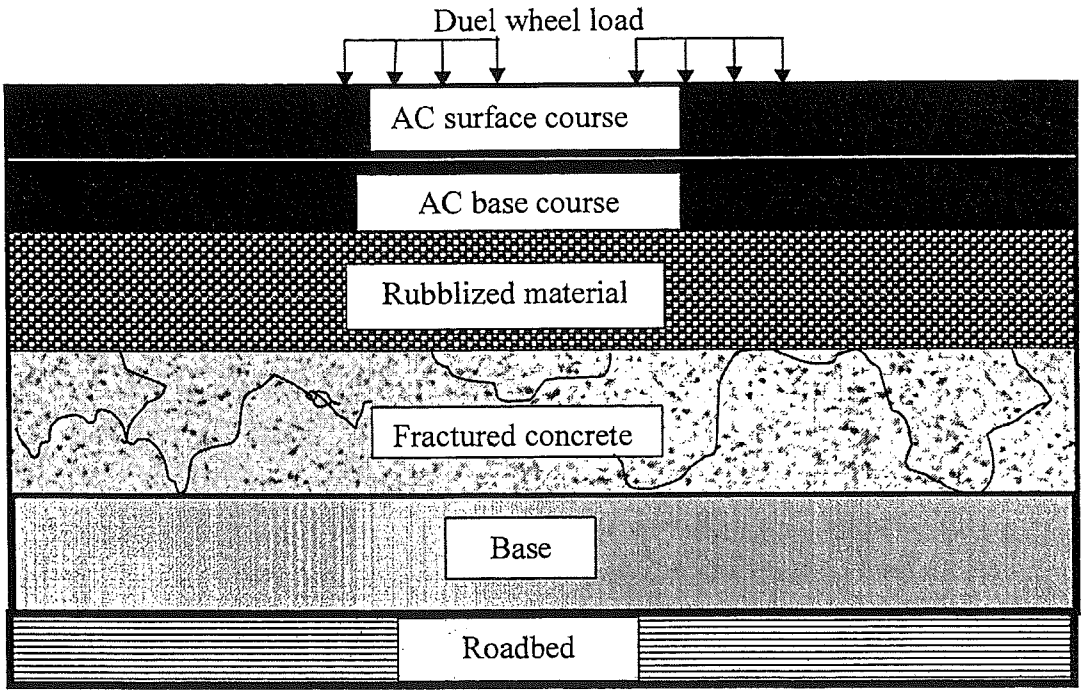

Figure 7.4 Six layer Rubblized pavement model with even interface

Table 7.1 provides a summary of the pavement cross-sections and material properties used in the analysis. As can be seen from the table, the layer thicknesses and engineering properties used in the analysis are:

1. One AC surface course thickness of 1.5 in. and three AC base course thickness of 1.5, 4.5, and 7.5 in. The two courses make the total AC thickness of 3, 6 and 9 in. This represents the spectrum of AC thicknesses used by MDOT. Results of the analysis were used to study the effect of the AC layer thickness on the maximum surface tensile stress.

2. A rubblized concrete thickness or base layer of 9 in.

3. A sand subbase layer thickness of 18 in.

4. The above thicknesses make the total pavement thickness of 30, 33, and 36 in. Such pavement thickness provides frost protection of the roadbed soil as per MDOT specifications.

5. Elastic moduli of the AC surface course of 50, 100, 150, 300, 450, 600, 1200 and 2400 ksi

6. Elastic moduli of the AC base course of 50, 75, 150, 300, 450, 600, 1200, and 2400 ksi.

7. Elastic moduli of the rubblized concrete slab or base layer of 30, 100, 500 and 2000 ksi.

8. An elastic modulus of the sand subbase of 20 ksi.

9. An elastic modulus of the roadbed soil of 5 ksi.

The variation in the AC modulus was thought to reflect different AC mix used by MDOT, to simulate aging (harder AC surface course) and the effect of temperature and differences in temperature (gradients) within the AC layer. The temperature simulation represents the following environmental conditions

1. Constant temperature throughout the AC layer.

2. Cooling cycle (night time and/or abrupt cold wave) where the AC surface course is colder than the AC base course (negative temperature gradient).

3. Heating cycle (day time and/or abrupt heat wave) where the AC surface course is hotter than the AC base course (positive temperature gradient).

The variation in the rubblized concrete slab or base layer modulus was set to serve two functions:

Table 7.1 Layer thicknesses and properties of the pavement models used in mechanistic analyses using the CHEVRONX and the MICHPAVE computer programs

Rubblized pavement cross-section and engineering properties			
Layer	Thickness (in.)	Elastic modulus (ksi)	Poisson's ratio
AC surface course	1.5	50, 100, 150, 300, 450, 600, 1200, 2400	0.3
AC base course	1.5, 4.5, 7.5	50, 75, 150, 300, 450, 600, 1200, 2400	0.3
Total AC thickness	3, 6, 9		0.3
Base/Rubblized concrete slab	9	30, 100, 500, 2000	0.25
Subbase	18	20	0.4
Roadbed soil		5	0.45

1. To simulate the actual condition of the rubblized pavement observed in the trenches. Hence, an elastic modulus of 30 ksi represents a full-depth rubblized concrete slab. Whereas the 2000 ksi modulus represents a full depth fractured concrete resulting from a poor rubblization process. Hence, studying the effects of variation in the base modulus is analogous to studying the effect of the quality of the rubblization process.

2. To simulate the various base layer materials used by MDOT in conventional flexible pavements. For example, the 30 ksi modulus represents a conventional aggregate base, while a 100 ksi modulus represents a stabilized base layer.

Finally, note that the range of the rubblized concrete modulus used in this study was designed to cover the range of moduli of the rubblized concrete slab that was obtained from the backcalculation of layer moduli (see table 5.13 of chapter 5, which is repeated here as table 7.2 for convenience). Further, given the range of layer moduli used in the mechanistic analyses, the results are applicable to both conventional flexible and rubblized pavements.

4.1 Results of Mechanistic Analyses of the 2-D Model

Tables 7.3 through 7.6 and figures 7.5 through 7.9 provide lists and plots of the results of the mechanistic analysis that were obtained from the CHEVRONX and the MICHPAVE computer programs. Examination of figures 7.5 through 7.9 and the data listed in the tables indicates that:

1. For the majority of the cases, both computer programs produce similar results relative to the magnitudes and locations of the maximum surface tensile stresses. Figure 7.5 illustrates a general relationship between the load-induced surface radial stress and the radial distance form the centre of load. As can be seen from the figure, the surface radial stresses can be divided into three zones

   - A high compression zone under the tire
   - A high tension zone around the edge of the tire
   - Low magnitudes compression and/or tension zones further away from the tire

   As it was expected, the magnitudes and locations of the surface radial stresses for each zone vary from one pavement to the other depending on the pavement cross section and the material properties (elastic modulus and Poisson's ratio) of each pavement layer. The magnitudes of the maximum surface tensile stresses for the three pavement sections are listed in tables 7.3, 7.5 and 7.6. For illustrative purposes, the locations of said stress for only one pavement section (total AC thickness of 6 in.) are provided in table 7.4. Note that the locations of the maximum surface tensile stress relative to the center of the loaded area reported in table 7.4 are very close to the field measured distances of the top-down cracks from the center of the wheel paths.

Table 7.2 Backcalculated and estimated pavement layer moduli of 18 rubblized pavements at the indicated test sites

Test site	No of FWD stations			Backcalculated moduli (ksi)					Estimated moduli (ksi)	
	Total	Converged	Accepted	AC	TCAC	RCS	Base	Roadbed soil	Rubblized material	Fractured concrete
10692-11	40	40	39	317	534	122	25	14	65	256
10692-12	40	40	40	295	573	159	29	17	73	352
10753-11	42	39	34	1,732	1,297	225	[illegible]	17	27	704
10753-12	43	31	20	2,104	1,701	182	[illegible]	19	14	600
11941-21	36	36	27	1,567	1,468	225	44	23	201	360
11941-22	43	42	20	1,247	1,500	182	37	21	144	322
20102-11	40	40	39	710	1,640	61	27	16	44	119
20102-12	40	40	35	517	1,657	46	23	16	31	92
20233-11	52	51	51	433	1,484	50	34	10	15	135
20233-12	26	26	25	150	743	114	29	9	46	287
20273-21	45	41	35	1,891	2,285	117	36	21	24	350
20273-31	40	40	29	470	936	55	17	13	36	109
20273-41	40	39	31	237	608	1,064	50	22	297	2,774
20311-11	40	40	35	637	1,620	414	40	22	191	949
30153-11	43	42	31	2,364	2,165	71	37	20	28	183
30373-51	40	40	35	411	1,192	275	31	16	179	561
30373-52	40	39	38	392	1,407	134	25	15	67	307
30373-61	33	26	17	2,126	2,337	234	38	16	90	592
Minimum				150	534	46	17	9	14	92
Maximum				2,364	2,337	1,064	50	23	297	2,774

TCAC = Temperature corrected asphalt concrete, RCS = Rubblized concrete slab

Table 7.3 Magnitudes of the maximum surface tensile stresses for pavements with different AC surface and base moduli

Modulus Ratio	Maximum surface tensile stress (psi)							
	Base Modulus 30 ksi		Base Modulus 100 ksi		Base Modulus 500 ksi		Base Modulus 2000 ksi	
	MICHPAVE	CHEVRONXX	MICHPAVE	CHEVRONXX	MICHPAVE	CHEVRONXX	MICHPAVE	CHEVRONX
0.7	2.3	16.5	8.0	24.5	13.2	30.5	17.2	35.0
1.3	3.1	4.8	6.9	15.9	14.3	26.0	21.2	35.5
2.0	3.7	1.8	8.3	10.1	17.3	24.2	26.4	35.0
4.0	10.7	8.0	16.4	13.4	26.5	23.2	39.4	35.7
6.0	18.8	14.8	24.7	19.6	35.2	30.4	50.7	45.4
8.0	26.3	21.3	32.4	26.9	43.8	36.6	60.4	53.2
16.0	50.2	43.9	57.5	49.3	70.3	58.5	90.2	76.3
32.0	79.7	71.7	87.2	77.1	103.8	86.3	128.2	107.7

Table 7.4 Locations of the maximum surface tensile stresses for pavements with different AC surface and base moduli

Modulus Ratio	Distance from center of load (in.)							
	Base Modulus 30 ksi		Base Modulus 100 ksi		Base Modulus 500 ksi		Base Modulus 2000 ksi	
	MICHPAVE	CHEVRONX	MICHPAVE	CHEVRONX	MICHPAVE	CHEVRONX	MICHPAVE	CHEVRONX
0.7	14.9	5.7	6.1	5.7	6.1	5.7	6.1	5.7
1.3	15.7	5.6	6.6	5.6	6.4	5.7	6.4	5.7
2.0	15.7	15.7	6.9	5.6	6.6	5.7	6.5	5.7
4.0	8.3	7.8	7.4	7.0	6.9	6.9	6.9	6.9
6.0	8.4	7.9	7.6	7.7	7.3	6.9	7.0	6.9
8.0	8.6	8.7	7.8	7.8	7.4	7.0	7.3	7.0
16.0	9.2	8.8	8.3	7.9	7.8	7.8	7.7	7.7
32.0	10.4	10.1	9.0	8.8	8.3	7.9	8.2	7.9

Table 7.5 Magnitudes of the maximum surface tensile stresses of rubblized pavements (base modulus = 100 ksi) with different AC surface moduli and AC thickness

Modulus Ratio	Max. radial tensile stress(psi)					
	3-in. AC layer		6-in. AC layer		9-in. AC layer	
	MICHPAVE	CHEVRONX	MICHPAVE	CHEVRONX	MICHPAVE	CHEVRONX
0.7	3.6	20.3	8.0	24.5	9.3	26.2
1.3	2.9	10.5	6.9	15.9	10.0	19.5
2.0	4.0	2.8	8.3	10.1	12.4	14.5
4.0	6.3	3.0	16.4	13.4	22.2	18.8
6.0	9.7	5.6	24.7	19.6	31.6	26.2
8.0	15.6	11.1	32.4	26.9	40.5	34.3
16.0	35.2	28.8	57.5	49.3	67.8	58.6
32.0	59.4	51.3	87.2	77.1	100.9	89.4

Table 7.6 Magnitudes of the maximum surface tensile stresses for conventional flexible pavements (base modulus = 30 ksi) with different AC surface moduli and AC thickness

Modulus Ratio	Max. radial tensile stress(psi)					
	3-in. AC layer		6-in. AC layer		9-in. AC layer	
	MICHPAVE	CHEVRONX	MICHPAVE	CHEVRONX	MICHPAVE	CHEVRONX
0.7	5.9	15.5	2.3	16.5	4.5	20.5
1.3	10.4	9.4	3.1	4.8	2.9	10.1
2.0	14.8	13.1	3.7	1.8	4.3	3.4
4.0	28.2	25.1	10.7	8.0	12.1	9.0
6.0	40.2	36.4	18.8	14.8	20.1	16.3
8.0	50.7	46.2	26.3	21.3	27.4	22.9
16.0	81.3	74.6	50.2	43.9	51.0	43.6
32.0	116.0	109.4	79.7	71.7	79.3	70.4

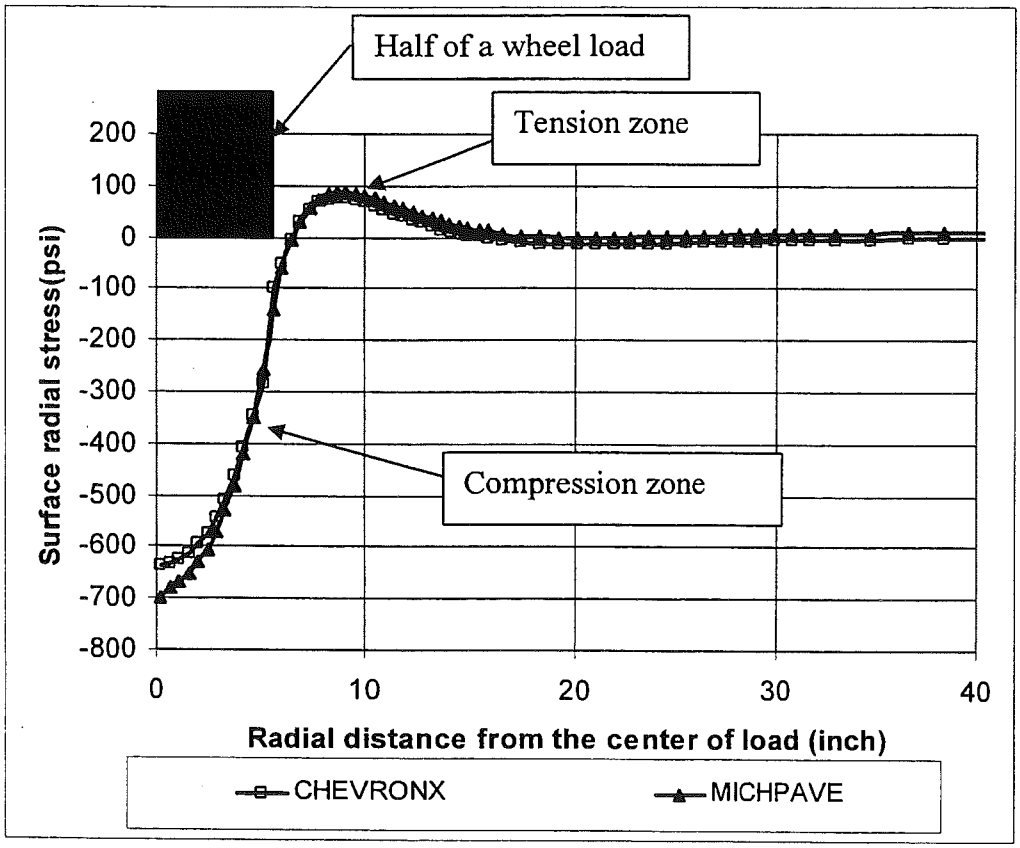

Figure 7.5 Surface radial stresses at various distances from the center of the load

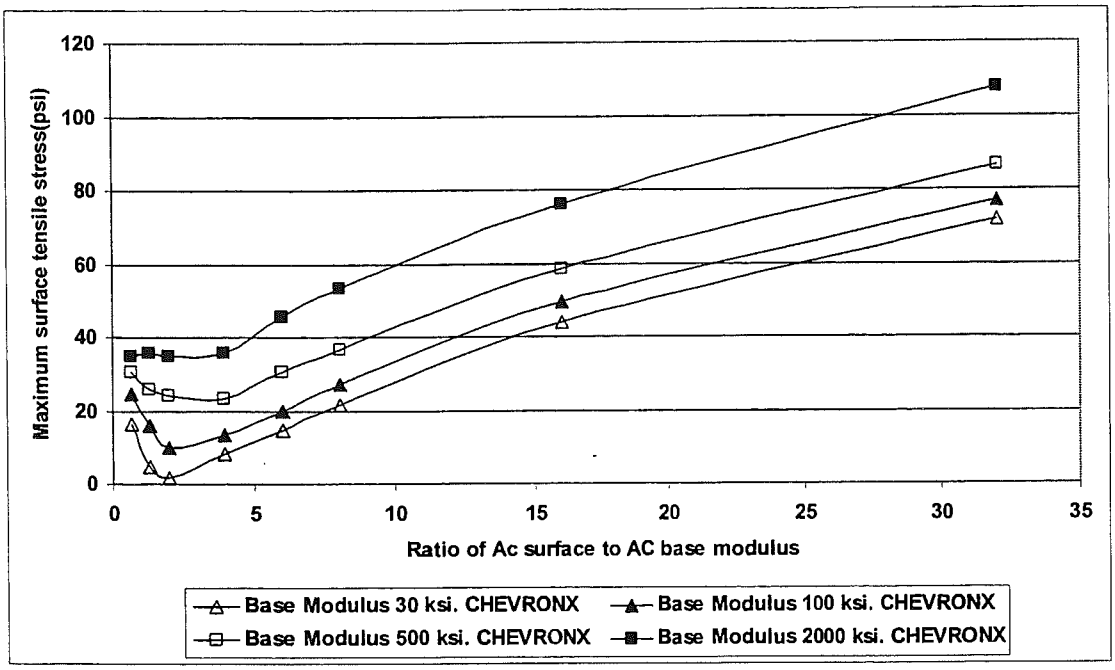

a) Results from CHEVRONX

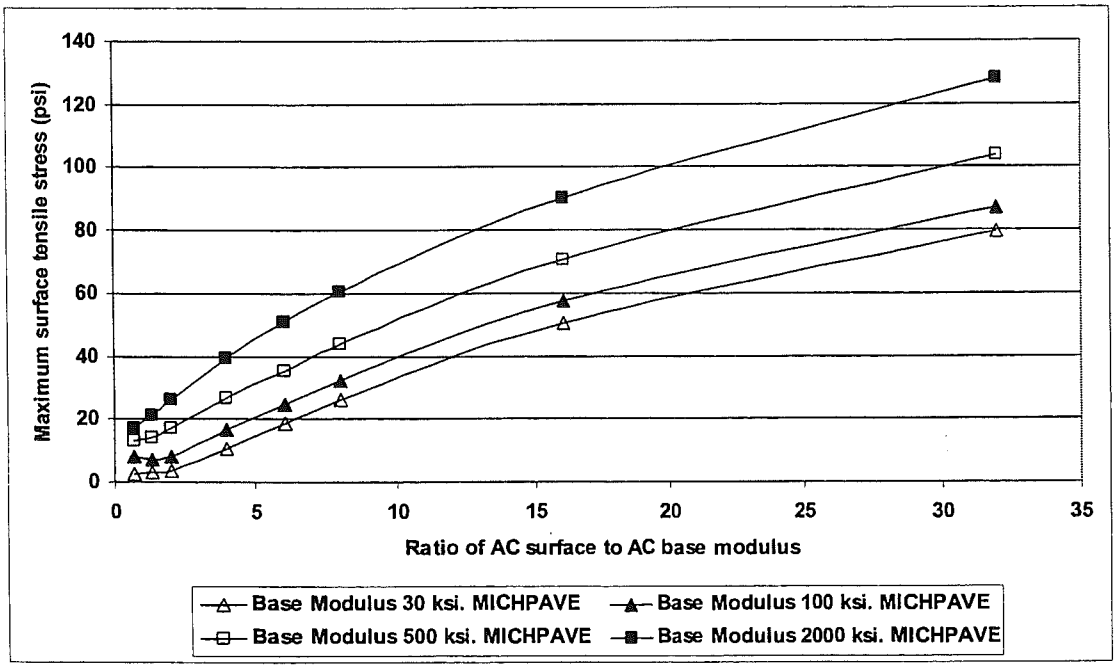

b) Results from MICHPAVE

Figure 7.6 The maximum surface tensile stress for different values of the base modulus as a function of the ratio of the AC surface to the AC base moduli

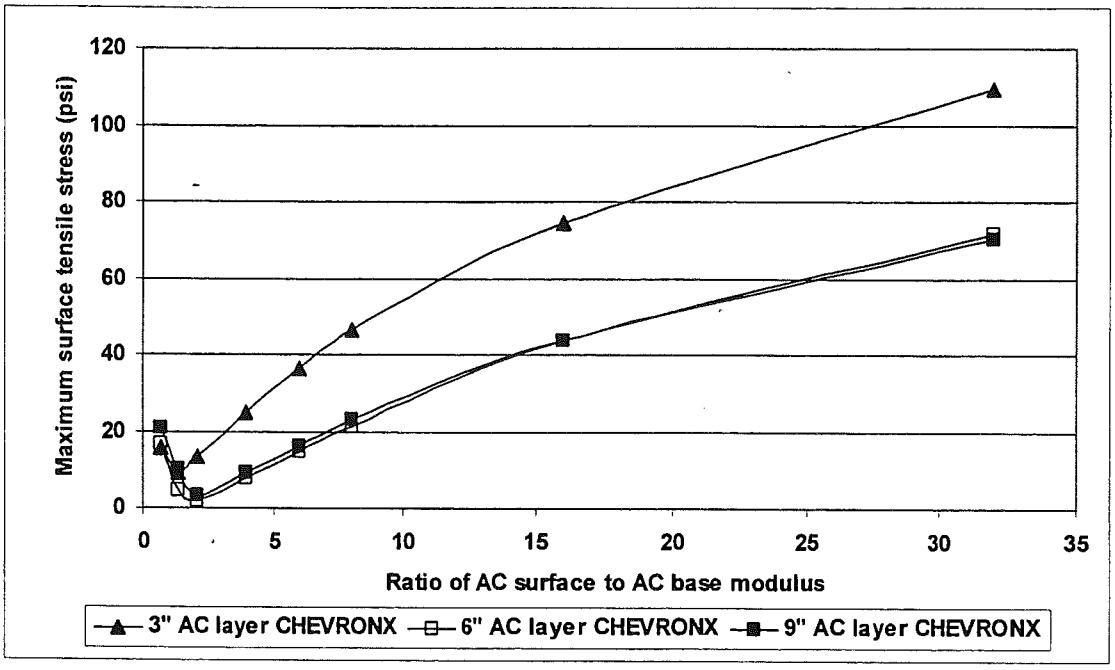

a) Results from CHEVRONX

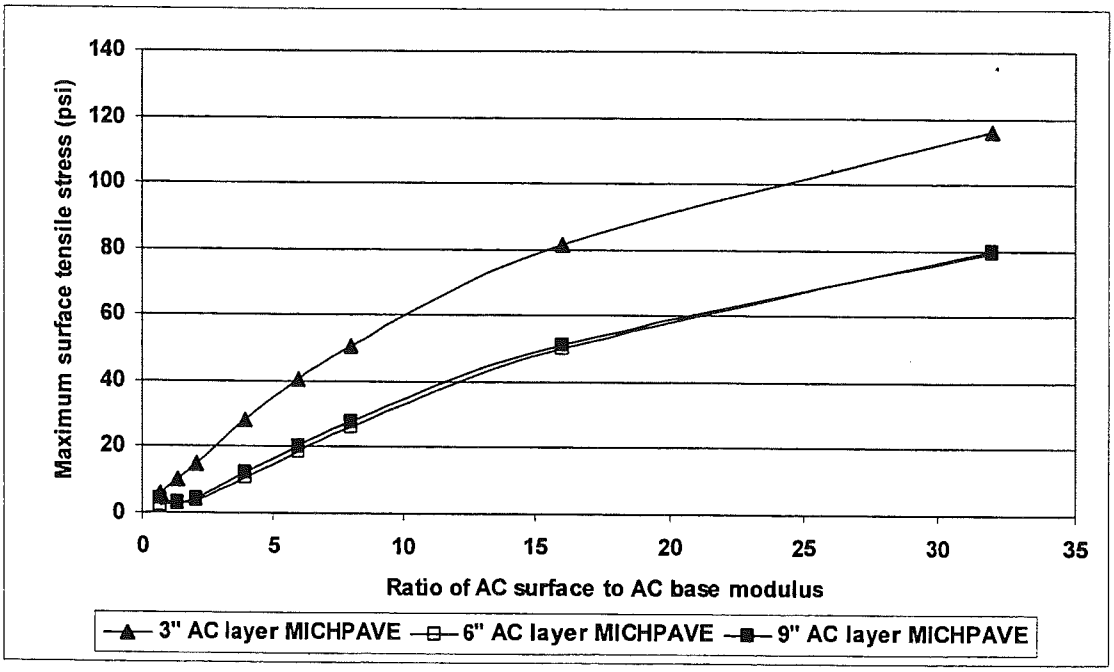

b) Results from MICHPAVE

Figure 7.7 The maximum surface tensile stress in conventional flexible pavements (base modulus = 30 ksi) with different AC layer thickness as a function of the ratio of the AC surface to the AC base moduli

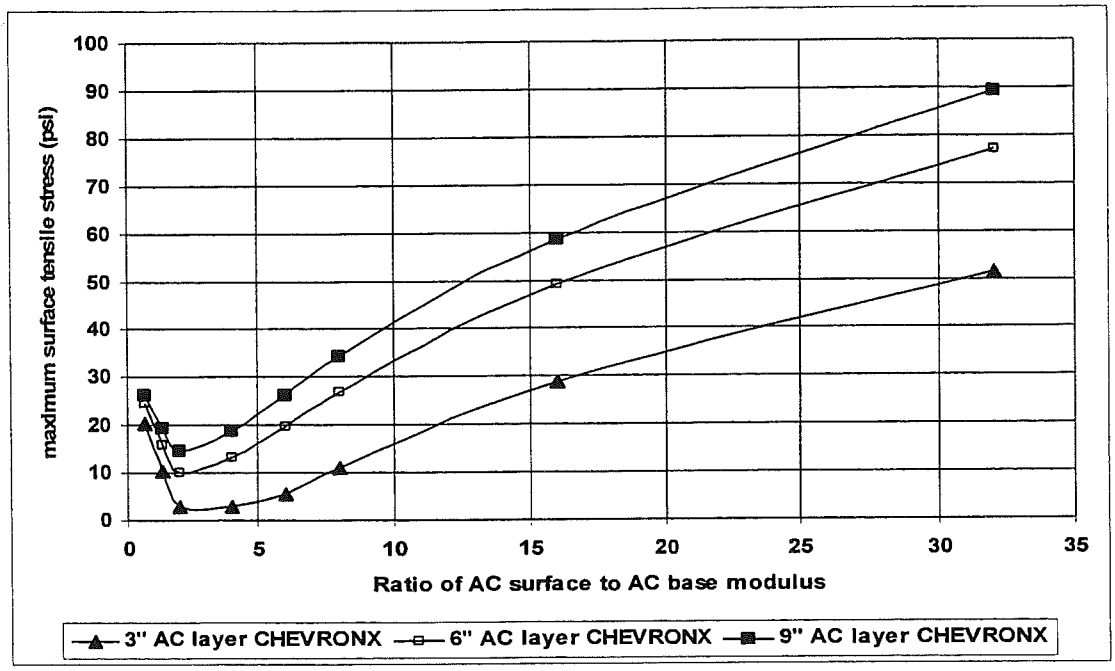

a) Results from CHEVRONX

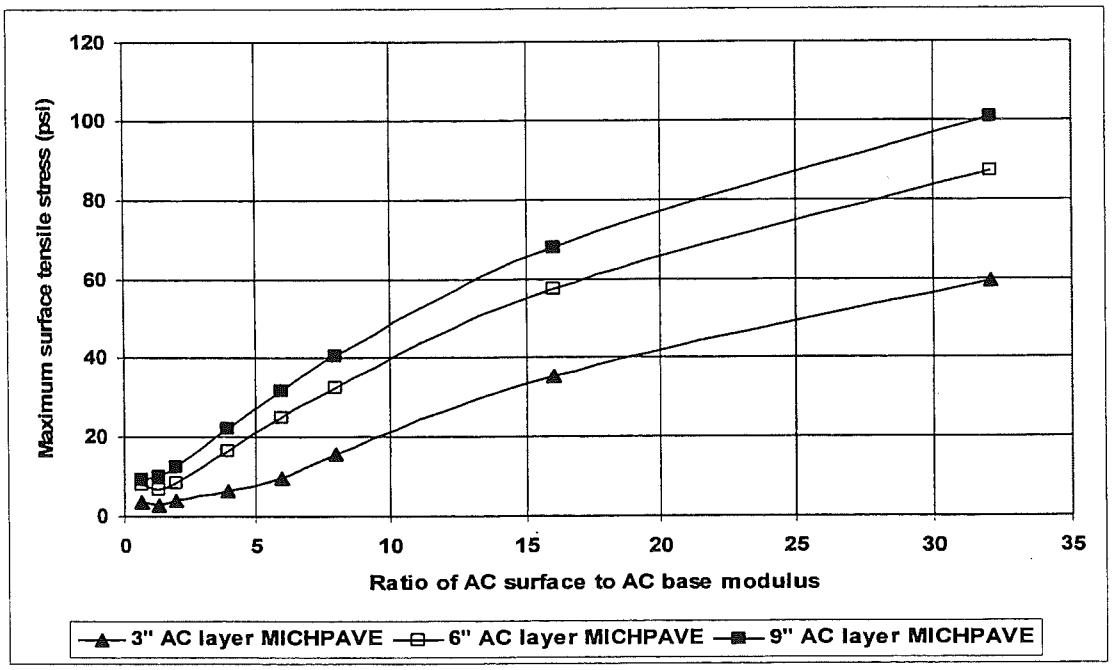

b) Results from MICHPAVE

Figure 7.8 The maximum surface tensile stress on rubblized pavements (base modulus = 100 ksi) with different AC layer thickness as a function of the ratio of the AC surface course to the AC base course moduli

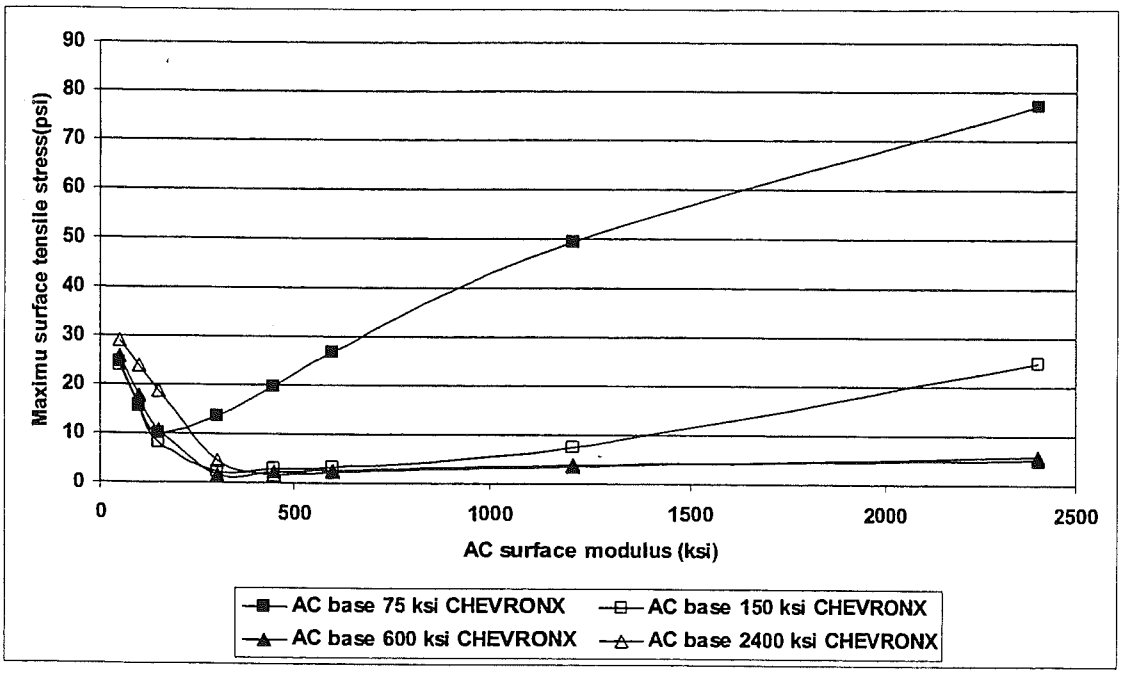

a) Results from CHEVRONX

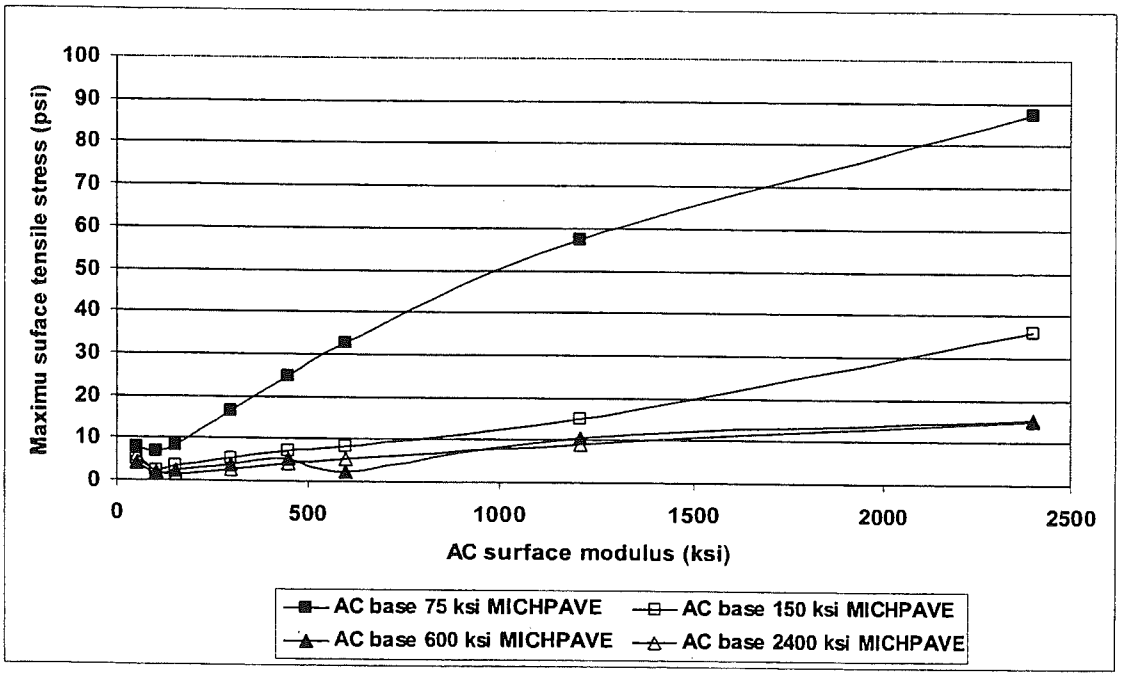

b) Results from MICHPAVE

Figure 7.9 The maximum surface tensile stress on rubblized pavements (base modulus =100 ksi) for different AC base course modulus as a function of the AC surface course modulus

2. Figure 7.6 shows that higher ratios of AC surface to AC base moduli cause higher surface tensile stresses. The high modulus of the AC surface course could be caused by many variables including temperature and age hardening. For example, night time, the temperature of the AC surface course is typically lower than that of the AC base course (a negative temperature gradient); hence, the modulus of the surface course is higher than that of the AC base course. Therefore pavements with higher AC surface modulus due to aging or temperature would have higher TDC potential. This finding supports those reported by Gerritsen et al (1), Wambura et al (2) and Duzauts and Rampal (3), (see Appendix K). The modulus ratio problem could be partially resolved by establishing a balanced asphalt mix design. For example, the asphalt mixes for the AC leveling and base courses could be designed to have higher modulus values than that of the AC mix designed for the surface course. When the pavement is subjected to a negative temperature gradient (lower temperature at the surface of the pavement) the modulus of the AC base course would not be much lower than the modulus of the AC surface course.

3. Two other points can also be deduced by the examination of figure 7.6 as follows:

   b) Higher modulus values of the base layer cause higher surface tensile stress. This is because the combination of a stiff base modulus, a stiff AC surface course modulus and a soft AC base course modulus create what is called a "sandwich model." A soft layer in the middle bordered by two stiff layers. Such a stiff-soft-stiff layer system causes high surface tensile stress.
   c) When the ratio of the AC surface to AC base courses moduli are less than two, the effect of the modulus of the base layer is minimized since the differential stiffness between the AC surface, AC base and the base layer are not high.

4. It can be seen from figures 7.7 and 7.8 that, as was expected, for flexible and rubblized pavements, the thickness of the AC layer has significant effect on the magnitude of the surface tensile stress. In conventional flexible or in full-depth rubblized pavements (figure 7.7) where the base modulus is 30 ksi, increasing AC thickness causes a decrease in the surface tensile stresses. For partial-depth rubblized pavements or for pavements with a stabilized base (figure 7.8) where the modulus of the base layer is 100 ksi, the scenario is reversed and higher AC thickness causes higher surface tensile stress. Note that for all AC layer thicknesses, the thickness of the AC surface course was kept constant at 1.5 in. while the thickness of the AC base course was changed. These findings contradict those reported by Matsuno and Nishizawa (4) and partially support the findings of Uhlmeyer et al (5). However, field observations made during this study indicate that pavements with AC thickness of 4.5 in. or more exhibit TDC, which contradicts the observations of Uhlmeyer et al, that TDC tend to occur in pavements with AC thicknesses of greater than 16 cm (6.3 in.). The crucial point herein is that, in order to minimize the effect of the AC thickness on TDC potential, the ratio of the AC surface to AC base moduli should be less than two. This is the same conclusion as the one stated in the previous paragraph.

5. The data in tables 7.3 through 7.6 and figures 7.5 through 7.9 indicate that all significantly high maximum surface tensile stresses occur between the edge of the tire and 1-ft from the edge of the tire. This finding is supported by field observations of the locations of TDC (see figures 7.19 and 7.20).

4.2 Verification of the Results of the Mechanistic Analysis Using the ABAQUS Program

The CHEVRONX (a close form solution), the MICHPAVE (a 2-D FEM) and the ABAQUS (a 3-D FEM) computer programs were used to analyze a pavement section. The one set of layer thicknesses and the three sets of material properties used in the analyses are listed in table 7.7 under the headings case 1, case 2 and case 3. Results of the analyses are listed in table 7.8. Figure 7.10 depicts three plots of the surface radial stresses obtained from the analysis of case 1 using the three programs. As can be seen from table 7.8 and figure 7.10, the results of the analysis using the ABAQUS program agree very well with the results from the CHEVRONX and the MICHPAVE computer programs. For all three cases, the programs give almost the same magnitudes and locations of the maximum surface tensile stresses. Based on these findings, it was concluded that the results of the 3-D analyses are accurate and comparable to those obtained from the other two programs. Therefore, 3-D analyses of rubblized pavement sections were conducted using the ABAQUS program and the results are discussed in the next section

5.0 MECHANISTIC ANALYSIS USING THE 3-D MODEL AND A DUAL-WHEEL LOAD

The objectives of the 3-D analyses of rubblized pavements using the ABAQUS program are to:

1. Evaluate the effect of the geometry of the interface between the rubblized and the fractured concrete layers on the maximum load-induced surface tensile stresses (TDC potential).

2. Analyze the effect of different differences in temperature within the AC layer on the maximum load-induced surface tensile stress on rubblized pavements with uneven interface between the rubblized and the fractured concrete layers

To accomplish the above objectives, Five3-D finite element models representing rubblized pavement structures were designed and are depicted in figures 7.11 through 7.15. The dimensions of each model were 150 in. in width and length and 100 in. in depth. Due to limitation in the storage capacity of the computer system, the full model was divided along two symmetrical planes into four symmetrical quarters. The dimensions of each quarter were 75 in. in width and length and 100 in. in depth. In all five models, the second tire of the duel wheel is on the right hand side of the figure (the right-hand side mirror image of the figure). In all analyses, the following inputs were used:

Table 7.7 Layer thicknesses and properties of the pavement models used in mechanistic analyses using the CHEVRONX, the MICHPAVE and ABAQUS computer programs

Layers	Thickness (in.)	Elastic modulus (ksi)			Poisson's ratio
		Case 1	Case 2	Case 3	
AC surface	1.5	2,400	1,200	1,200	0.30
AC base	4.5	75	75	150	0.30
Base	9.0	100	100	500	0.25
Subbase	18.0	20	20	20	0.40
Roadbed	67.0	5	5	5	0.45

Table 7.8 Comparison of results of mechanistic analyses using the CHEVRONX, the MICHPAVE and ABAQUS computer programs

	Maximum radial tensile stress	
	Magnitude (psi)	Distance from the center of loaded area (in.)
Case 1		
CHEVRONX	77.0	8.7
ABAQUS	79.6	8.8
MICHPAVE	87.5	9.1
Case 2		
CHEVRONX	49.1	7.8
ABAQUS	52.3	8.0
MICHPAVE	57.8	8.3
Case 3		
CHEVRONX	16.1	6.9
ABAQUS	19.0	7.5
MICHPAVE	29.1	7.4

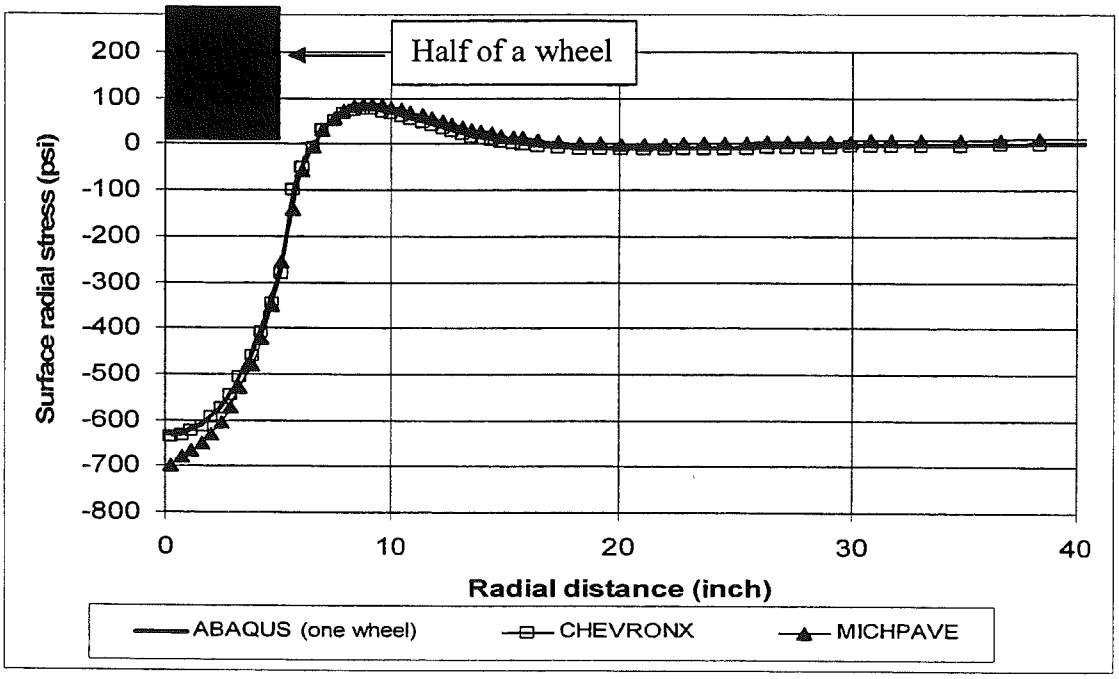

a) Overall view of the three stress zones

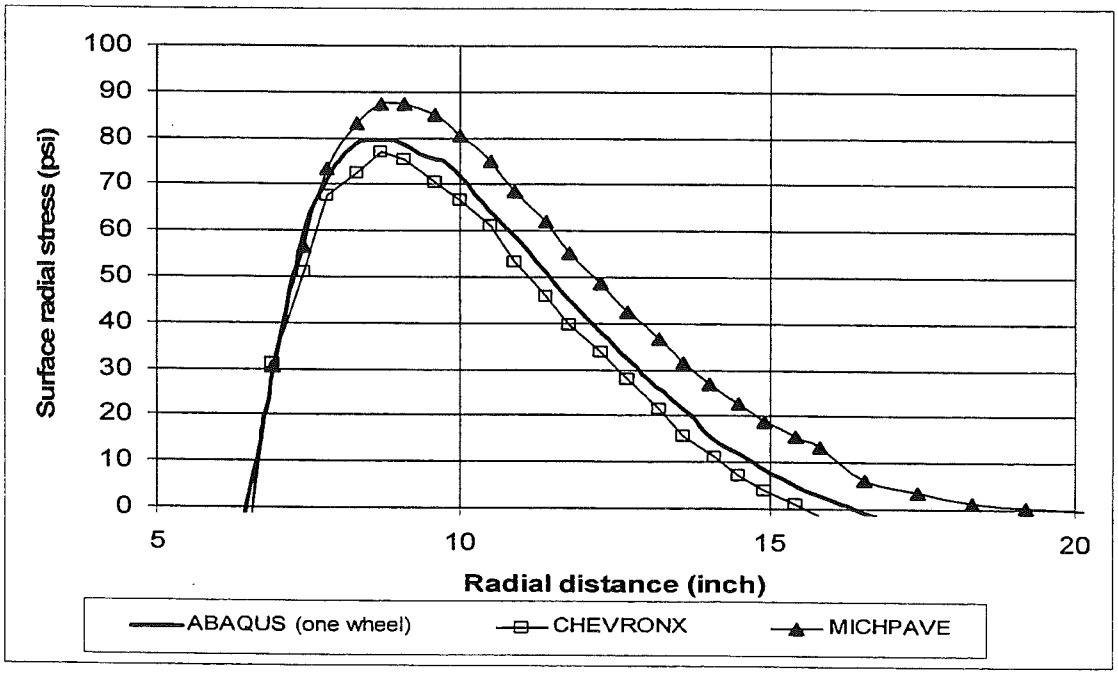

b) Close-up view of the surface tension zone

Figure 7.10 Results of mechanistic analyses of a rubblized pavement subjected to a single-wheel load using CHEVRONX, MICHPAVE and ABAQUS programs

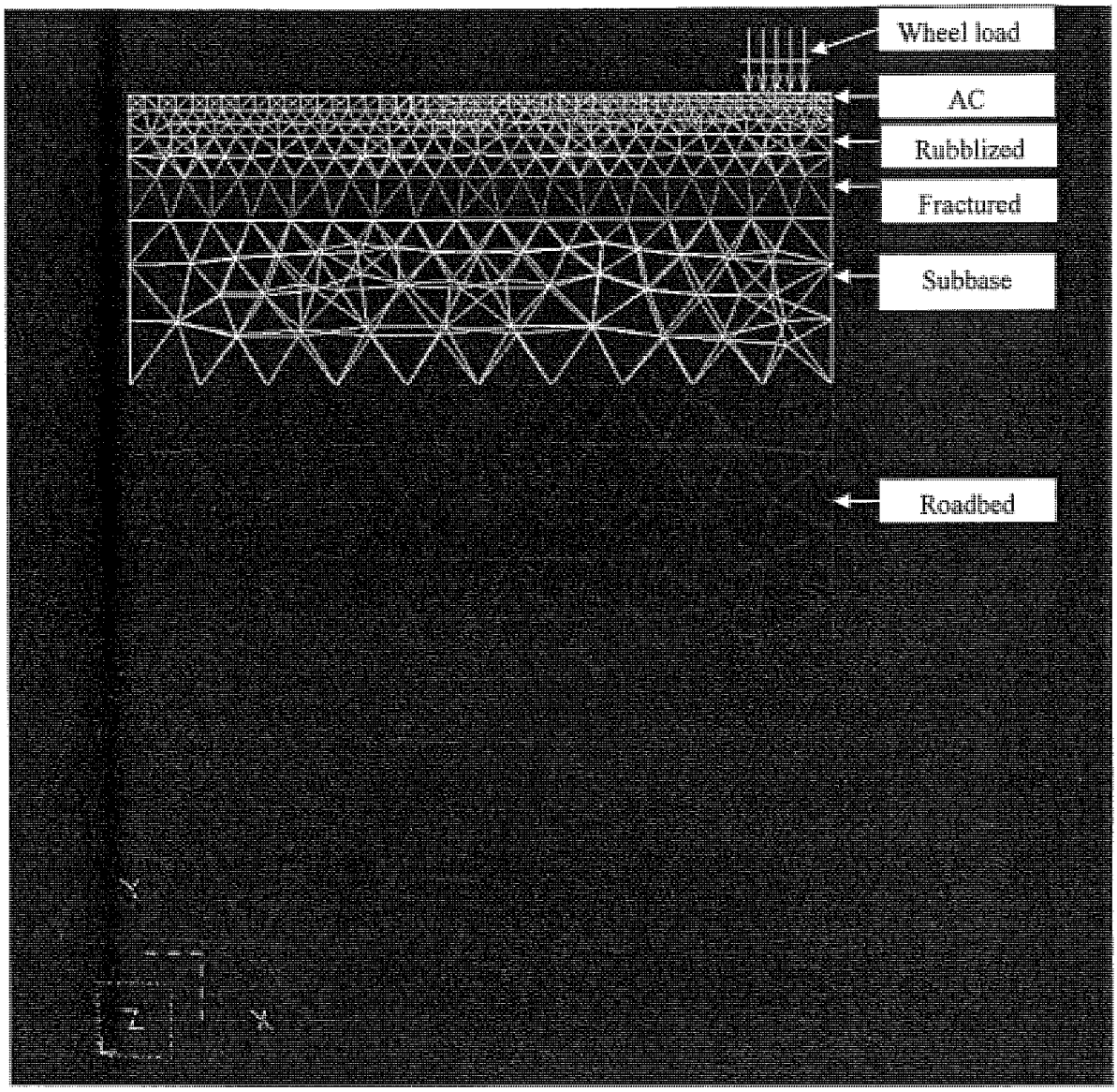

Figure 7.11 The first 3-D model 1 with even interface and equal thickness (4.5 in.) between the rubblized material and the fractured concrete layers

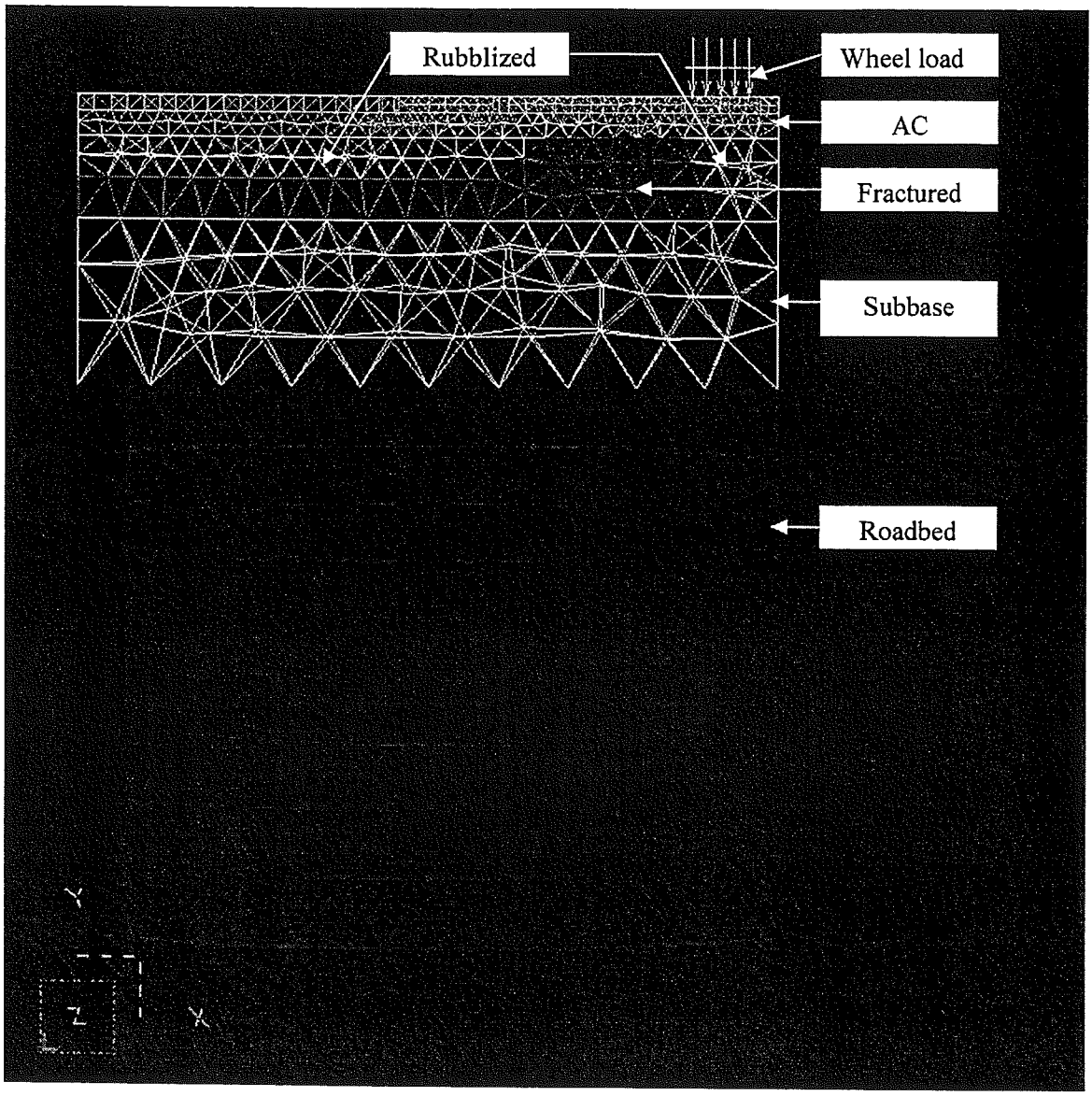

Figure 7.12 The second 3-D model with uneven interface between the rubblized material and the fractured concrete layers and the absence of the fractured concrete layer under the dual-wheel

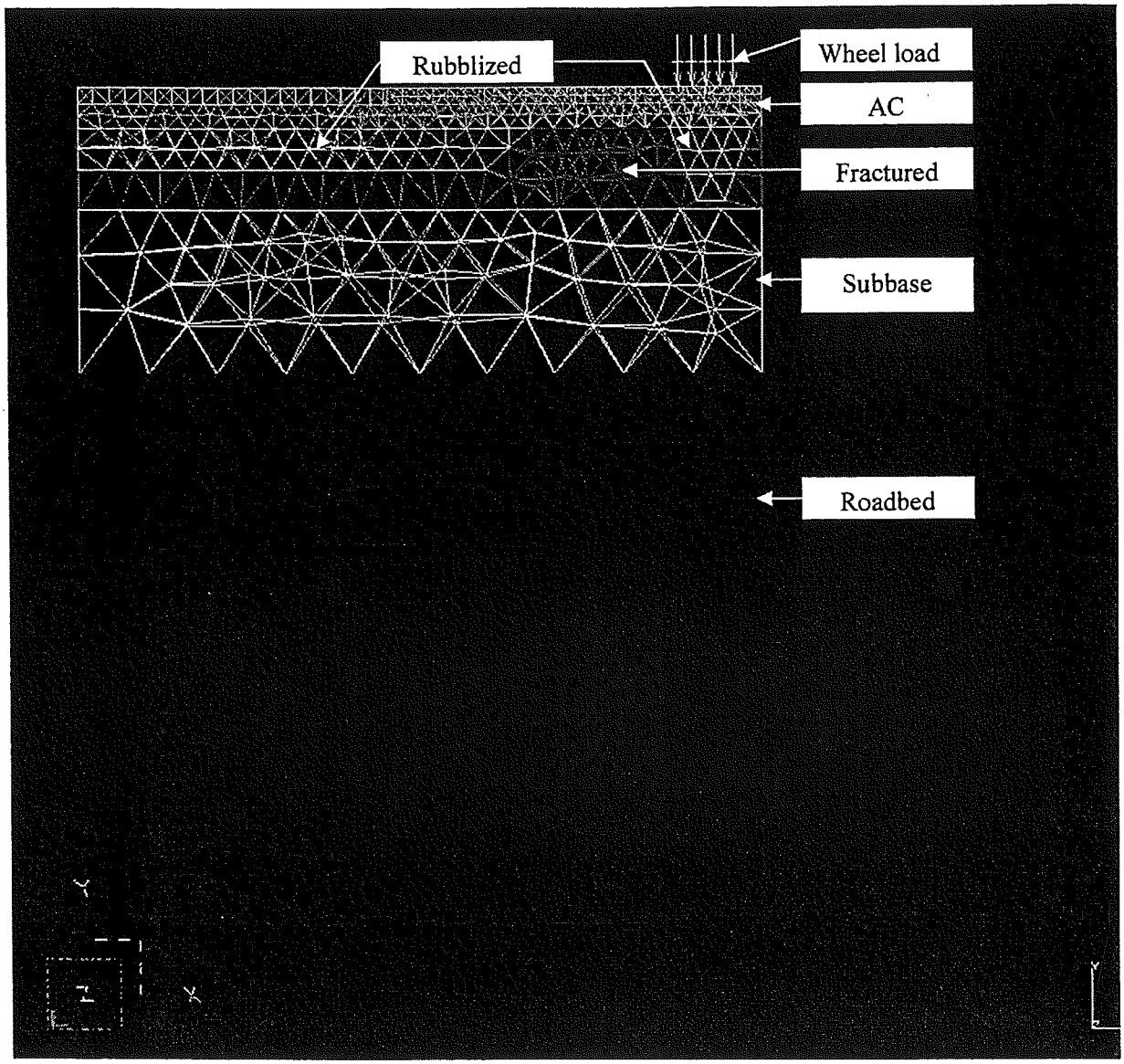

Figure 7.13 The third 3-D model with uneven interface with the presence of fractured concrete under the edges and the center of the dual wheel

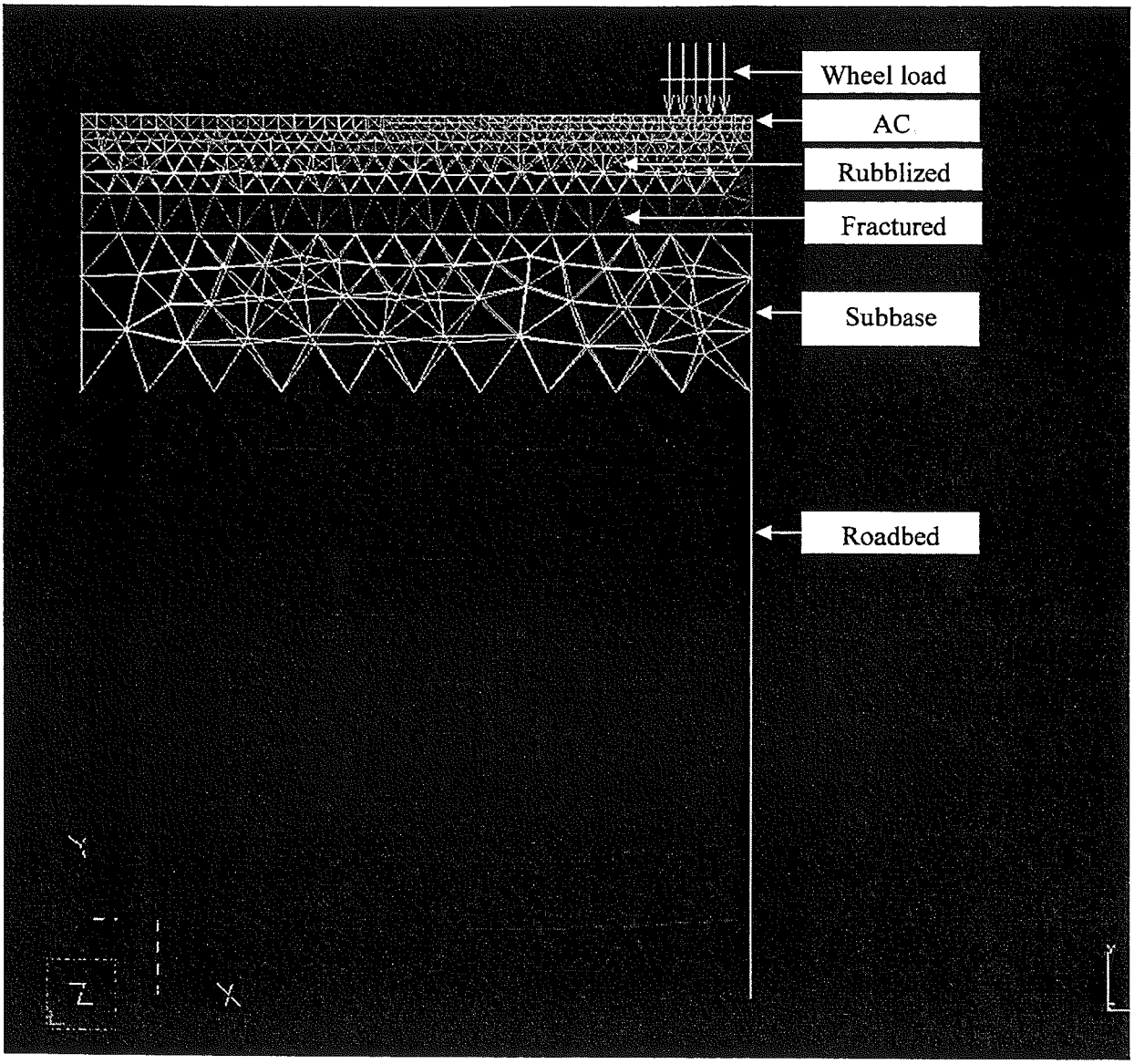

Figure 7.14 The fourth 3-D model with uneven interface with the presence of fractured concrete at the center of the dual-wheel

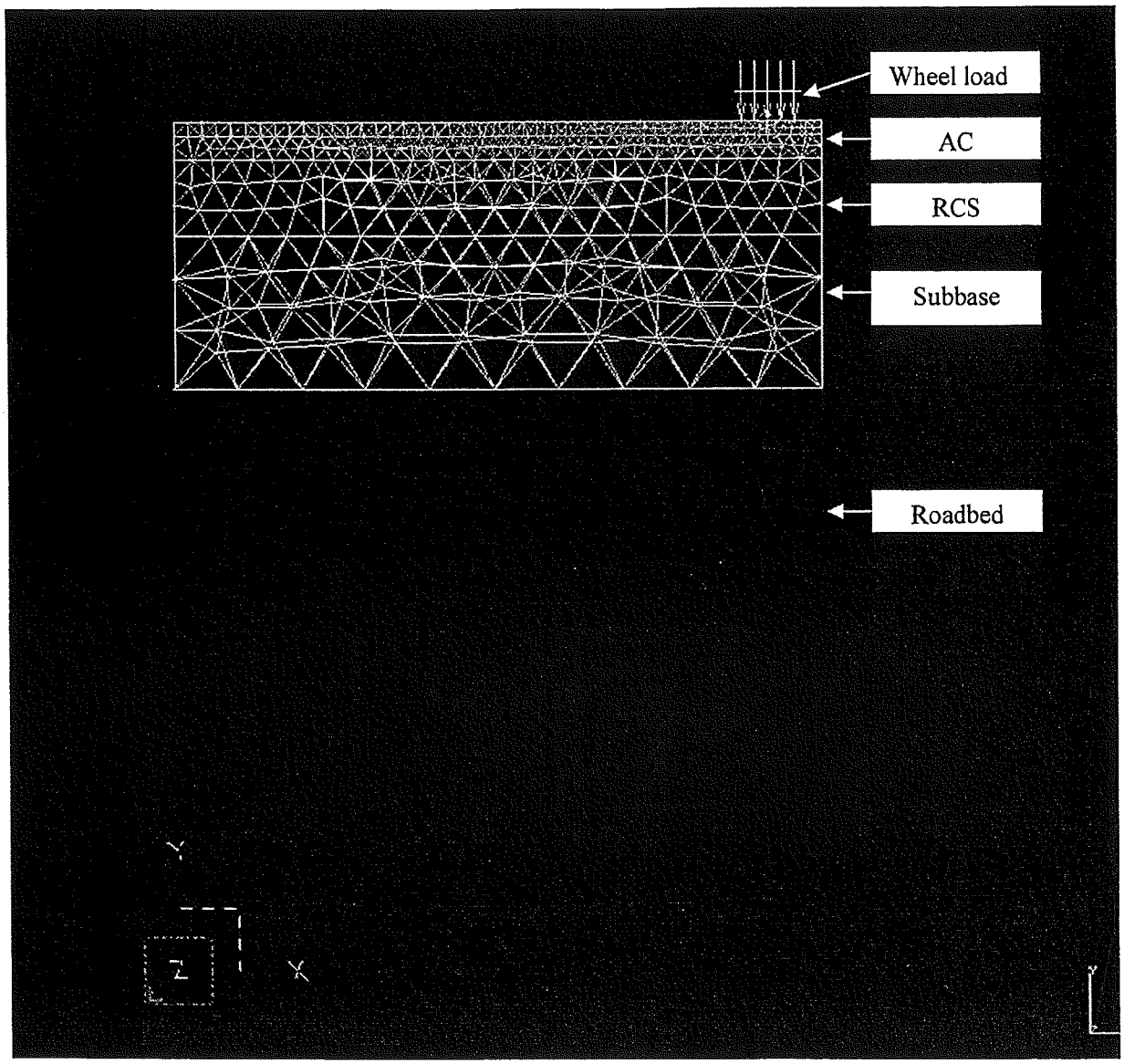

Figure 7.15 The fifth 3-D model with a 9-in. rubblized concrete slab (RCS) representing the rubblized material and fractured concrete layers

A 9000-lb dual wheel load applied to a uniform circular contact area with a radius of 3.785 in. and a tire pressure of 100 psi. The distance between the duel tires was set at 4.43 in.

1. The layer thicknesses and properties of the following four rubblized pavements that were investigated during the Phase II Study:

   - I-69 EB section 1 test site 1, control section 76023 and job number 36020
   - I-75 SB section 1 test site 1, control section 10692 and job number 25559
   - M-15 SB section 1 test site 1, control section 25092 and job number 45534
   - M-37 SB section 6 test site 1, control section 41033 and job number 26691

Each of the five models was used to analyze the effects of certain variable on the maximum surface tensile stress and hence, on TDC potential. Results of the analyses are presented in the next section.

5.1 Results of Mechanistic Analyses Using the 3-D Models

The five 3-D models shown in figures 7.11 through 7.15 were used to conduct detailed mechanistic analyses on the pavement section of I-75, SB, section 1, test site 1. The results of the analyses were divided into two categories as follows:

1. Those results that address the effects of the geometry of the interface between the rubblized material and the fractured concrete layers on the maximum surface tensile stress.

2. Those results that address the effects of differential stiffness in the AC layer (the effects of differences in temperature and/or hardening) on the maximum surface tensile stress.

The two categories are presented below. In addition, after the mechanistic analyses of I-75 SB were completed, the combination of variables (the interface geometry and the differences in temperature) that yielded the highest surface tensile stress were chosen and applied in the mechanistic analysis of the other three pavement sections listed above. Results of the latter analyses are presented in section 5.2.

5.1.1 The Effects of the Geometry of the Interface

Detailed analyses of the effect of different geometry of the interface between the rubblized material and the fractured concrete layers on the maximum load-induced surface tensile stresses were conducted on pavement models representing the rubblized pavement on I-75 SB, section 1 and test site 1. Four different geometries of the interface were used in the analyses as follow:

1. Even interface between the rubblized material and the fractured concrete layers as shown in model 1 of figure 7.11.

2. Uneven interface with the absence of the fractured concrete layer under the dual-wheel as shown in model 2 of figure 7.12.

3. Uneven interface with the presence of fractured concrete at the middle between and at the edge of the dual-wheel as shown in model 3 of figure 7.13.

4. Uneven interface with the presence of fractured concrete at the middle between the dual-wheel as shown in model 4 of figure 7.14.

Further, two 3-D FEM analyses were conducted using the rubblized pavement models with a 9-in. rubblized concrete slab layer as shown in model 5 of figure 7.15. Two modulus values were assigned to the rubblized concrete slab to simulate the following scenarios:

1. A full depth rubblized material layer was simulated through the assignment of a 27,000-psi modulus value to the 9-in. thick rubblized concrete slab.

2. A full depth fractured concrete layer was simulated using a 1,174,000-psi modulus value to the 9-in. thick rubblized concrete slab layer.

In all analyses, negative differences in temperature were assigned to the AC layer such that the AC surface course temperature was 60^0F and the AC base course temperature was 90^0F. The temperature corrected moduli of the AC surface and base courses were calculated using equation 7.1 (6).

$$E_T = E_{20} / 10^{0.0224(T-20)} \qquad (7.1)$$

where

E_T = elastic modulus of the AC course at temperature T ^{0}C
E_{20} = the AC modulus at the standard temperature of 20°C (68°F), which was obtained from the backcalculated and temperature corrected modulus

Results of the 3-D analyses are summarized in table 7.9. Figures 7.16 and 7.17 show the load-induced surface tensile stress as a function of the radial distance from the center of the loaded area (the center of the duel wheel). Examination of the results of the analyses listed in table 7.9 and depicted in figures 7.16 and 7.17 indicates that:

1. Pavement model 2 (uneven interface between the rubblized material and the fractured concrete layers, the duel wheel is setting on a pool of rubblized material and the fractured concrete extends to the bottom of the AC layer at the outer edges of the tires) yielded the highest load induced surface tensile stress. This model simulates the pavement section shown in figure 7.1, depicted in figure 7.2 and the 3-D analysis model is shown in figure 7.12. The maximum load-induced surface tensile stress obtained from model 2 is 86.8 psi. This tensile stress magnitude is much higher than that obtained from

Table 7.9 A summary of the results obtained from 3-D FEM analyses with 6 different conditions of the rubblized concrete slab

Geometry / thickness of the rubblized material	Temperature (°F)		Modulus (ksi)		Maximum surface radial tensile stress	
	AC surface	AC base	AC surface	AC base	Location (in.)	Magnitude (psi)
Even interface and equal thickness between two layers (model 1)	60	90	1,631	690	17.3	20.0
Uneven interface with the absence of fractured concrete under the dual-wheel (model 2)	60	90	1,631	690	11.5	86.8
Uneven interface with the presence of the fractured concrete at the middle and at the edges of the dual-wheel (model 3)	60	90	1,631	690	0.7	77.3
Uneven interface with the presence of the fractured concrete at the middle of the dual-wheel (model 4)	60	90	1,631	690	24.6	43.6
Full depth rubblized material (model 5)	60	90	1,631	690	24.6	29.3
None rubblized material (full depth fractured concrete), (model 5)	60	90	1,631	690	52.8	1.74

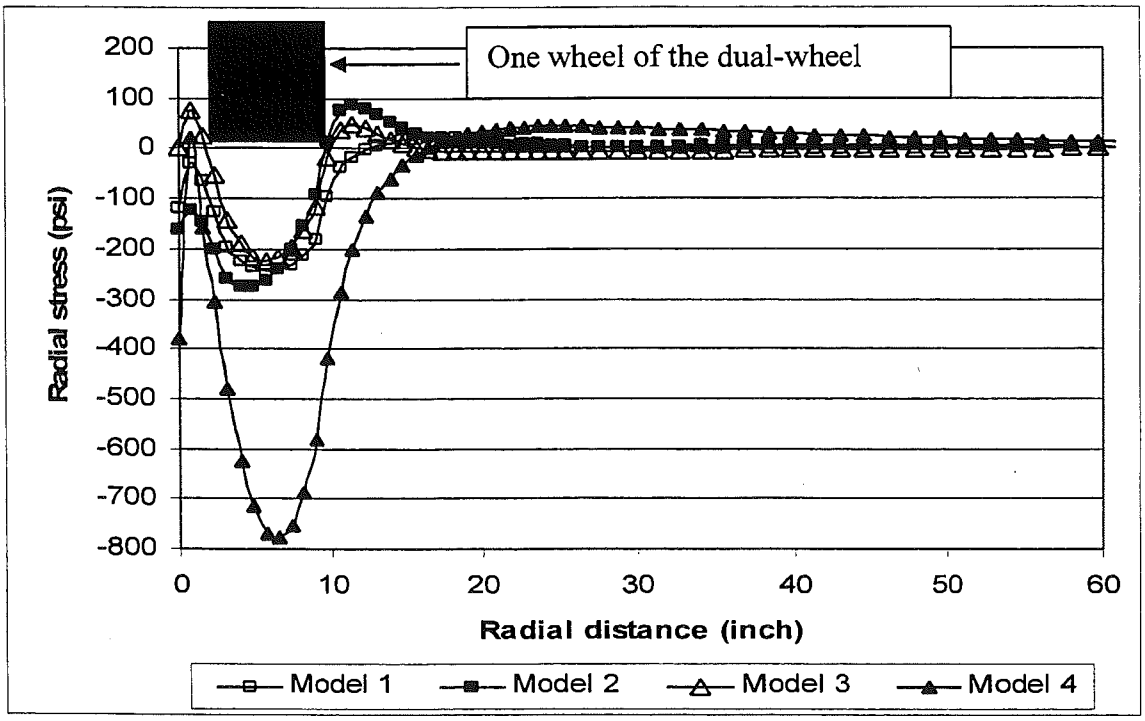

Figure 7.16 Variation in the surface radial stress with the radial distance from the center of the load (analyses of models 1 through 4)

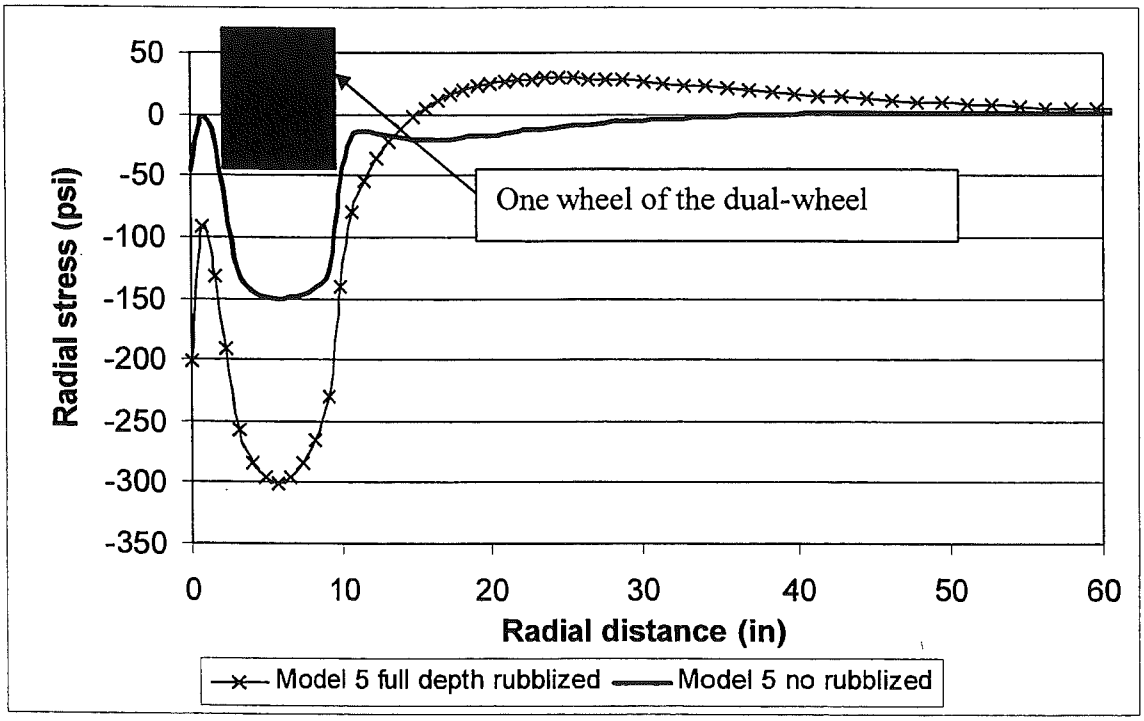

Figure 7.17 Variation in the surface radial stress with the radial distance from the center of the load (analyses of model 5)

model 1, which simulates even interface and equal thickness between the rubblized and the fractured concrete layers. The latter model produced maximum load-induced surface tensile stress of only 20.0 psi.

2. The location of the maximum surface tensile stress in model 2 is 11.7 in. from the center of the load. It is just to the left of the edge of the wheel, which is about 10 in. from the center of the load. For a full depth fractured concrete layer (no rubblized material), the location of the maximum surface tensile stress obtained from the other models, except models 3 and 5, varies from the edge of the wheel to 15 in. away from the edge of the wheel. These locations are similar to those of the maximum surface tensile stress found for the single wheel load case reported in the previous section. The location of the maximum load-induced surface tensile stress for model 3 is at the middle between the two tires (the center of the dual-wheel). This scenario implies that the TDC potential exists in and around the wheel paths. These are the exact locations where TDC were found in real pavements.

3. Although model 5 with full depth fractured concrete or no rubblized material produces low load-induced surface tensile stress, which indicates low TDC potential, it does not mean that this model represents a good rubblized pavement. Since the rubblization operation delivered no rubblized material to the rubblized concrete slab, the integrity of the slab and joint were not destroyed, that is the main objective of the rubblization operation has not been accomplished. As a result, reflective cracks will develop in this pavement within a relatively short period of time.

Based on the above 3-D analyses the geometry of the interface in model 2 has been selected as the critical condition that will create the highest load-induced surface tensile stress. Therefore, model 2 was used to further analyze the effects of differences in temperature within the AC layer on the load-induced surface tensile stress in rubblized pavement. The results of such analyses are presented in the next section.

5.1 The Effects of Differences in Temperature on Load-Induced Surface Tensile Stress

First, recall that the properties of asphalt mixes are temperature dependent. The mix becomes stiff and solid at low temperatures and soft and viscous at higher temperatures. In the field, the temperature in the asphalt layer varies from top to bottom. Hence, temperature gradient exists in the asphalt layer most of the time. As noted earlier, the temperature gradient could be positive where the AC surface course is hotter than the AC base course (day time gradient) or negative (night time gradient) with a reversed temperature scenario. The effects of temperature gradient on the load-induced stresses in rubblized pavements was studied by using different modulus values for the AC surface and AC base courses. For example, for the single wheel load that was analyzed using the CHVERONX and the MICHPAVE computer programs, the effects of the temperature gradients in the AC layers were simulated by

differential stiffness (modulus ratio between the AC surface and AC base courses). The results were reported in the previous section. Similarly, in the 3-D analysis, the AC layer was divided into two courses; AC surface and AC base courses. Each course was assigned a temperature and its modulus at that temperature was calculated using the backcalculated modulus value and equation 7.1. Four temperature scenarios were assigned to the AC surface/AC base courses as follows 60°F/80°F, 60°F/70°F, 30°F/60°F and 90°F/120°F and their respective modulus values were calculated. These four temperature scenarios are in addition to the 60°F/90°F scenario that was already analyzed in the previous section. In the analyses of the four temperature scenarios, model 2 shown in figure 7.12 was used. Table 7.10 provides a list of the results of the analyses and figure 7.18 shows the relationship between the differences in temperature and the maximum load-induced surface tensile stress. Examination of the results in table 7.10 and figure 7.18 indicates that, for the same temperature of the AC surface course, the maximum load-induced surface tensile stress increases with increasing negative differences in temperature between the two AC courses. Further, figure 7.18 clearly shows that the maximum load-induced surface tensile stress is linearly related to the differences in temperature between the AC courses. This is because the temperature of the AC surface course for the three data points making-up the straight line in the figure was held constant at 60oF while the AC base course temperature was increased from 70 to 80 and to 90°F. The two data points in the figure that are at a temperature difference of –30°F and are outside the straight line belong to an AC surface course at temperatures of 30 and 90°F. Hence, for the same temperature difference, the maximum load-induced stress is not the same. Stated differently, the effect of differences in the temperature between the AC surface and the AC base courses on the maximum load-induced surface tensile stress is a function of the magnitude of the difference in temperature and the reference temperature of the AC surface course.

The above scenario could also be explained using the data in table 7.10. The data in the table is divided into two groups; a constant AC surface temperature and a variable AC surface temperature. As can be seen from the table, three pavement sections with the same temperature difference of -30°F (30°F/60°F, 60°F/90°F and 90°F/120°F) lead to the same ratio of the AC surface and AC base moduli but not the same maximum load-induced surface tensile stress. Hence, the maximum load-induced surface tensile stress cannot be expressed as a function of the modulus ratio.

5.2 Implementation - Mechanistic Analysis of Four Rubblized Pavements

The results of the mechanistic analyses presented and discussed in the previous sections were based on assumed but reasonable modulus values of the various pavement layers. As stated earlier, the main objective was to discuss the sensitivity of the TDC potential to various input variables. Such variables reflect variations in the rubblization process, construction, material properties and the environment. In this section, results of mechanistic analyses of four rubblized pavement sections are discussed.

Table 7.10 A summary of the results of 3-D FEM analyses with 5 temperature gradients

Geometry of the interface	Temperature profile	Temperature (°F)		Difference in temperature (°F)	Modulus (ksi)		Modulus ratio	Maximum surface radial tensile stress	
		AC surface	AC base		AC surface	AC base		Location (in.)	Magnitude (psi)
Uneven interface with the absence of fractured concrete under the dual-wheel	Constant AC surface course temperature and variable AC base course temperature	60	70	-10	1,631	1,225	1.33	11.5	63.6
		60	80	-20	1,631	919	1.77	11.5	74.9
		60	90	-30	1,631	690	2.36	11.5	86.8
	Variable AC surface and base courses temperature	30	60	-30	3,852	1,631	2.36	12.3	73.6
		60	90	-30	1,631	690	2.36	11.5	86.8
		90	120	-30	690	292	2.36	11.5	80.1

Table 7.11 Layer thickness and layer properties of four rubblized pavements

Pavement	Thickness (in.)				Modulus (ksi)					
	AC surface	AC base and leveling	Total AC	Base	AC surface course at 60F	AC base and leveling at 90F	Rubblized material	Fractured concrete	Base	Roadbed soil
I-69	1.50	6.70	8.2	16	492	301	65	256	25	14
I-75	1.7	2.80	4.5	18	1,631	690	27	704	17	17
M-15	1.50	4.00	5.3	12	2,861	1,130	27	183	37	20
M-37	1.60	4.10	5.7	12	3,129	1,212	90	592	38	16

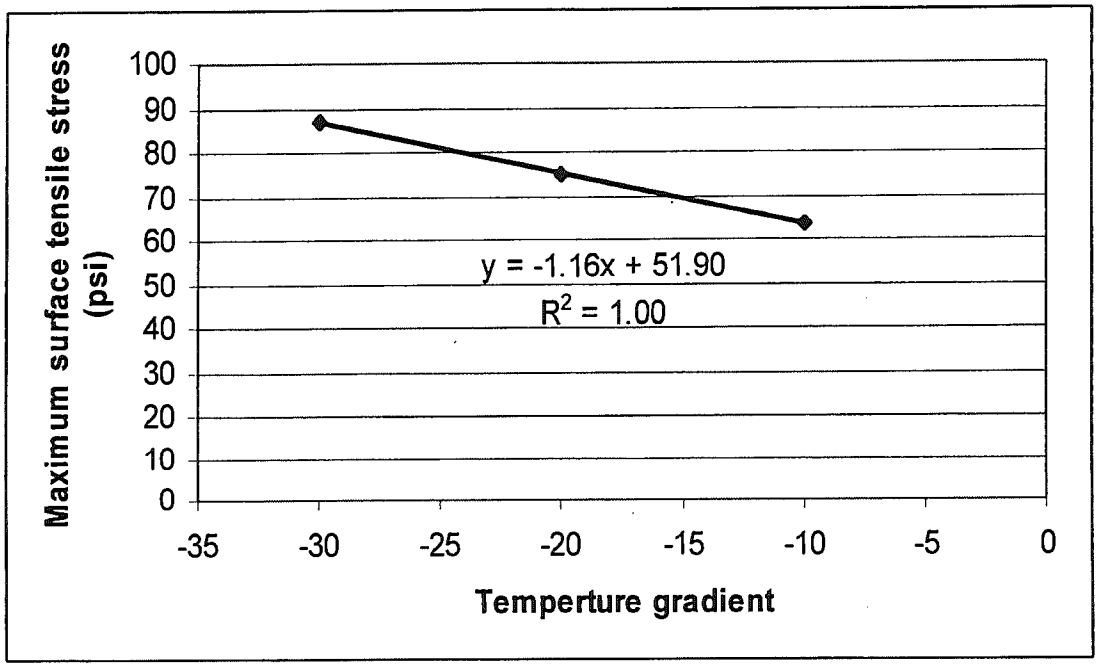

Figure 7.18 Relationship between temperature gradient and the maximum surface tensile stress

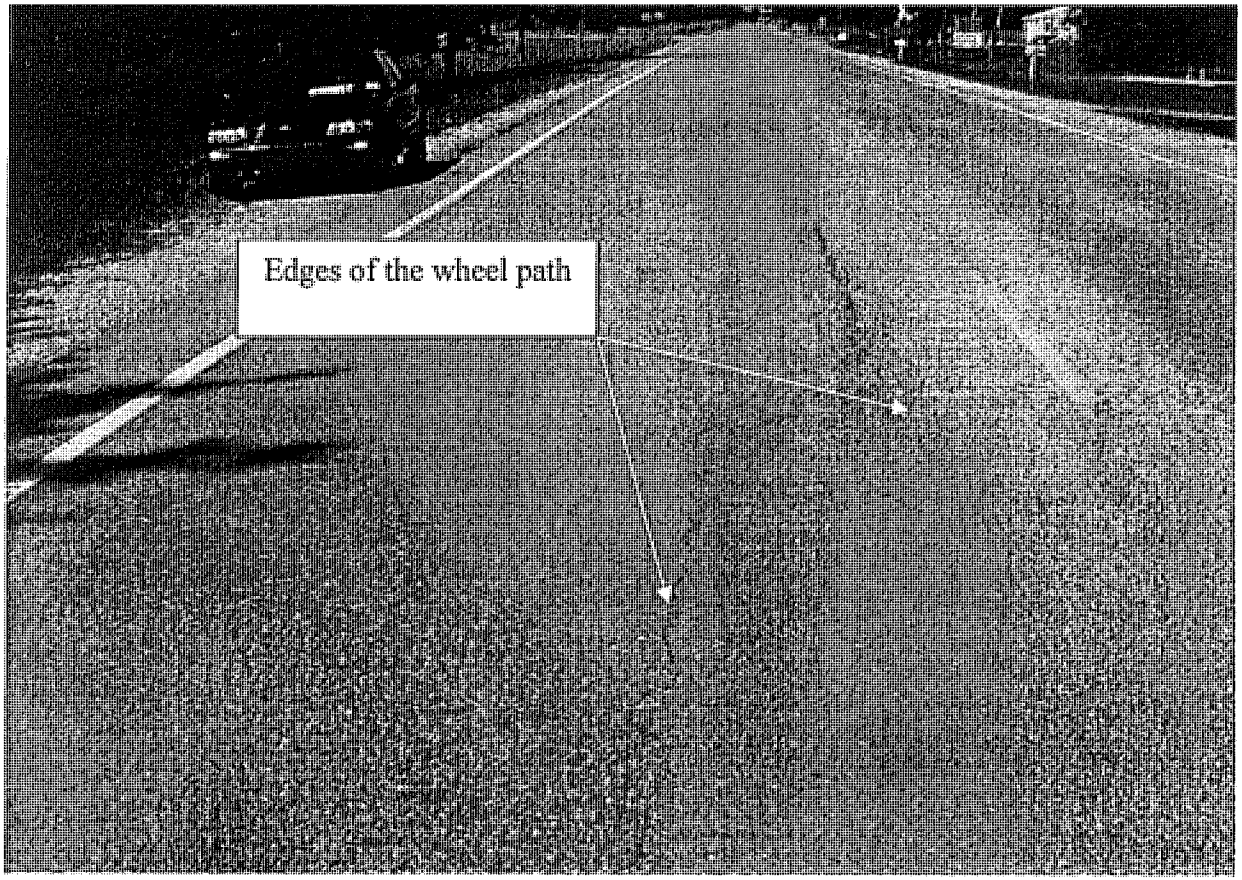

Figure 7.19 Longitudinal top-down cracks at the edges of the wheel path on Saginaw road, CS 36555, JN 35266, August 2001

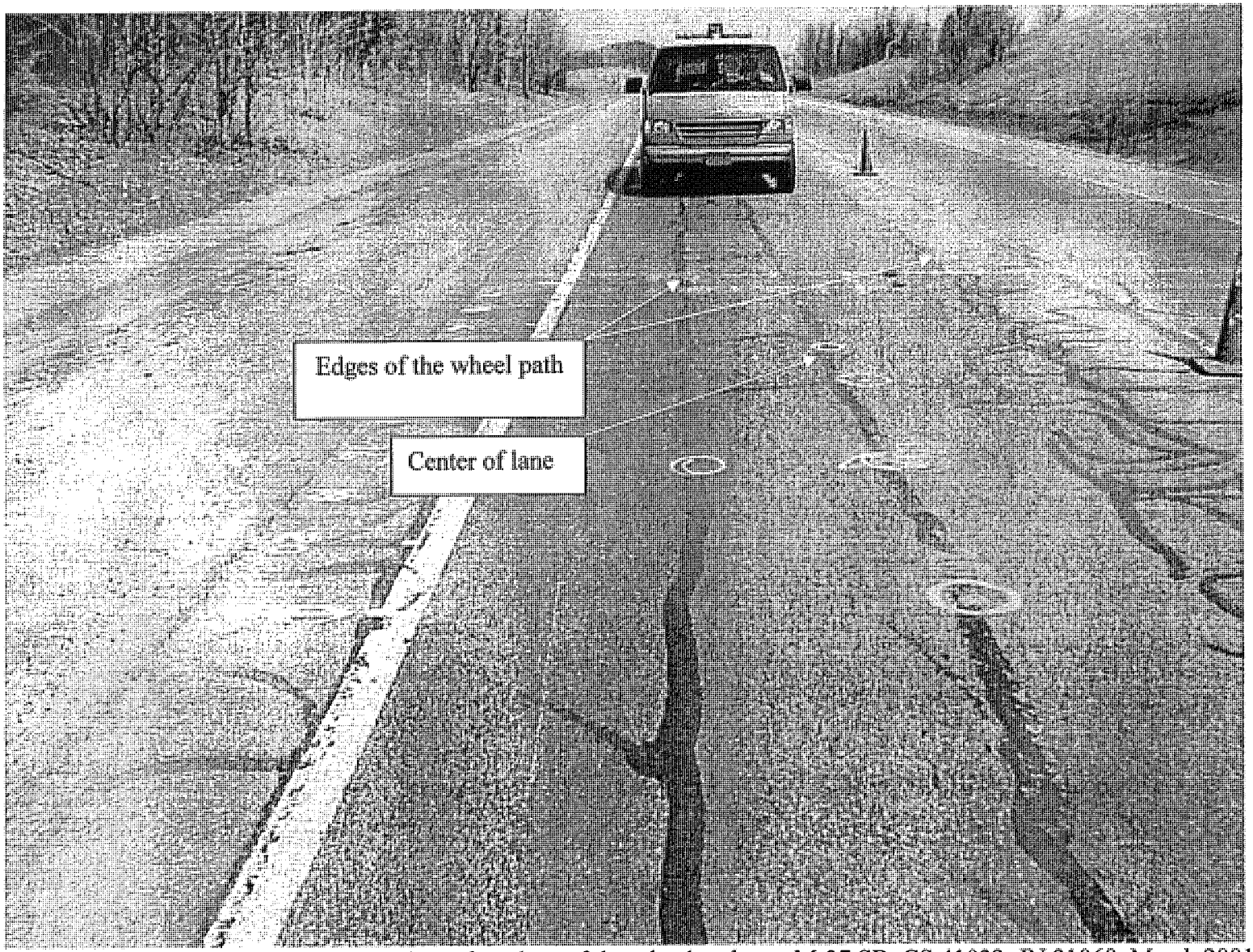

Figure 7.20 Longitudinal top-down cracks at the edges of the wheel paths on M-37 SB, CS 41033, JN 31068, March 2001

In the 3-D analyses of the maximum load–induced surface tensile stress of the four rubblized pavement sections of table 7.11, the geometry of the interface between the rubblized material and the fractured concrete layers of the fifth 3-D model (see figure 7.15) was selected and used. For each pavement section, the moduli of the AC surface and the AC base courses were refigured based on their assigned temperatures of 60°F and 90°F, respectively (a typical night time temperature gradient). The refigured modulus values of the AC courses and the layer thicknesses used in the analyses are listed in table 7.11. Note that the selection of the interface geometry and the temperature difference between the AC surface and the AC base courses was based on:

1. Two and three dimensional analyses of the load-induced surface tensile stress using various interface geometry. The selected interface geometry yielded relatively high tensile stresses.

2. Field observations of rubblized concrete pavements where, prior to placing the AC layer, trenches were excavated in the rubblized material layer to expose the fractured concrete layer (see figures 7.1 and 7.2).

3. Field measurements of night time temperatures of the AC surface and the AC base courses.

In the analyses, the average AC core thickness and the actual thicknesses of the other pavement layers were used. Results of the 3-D mechanistic analyses of the four pavement sections are summarized in table 7.12. The load-induced surface tensile stress on the I-75 section is the highest among the four pavements. This is because the pavement section on I-75 has the lowest rubblized material modulus compared to the other sections. Given the high AC modulus, low rubblized material modulus and high fractured concrete modulus, the effects of the stiff-soft-stiff layers (the sandwich model) on the surface tensile stress is very high. Although the pavement section on M-37 has a rubblized material modulus close to that of the I-75 section, the modulus of the fractured concrete layer is much lower. Hence the effect of the stiff-soft-stiff system is also much lower. Likewise, the AC modulus on the I-69 pavement section is the lowest among the other three sections; this implies lower effects of the sandwich model and, hence, lower surface tensile stress.
Indeed, among the four pavement sections, the I-69 section is the only pavement free of TDC. Based on the distress surveys conducted in 2001 and 2002, the other three sections exhibit TDC that were initiated within medium or high degree segregated areas and have propagated outward. For the I-75 pavement section only, TDC were also found outside the segregated areas. However, the cracks were tighter and exhibited less associated distresses than the ones located within the segregated areas. The implication of this last observation is that TDC in segregated areas were initiated and propagated at much earlier time than those outside the segregated areas.

Note that the thickness and moduli of the pavement layers, especially the rubblized material and the fractured concrete layers, vary from one location to the others. At certain locations the combination of the thicknesses and moduli of the rubblized and fractured concrete layers create more favorable condition for the initiation of

Table 7.12 A summary of the results of 3-D FEM analyses of four rubblized pavements

Pavement	Geometry of the interface	Temperature (°F)		Modulus (ksi)		Maximum surface radial tensile stress	
		AC surface	AC base	AC surface	AC base	Location (in.)	Magnitude (psi)
I-69	Uneven interface with the absence of fractured concrete under the dual-wheel	60	90	492	301	12.1	16
I-75		60	90	1,631	690	11.5	87
M-15		60	90	2757	1089	14.3	25
M-37		60	90	3129	1212	12.3	25

Table 7.13 Applied stress ratio, existence of TDC, degree of segregation and the pavement/surface age for four rubblized pavements

Pavement	Maximum tensile stress (psi)	Indirect tensile strength (psi)	Stress ratio	TDC	Degree of segregation	Pavement/surface age (years)
I-69	16	97	0.16	No	Low	4
I-75	87	146	0.59	Yes	High	13
M-15	25	172	0.14	Yes	Medium	4
M-37	25	143	0.17	Yes	Medium	10

TDC than in other locations. They cause increases in the magnitude of the maximum load-induced surface tensile stress. Hence, the magnitude of the maximum load-induced surface tensile stress listed in table 7.12 may not be the absolute maximum along the pavement section. The results in the table are based on the average values of the layer thicknesses and moduli, which may not be the optimum conditions for the initiation of TDC.

6.0 CAUSES OF TOP-DOWN CRACKS ON THE FOUR PAVEMENT SECTIONS

Results of the 3-D mechanistic analyses of the four pavement sections discussed in the previous section, and the distress data obtained from two distress surveys that were conducted in 2001 and 2002, indicate that the TDC on the three pavement sections along I-75, M-37 and M-15 are caused by the construction and rubblization processes. Construction of the AC caused segregation whereas the rubblization process created differential stiffness between the pavement layers.

The potential for the initiation of TDC depends on the ratio of the applied stress to the available tensile strength of the AC mix (also called the stress ratio). Such ratio can be calculated using the following equation.

$$\text{Stress ratio} = \text{Maximum surface tensile stress} / \text{Tensile strength} \qquad (7.2)$$

Table 7.13 provides the stress ratio and some other information of the four rubblized pavements. As can be seen from the table, only the pavement section along I-69 does not exhibit TDC. Although the pavement age and the stress ratio of the I-69 section are very similar to the M-15 section, the degree of segregation on M-15 section is higher than that on I-69 section. Segregation is a factor that significantly affects the stress ratio and the initiation of TDC. In the area where the pavements experience segregation, the tensile strength of the AC mix will substantially lower than in non-segregated areas. Note that the tensile strengths reported in table 7.13 and in the other tables in this report were obtained from laboratory testing of AC cores that were extracted from non-segregated areas. Hence, the actual stress ratio of the four rubblized pavement sections could be much lower than the values reported in table 7.13.

Finally, it would be of interest to monitor the pavement performance along the I-69 section. Although the pavement did not exhibit any type of distress as of the last distress survey of 2002, the section has been capped by a relatively dry AC mix having high air voids and low tensile strength. It is likely that TDC and other distress (e.g., rut) may initiate on this section within few years.

7.0 SUMMARY

Two- and three- dimensional finite element analyses were conducted on various rubblized pavement sections using various techniques to model the geometry of the interface between the rubblized material and the fractured concrete layers. A single and a dual wheel loads were used in the analyses. The results indicate that:

1. The magnitude and location of the maximum load-induced surface tensile stress are functions of the following variables:

   - Layer thickness and properties
   - Geometry of the interface between the rubblized material and the fractured concrete layers
   - Load configurations

2. The interface geometry between the rubblized material and the fractured concrete layers has a significant impact on TDC potential. For example, analysis of the I-75 section using model 1 (even interface) yielded maximum surface tensile stress of only 20 psi whereas model 2 (uneven interface) produced maximum surface tensile stress of 87 psi.

3. Higher temperature differences between the AC surface and the AC base courses cause increases in the maximum surface tensile stress.

4. For a single wheel loads, the location of the maximum surface tensile stress is in the vicinity of the edge of the tire. For a dual wheel load, the location of the maximum surface tensile stress could be either at the center of the dual or in the vicinity of the tire edges. The exact location is a function of the pavement layer thickness and properties and the geometry of the interface between the rubblized and the fractured concrete layers. These locations agree very well with the locations of the TDC observed during the field investigation.

5. Segregation is a very important construction factor affecting the TDC potential. Segregation causes decrease in the AC tensile strength and increases in the stress ratio. The latter decreases the fatigue life of the mix. In this regard, note that during the 2002 distress survey of rubblized pavements, 42 pavement sections exhibited medium or high degree of segregation out of the 48 pavement sections that exhibited longitudinal TDC. Further, all transverse TDC were located within segregated areas.

REFERENCES

1. Gerritsen, A.H., C. A. P. M. van Gurp, J. P. J. van der Heide, A. A. A. Molenaar and A. C. Pronk. Prediction and Prevention of Surface Cracking in Asphaltic Pavements, Proc. 6th International Conference on the Structural Design of Asphalt Pavements, Ann Arbor, 1987

2. Dauzats, M., and A. Rampal. Mechanism of Surface Cracking in Wearing Courses, Proc. 6th International Conference on the Structural Design of Asphalt Pavements, Ann Arbor, 1987

3. Wambura, J. H. G., J. Maina and H. R. Smith. Kenya Bituminous Materials Study. In Transportation Research Record 1681, TRB, National Research Council, Washington, D.C., 1999, pp. 129-137

4. Matsuno, S., and T. Nishizawa. Mechanism of Longitudinal Surface Cracking in Asphalt Pavement, Proc. 7th International Conference on the Structural Design of Asphalt Pavements, Ann Arbor, 1992

5. Myers, L. A., R. Roque, and B. E. Ruth. Mechanisms of Surface-Initiated Longitudinal Wheel Path Cracks in High-Type Bituminous Pavements. Journal of the Association of Asphalt Paving Technologists, Vol. 67 pp. 401-432, 1998

6. Buch, N., R. S. Harichandran, G. Y. Baladi, D. Park, and H. Kim. Calibration of Michpave's Rut and Fatigue Distress Models and Development of an Overlay procedure in Michback, Research Report RC-1383 , Michigan Department of Transportation, 1999

CHAPTER 8
CONCLUSIONS AND RECOMMENDATIONS

Based on the results of the laboratory and field investigation, analyses of the FWD and the laboratory test data, various conclusions were drawn and recommendations were made. These conclusions and recommendations can be divided into four categories as follows:

1. General

2. Factors influencing the performance of rubblized concrete pavement

   - Project selection
   - The rubblization process
   - The construction procedure
   - The pavement design process
   - The pavement materials
   - Traffic

3. The MDOT special provision for rubblization of concrete pavements

4. Rubblized pavement design parameters

The conclusions and recommendations for each of the above four categories are presented below.

1.0 GENERAL CONCLUSIONS AND RECOMMENDATIONS

During the study, the performance of every MDOT rubblized pavement project in the state of Michigan was studied. In the mean time, in a parallel study, the performance of several conventional asphalt pavement projects was also analyzed. Based on both studies, the following conclusions were made:

1. Rubblization of deteriorated concrete pavements is a viable rehabilitation option that requires more detailed quality control measures than conventional asphalt pavements. That is the performance of rubblized concrete pavements appears to be more sensitive to variation in various pavement parameters than conventional asphalt pavements. Therefore, it is strongly recommended that quality control measures be revisited, tightened and strictly enforced. For example, the MDOT special provision for rubblizing concrete pavements should be modified to include the recommended calibration scheme and should be strictly enforced. Another example is that medium and heavy segregated areas should be milled and repaved.

2. Various distress types that affect the performance of rubblized concrete pavements such as top-down longitudinal and transverse cracking and raveling were also found, but to a slightly lesser extent, on various conventional asphalt pavement projects. In most cases, the TDC were located in segregated areas.

3. Based on several observations of the rubblization operations of the sonic and the multi-head breaker and on the finding in the excavated trenches, it is concluded that the sonic and the multi-head breaker did not deliver the best possible quality of rubblized concrete. In this regard, the sonic breaker delivers, on average, better and more uniform rubblized products than the multi-head breaker. The latter conclusion is based on the following observations:

   a) The resonant frequency breaker delivers much higher percent of debonded steel than the multi-head breaker.
   b) The resonant frequency breaker delivers, on average, higher and more uniform thickness of the rubblized material.
   c) The resonant frequency breaker delivers higher percent of joints where the integrity of the joint is completely destroyed than the multi-head breaker.
   d) The multi-head breaker has higher potential of damaging the newly paved AC layer on the adjacent lane than the resonant frequency breaker.

2.0 FACTORS INFLUENCING THE PERFORMANCE OF RUBBLIZED CONCRETE PAVEMENT

Many factors were found to influence the performance of rubblized concrete pavement projects. Each factor belongs to a certain action that has been taken during the course of project inception to project construction. Therefore, the factors are divided into six groups depending on the type of action (the cause and effects) as presented in the next six subsections.

2.1 Project Selection

For few rubblized pavement projects, some of the factors affecting their performance can be traced back to the project selection process. Such factors could be minimized or eliminated if the following recommendations are implemented:

2.1.1 Candidate Projects

The following deteriorated concrete pavements should not be considered for rubblization options:

2. Concrete pavements that have been cracked and seated in the past.
3. Concrete pavements that are supported on a relatively soft roadbed soil (less than 3000 psi modulus).

4. Concrete pavements with extensive amount of cracking as defined in the MDOT PMS distress manual.

2.1.2 Testing of Candidate Projects

After selecting a candidate project for rubblization, the compressive strength of the existing concrete pavements should be determined. If the concrete pavement consists of two types of concrete (e.g., a widening strip, an added lane and so forth), both concrete types should be tested. The compressive strength data can be used to determine whether or not the pavement should be rubblized using different settings of the rubblizer parameters. For example, if the average compressive strength of the better concrete minus one standard deviation is higher than the average strength of the other concrete plus one standard deviation, then the rubblizer parameters should be calibrated for each type of concrete.

2.2 The Rubblization Process

For each candidate project, the contractor should obtain the compressive strength data of the concrete slab to determine the number of locations at which the operating parameters of the rubblizer should/must be calibrated as per the recommended calibration procedure presented in chapter 4. The operator of the rubblizing equipment should be trained to be cognizant of the impact of the rubblizing process on pavement performance. The following steps could be used as guidelines.

1. Stop the rubblization process and recalibrate the operating parameters if any of the following situations arises:

   a) The steel is not debonded or the concrete pavement is rubblized to shallow depths (less than 4.5 in.).
   b) The integrity of the concrete longitudinal and/or transverse joints is not completely destroyed.
   c) The rubblization is producing numerous large concrete pieces (more than 8 in.).

2. Re-examine the rubblization operation if strips of coarse rubblized material (0.5 to 3 in.) are separated by about 1-in. wide strips consisting of fine materials and/or dust. This indicates an uneven rubblization across the lane.

3. Stop the rubblization operation if the rubblizer causes large concrete pieces especially at the corner of the slab to break free and to rotate and penetrate the base material. This implies that the roadbed soil is soft and that the base layer is being subjected to shear failure, which would be reflected through the finished pavement. It is possible to alleviate the situation by recalibrating the operating parameters of the rubblizer.

4. Stop the rubblization operation and recalibrate if the hammers or the sonic shoe bounce off the pavement surface.

2.3 The AC Construction

Distress survey of all rubblized projects in the State of Michigan indicates that more than sixty percent of the projects have experienced premature distress due mainly to the construction of the asphalt mat. For almost every underperforming project, the premature distress could have been eliminated at no additional cost. Field observations and the premature distress data indicate that, for future projects, premature distress can be eliminated if the following steps are taken:

1. The rubblized concrete is thoroughly inspected for potential defects and variability prior to the placement and compaction of the AC mix.

2. Large but broken concrete pieces are replaced with approved filler aggregate.

3. Areas where asphalt patches were removed are filled with approved filler aggregate and compacted properly.

4. Areas where large concrete pieces were rotated and penetrated the base layer are excavated to the roadbed soil and all the excavated materials are replaced with approved filler aggregate and compacted properly.

5. The asphalt mix is examined to determine whether or not a dry mix is being used; a dry mix would have high potential for raveling and TDC.

6. The paver parameters (speed, the auger rotation rate, the opening of the supply window and the rate at which the AC is being fed to the auger) are calibrated as to eliminate segregation under the gear box and the ends of the auger. Note that, the new AC mixes have high segregation potential and therefore are very easily segregated if any of the above parameter is slightly off the mark. The potential for aggregate segregation could be substantially reduced or eliminated if a windrow step is included in the paving operation.

7. The hopper of the paver is not emptied at any time. This will cause an end of load segregation.

8. The asphalt mat is promptly and evenly compacted as to avoid temperature segregation prior to compaction.

2.4 The Pavement Design Process and Design Parameters

Mechanistic analyses of various rubblized pavement sections indicate that most sections are adequately designed. For few projects such as the one on US 23 by Alpena, the

finished pavement sections are thin and lack frost protection of the roadbed soil. Rubblized pavement sections could be designed using either two rubblized concrete layers (one rubblized material and one fractured concrete layers) or one rubblized concrete layer. Regardless of the number of layers used, the layer properties and coefficients stated in chapter 6 are strongly recommended.

2.5 The Pavement Materials

The new superpave mixes being used by the MDOT appear to be very sensitive to the asphalt content and very easy to segregate during the mixing, transportation and paving operations. Slight fluctuation in the ac content may cause a superpave mix to be dry or fat. Further, the high coarse aggregate contents (+ no. 4 sieve) of the mix makes it susceptible to particle segregation due to the slightest variation in the paver operation. The problem could be resolved by using windrow equipment as a part of the paving operation.

2.6 Traffic Control During the Rubblization Operation

Field investigation during the rubblization operation revealed that on some projects, one lane was kept open to traffic while the adjacent lane was being rubblized. When the rubblization of the lane was finished, the rubblized material was capped with AC, the finished pavement on one lane was opened to traffic, and the rubblization of the adjacent lane was commenced. It was observed that while the second lane is being rubblized, the applied pressure due to the hammer impact caused vertical movements in the paved lane (a stone on the pavement lane bounced off the pavement by about 1 in.). Such movement causes cracks or micro cracks in the finished asphalt mat along the paved lane. Over time, such cracks would open up and propagate in various directions. This construction built distress could be eliminated if one of the following steps is taken.

1. If feasible, do not allow any traffic along the project until the rubblization of adjacent lanes is completed. For 2-lanes 2-direction roads, this may imply traffic detour. For 2-lane in one direction roads, this imply diverting the traffic to one of the other two lanes in the opposite direction.

2. If traffic detour or diversion is not possible, rubblize one lane and surface it with 2-in. base course only. Divert the traffic to this lane while the adjacent lane is being rubblized. After the rubblization operation is completely finished, surface the newly rubblized lane using base, leveling and surface courses as needed. Divert the traffic to the finished pavement along one lane and finish paving the other lane.

3.0 THE MDOT SPECIAL PROVISION FOR RUBBLIZATION OF CONCRETE PAVEMENTS

Over time, MDOT has developed a sound and balanced special provision for rubblization of concrete pavements. However, it was observed during construction that, on most projects, the special provisions are totally or partially ignored by the contractors. For example, on certain projects, existing asphalt patches were not completely removed as stated in the provision. It is strongly recommended that the special provisions be strictly enforced.

The following modifications of the special provision are recommended:

1. Include the calibration plan of the rubblizing equipment as stated in chapter 4.

2. Include the items stated in the project selection (section 2.1) of this chapter.

3. Include the traffic control provision of section 2.6.

4. Include a provision for the inspection of the rubblized concrete at joints and mid-slab.

Based on field investigation and distress survey (see table 3.6, which, for convenience, is included herein as table 8.1) of 84 rubblized pavements, the under performance and the causes of the under performance of rubblized concrete pavements are summarized in table 8.2. The data in the table indicate that:

1. Ten projects (12 percent) exhibit no distress as of 2002. All these projects are only 2 to 4 years old.

2. Forty eight projects exhibit longitudinal TDC and twenty eight projects (33 percent) exhibit transverse TDC. All projects that exhibit transverse TDC also exhibited longitudinal distress. All transverse TDC are located in segregated areas and are mainly caused by segregation. On the other hand, 90 percent of all longitudinal TDC are caused by segregation (the cracks were initiated in segregated areas and propagated outward). The other 10 percent of the longitudinal TDC are caused by opening of the paving joints between the two lanes.

3. Twenty six projects (31 percent) exhibit joint reflective cracks and twelve projects (14 percent) are showing the initiation of reflective cracks (rough joints). The main cause of reflective cracks is the failure of the rubblization process to destroy the integrity of the concrete joints.

4. Eleven projects (13 percent) exhibit regular reflective cracks from the underlying concrete pavement. The main cause of these cracks is the failure of the

rubblization operation to rubblize the concrete in the vicinity of the original crack (at discontinuity)

5. Twenty projects (24 percent) exhibit rut. The rut depth varied from about 0.75 to about 0.125 in. with the majority of rut depths below 0.5 in. All rut channels are narrow and therefore the rut problem resides within the AC mix.

6. Finally 19 projects (23 percent) exhibit raveling, which is caused by segregation.

Note that, some pavement projects exhibit more than one type of distress while others exhibit a single distress type.

Alternative to modifying the special provision for rubblizing concrete pavements, the department could develop design, built and warranty provision for rubblized concrete pavements. For this scenario, based on field investigation, the following pavement performance measures are recommended for inclusion in a 5-year warranty period:

1. No longitudinal and/or transverse top-down cracks.
2. No reflective longitudinal or transverse cracks
3. No shear failure
4. No raveling
5. Less than 0.25-in. rut depth

Table 8.1 The number of projects exhibiting the indicated distress observed during the 2002 distress survey

Distress type	No of projects	JTC	TTDC	RTC	LTDC	RLC	ALC	S	R	P	PH	RJ	Rut	B	BC	B-up	D
LTDC/TTDC/S/JTC/R/RTC/RLC/P/PH	1	1	1	1	1	1		1	1	1	1						
LTDC/TTDC/S/JTC/R/P/PH/Rut	1	1	1		1			1	1	1	1		1				
LTDC/TTDC/S/JTC/R/P/Rut/Break up	1	1	1		1			1	1	1			1			1	
LTDC/TTDC/S/JTC/R/P/Bleeding	1	1	1		1			1	1	1				1			
LTDC/TTDC/S/JTC/R/P	1	1	1		1			1	1	1							
LTDC/TTDC/S/JTC/R/RJ	1	1	1		1			1	1			1					
LTDC/TTDC/S/JTC/R/Rut	1	1	1		1			1	1				1				
LTDC/TTDC/S/JTC/RLC/Rut	1	1	1		1	1		1					1				
LTDC/TTDC/S/JTC/Rut/Bleeding	1	1	1		1			1					1	1			
LTDC/TTDC/S/JTC/Rut	2	2	2		2			2					2				
LTDC/TTDC/S/JTC	3	3	3		3			3									
LTDC/TTDC/S/R/P/Rut	1		1		1			1	1	1			1				
LTDC/TTDC/S/R/RLC/P/Block crack	1		1		1	1		1	1	1					1		
LTDC/TTDC/S/R/RLC/Rut	1		1		1	1		1	1				1				
LTDC/TTDC/S/R/Rut	1		1		1			1	1				1				
LTDC/TTDC/S/R	2		2		2			2	2								
LTDC/TTDC/S/RTC	1		1	1	1			1									
LTDC/TTDC/S/RLC	1		1		1	1		1									
LTDC/TTDC/S/Rut	1		1		1			1					1				
LTDC/TTDC/S	3		3		3			3									
LTDC/JTC/S/R/RTC	1	1		1	1			1	1								
LTDC/JTC/S/R/RLC/Rut	1	1			1	1		1	1				1				
LTDC/JTC/S/RTC/RLC/Rut	1	1		1	1	1		1					1				
LTDC/JTC/S/RTC	1	1		1	1			1									
LTDC/JTC/S	2	2			2			2									
LTDC/S/R/RTC/RLC	1			1	1	1		1	1								
LTDC/S/R/RLC/P/PH/RJ	1				1	1		1	1	1	1	1					
LTDC/S/R	1				1			1	1								
LTDC/S/RLC/RJ/Break up	1				1	1		1				1				1	
LTDC/S/RLC/RJ	1				1	1		1				1					
LTDC/S/RLC/P	1				1	1		1		1							
LTDC/S/Rut	1				1			1					1				

Table 8.1 The number of projects exhibiting the indicated distress observed during the 2002 distress survey (continued)

Distress type	No of projects	JTC	TTDC	RTC	LTDC	RLC	ALC	S	R	P	PH	RJ	Rut	B	BC	B-up	D
LTDC/S	4				4			4									
LTDC/RTC/P	1			1	1					1							
LTDC/RLC/RJ	1				1	1						1					
LTDC/Rut	1				1								1				
LTDC	2				2												
TTDC/JTC/S/RLC/RJ	1	1	1			1		1				1					
TTDC/JTC/ALC/Rut	1	1	1				1						1				
JTC/RTC	1	1		1													
JTC/RLC/Rut	1	1				1							1				
JTC/RLC	1	1				1											
JTC	1	1															
S/R/RLC/P/PH	1					1		1	1	1	1						
S/P	1							1		1							
S/PH	1							1			1						
S/RJ	1							1				1					
S/RLC	1					1		1									
S/Depression	1							1									1
S	3							3									
RTC/RLC	2			2		2											
RTC	1			1													
RLC/RJ	1					1						1					
RLC	1					1											
RJ/Rut	2											2	2				
RJ	2											2					
Rut	1												1				
Bleeding	1													1			
No distress	10																
Total	**84**	**26**	**28**	**11**	**48**	**22**	**1**	**53**	**19**	**12**	**5**	**12**	**20**	**3**	**1**	**2**	**1**
Did not survey	2																
Not rubblized	2																

LTDC = Longitudinal top-down cracks, TTDC = Transverse top-down cracks, S = segregation, JTC Joint transverse crack, R = Raveling, RTC = Regular transverse crack, RLC = Regular longitudinal crack, P = Patch, PH = Pothole, RJ = Rough joint, D = Depression, B = Bleeding, ALC = Alligator cracks, BC = Block cracking, and B-up = Break up

Table 8.2 A summary of the attributes to the under performance of rubblized pavements and the associated causes

Attribute of underperformance	Percent of projects showing the underperformance attribute	Causes of the under performance attribute		
		HMA segregation (construction)	Rubblizing procedure	HMA mix (construction)
No distress	12			
Longitudinal TDC	57	90		10
Transverse TDC	33	100		
Joint reflective cracking	31		100	
Reflective cracks	13		100	
Rut	24			100
Rough joint	14		100	
Raveling	23	100		
Potholes	15	83	17	